RCA REVIEW

a technical journal

RADIO AND ELECTRONICS
RESEARCH · ENGINEERING

VOLUME VIII   JUNE 1947   NO. 2

RCA REVIEW

a technical journal

RADIO AND ELECTRONICS
RESEARCH · ENGINEERING

CONTENTS

RCA REVIEW

FOREWORD

FROM time to time inquiries are received concerning technical literature published by the RCA REVIEW Department of RCA Laboratories Division. In general, all subscribers are informed of available material by direct mail; however, it is felt that the following outline will be of interest.

At the present time, in addition to the quarterly technical journal, RCA REVIEW publishes an Index, occasional pamphlets, and a Technical Book Series. Two volumes of the Index have been published to date: RCA TECHNICAL PAPERS (1919-1945)—INDEX, Volume I, and (1946)—INDEX, Volume II(a). One pamphlet has been issued: TELEVISION—A Bibliography of Technical Papers by RCA Authors (1926-1946).

Three volumes of the Technical Book Series are currently available: TELEVISION, Volume III (1938-1941), and Volume IV (1942-1946), both published in 1947; and RADIO FACSIMILE, Volume I, published in 1938. These books consist of technical papers by RCA Authors on the subject indicated. Some of the papers have not been published elsewhere.

Further information on any of these publications, as well as on RCA REVIEW, may be obtained by writing to:

RCA REVIEW
Radio Corporation of America
RCA Laboratories Division
Princeton, N. J.

The Manager, RCA REVIEW

THE RATIO DETECTOR*

BY

STUART WM. SEELEY AND JACK AVINS

Industry Service Laboratory, RCA Laboratories Division,
New York, N. Y.

Summary—A new circuit for f-m† detection known as the ratio detector is coming into wide use. In this circuit two frequency-sensitive voltages are applied to diodes and the sum of the rectified voltages held constant. The difference voltage then constitutes the desired a-f† signal. This means of operation makes the output insensitive to amplitude variations.

The basic principles governing the operation and design of the ratio detector are described. The ratio between the primary and secondary components of the frequency-sensitive voltages in a phase-shift type of ratio detector is a function of the instantaneous signal amplitude. The a-m† rejection properties, however, are shown to depend upon the mean ratio between these voltages. An expression which is developed for this ratio in terms of the circuit parameters provides the basis for arriving at an optimum design. The measurements necessary in the design of a ratio detector and in checking its performance are described.

GENERAL DESCRIPTION

THE principle underlying most circuits for f-m detection has been the peak rectification of two i-f† voltages whose relative amplitudes are a function of frequency, together with means for combining the rectified voltages in reversed polarity. This introduces a difference voltage, proportional to the difference of the two applied i-f voltages, which is a function of the instantaneous applied frequency. A representative circuit of this type is shown in Figure 1(a).

While this circuit represents a considerable improvement over unbalanced f-m detectors in that it is amplitude-insensitive at the center frequency, it has the disadvantage that changes in amplitude at other than the center frequency will cause the audio output to fluctuate proportionally as shown in Figure 1(b). This has been recognized and has resulted in the use of limiter circuits to remove extraneous amplitude variations from the applied signal.

In the ratio type of f-m detector, the problem of making the de-

---

* Decimal Classification: R362 × R361.111.

† Throughout this paper the following abbreviations are used: f-m: frequency modulation or frequency-modulated; a-m: amplitude modulation or amplitude-modulated; a-f: audio frequency; i-f: intermediate frequency.
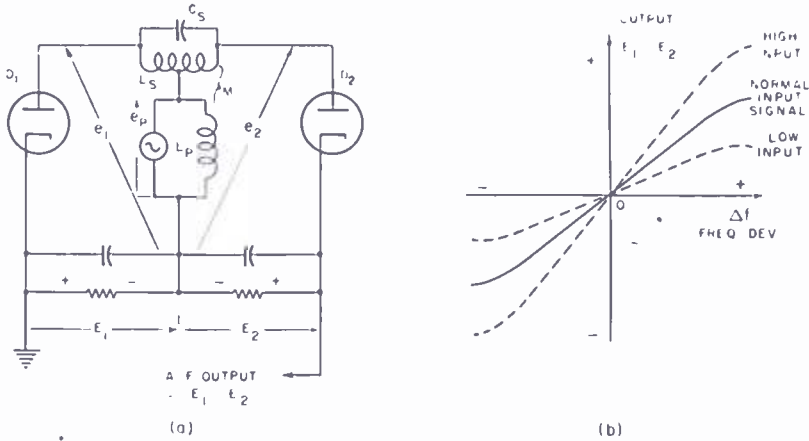
Fig. 1—Basic circuit of a balanced discriminator. The output characteristic in (b) shows the dependence of the output on the input signal amplitude.

tector insensitive to amplitude variations has been met by splitting the rectified i-f voltages into two parts in such a way that the ratio of the rectified voltages is proportional to the ratio of the applied frequency-sensitive i-f voltages. It follows that if the sum of these rectified voltages is maintained constant by a suitable means, *and if their ratio remains constant,* the individual rectified voltages will also remain constant. The output will therefore tend to be independent of amplitude variations in the input signal. A representative simplified ratio-detector circuit is shown in Figure 2. The circuit connections are such that both diodes carry the same direct current. The rectified voltages add to produce the sum voltage, which is held constant.

The sum voltage may be stabilized by using a battery or by shunt-
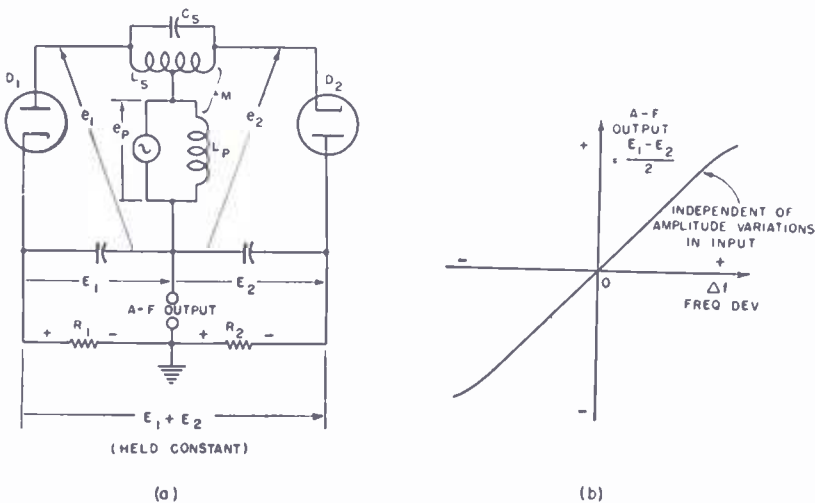
Fig. 2—Basic circuit of a ratio detector using the same phase shift input circuit as in Figure 1. The rectified voltage is stabilized so that the output can be independent of the input amplitude.

ing a large condenser across the load resistors. If a battery is used, operation is limited to a signal at least strong enough to overcome the fixed bias created by the battery. On the other hand, if a large condenser is used, the voltage across the condenser will vary in proportion to the average signal amplitude and thus automatically adjust itself to the optimum operating level. In this way amplitude rejection can be secured over a wide range of input signals, the lowest signal being determined by deterioration of the rectifier characteristics at low levels.

When a condenser is used to stabilize the rectified output voltage its capacitance must be large enough so that the rectified output
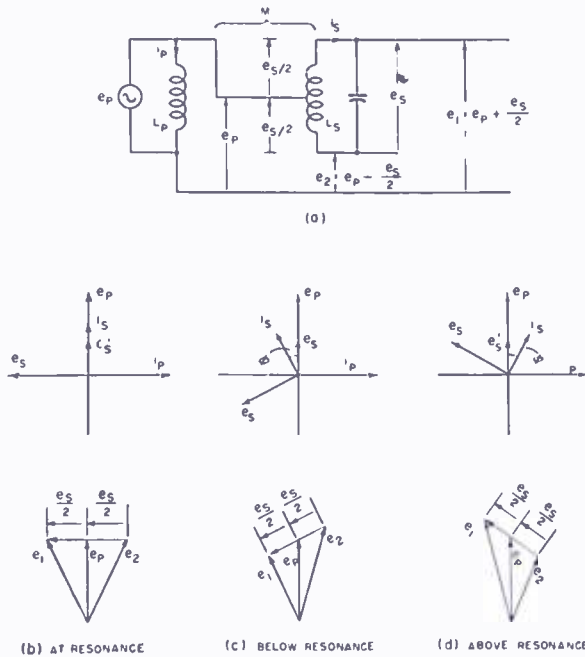
Fig. 3—Basic phase shift circuit used in frequency discriminators and ratio detectors. The phase relations between the primary and secondary voltages are shown, as well as the resultant voltages which are applied to each diode.

voltage does not vary at audio frequency. This calls for a time constant on the order of 0.2 second and for capacitance values on the order of several microfarads.

Elementary Operation

Although the exact analysis of a practical ratio detector is complicated by many factors, it is not difficult to obtain a qualitative understanding of the method of operation. A more detailed investigation of the circuit is made later.

Since the ratio detectors described here use the balanced phase shift type of input circuit, the characteristics of this circuit are briefly reviewed. Figure 3 shows the basic phase shift circuit and the manner in which the two frequency-sensitive voltages are obtained. These voltages are combined in the ratio detector as shown in Figure 4(a). The variations in the open-circuit voltages e_1 and e_2 are conveniently described by Figure 4(b). The rectified voltages E_1 and E_2 are approximately proportional to OA and OB. The phase angle ϕ is zero at the center frequency and increases as the deviation increases.

Using this diagram it is possible to draw the detector output characteristic as shown by the $(E_1\text{-}E_2)$ curve in Figure 5. This is

$$\tan\phi \cdot m = Q_{sec}\left(1 - \frac{f^2}{f_0^2}\right) \cong 2Q_{sec}\frac{f-f_0}{f_0} = 2Q_{sec}\frac{\Delta f}{f_0} \cdot 2Q_{sec}\delta$$

(a)   (b)
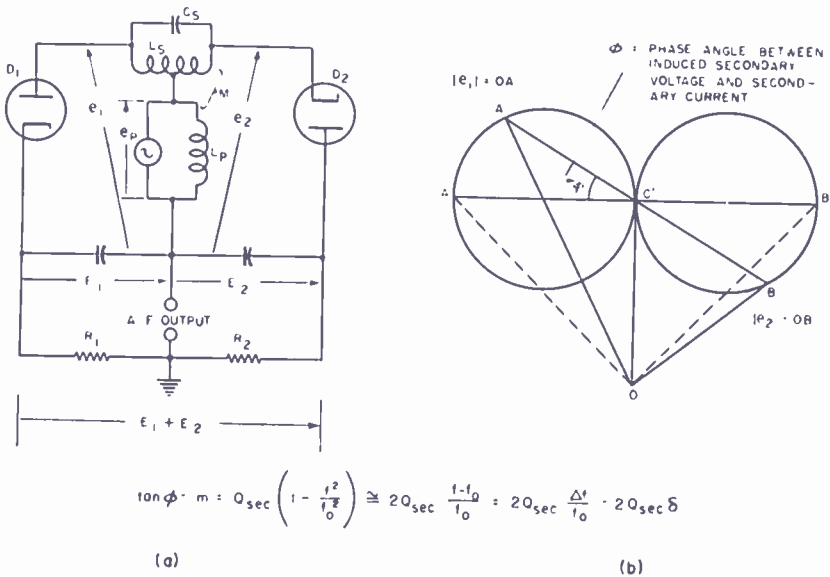
Fig. 4—Basic ratio-detector circuit showing the variation with frequency of the voltages applied to each of the diodes.

similar to the characteristic obtained with a conventional discriminator. A factor ½, however, should be applied to indicate the six-decibel loss which is inherent in the reversed polarity connection of the diodes and the change in the a-f take-off point. Thus, when, $E_1\text{-}E_2$ changes by a given amount, the change in potential at the a-f take-off point in Figure 4 is $(E_1\text{-}E_2)/2$.

If now the rectified voltage is stabilized as in Figure 2, the output characteristic changes. Over the region where $E_1 + E_2$ is constant, i.e. for small deviation from the center frequency, Figure 5 shows that a ratio detector will have essentially the same output (in the absence of amplitude modulation) as a conventional discriminator using the same transformer and load resistors but with one of the diodes reversed. For large deviations, $E_1 + E_2$ falls and the application of
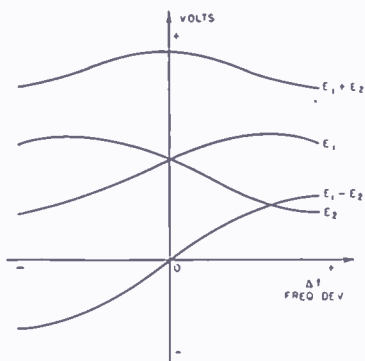
Fig. 5—The voltages E_1, E_2, $E_1 + E_2$, E_1-E_2 which are present in Figure 4(a) can be plotted as shown, with the aid of ·Figure 4(b).

the stabilizing voltage to maintain $E_1 + E_2$ constant has the effect of improving the linearity of the detector characteristic and extending the maximum deviation that can be handled for a given amount of distortion.

The manner in which the ratio detector maintains a constant output independent of amplitude modulation may be seen by reference to Figure 6. If the amplitude of the input signal is constant as in (a), the stabilizing current is zero and the circuit has essentially the same output characteristic as a balanced discriminator. On the other hand, if the input signal increases as in (b), the diodes are driven harder, the average diode current increases, and this increased direct current flows into the stabilizing voltage source. Similarly, if the input signal decreases, as in (c), the diode current decreases and the stabilizing
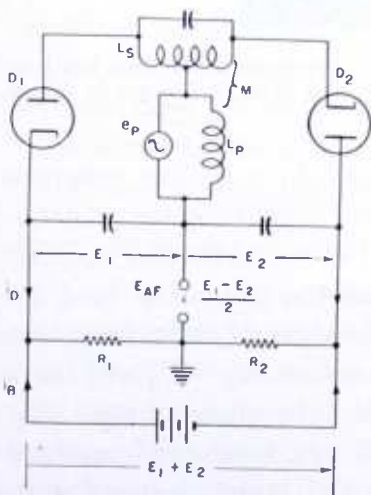
(a) Constant normal input amplitude $e_p = e_0$
Stabilizing current $I_B = 0$
Diode current $I_0 = \dfrac{E_1 + E_2}{R_1 + R_2}$
Effective diode load resistance $= R_1 + R_2$

(b) Increase in input amplitude $e_p > e_0$
Stabilizing current $L_B < 0$
Diode current $I_0 > \dfrac{E_1 + E_2}{R_1 + R_2}$
Effective diode load resistance $< R_1 + R_2$

(c) Decrease in input amplitude $e_p < e_0$
Stabilizing current $I_B > 0$
Diode current $I_D < \dfrac{E_1 + E_2}{R_1 + R_2}$
Effective diode load resistance $> R_1 + R_2$

Fig. 6—The effect of changes in input signal level on the diode current, the stabilizing current, and the effective load resistance presented to the diodes. The stabilizing voltage $E_1 + E_2$ is held constant at the voltage equal to the rectified output when $e_p = e_0$.

voltage makes up the decrease in diode current in order to maintain the sum voltage across the two diode load resistors constant. Stabilizing the rectified voltage, therefore, results in the equivalent load resistance varying in such a way that it decreases when the input signal rises and increases when the input signal falls.

This action of the stabilizing voltage in varying the effective diode load resistance provides a convenient method for analyzing the mechanism of amplitude rejection. A first approximation to the behavior of the ratio detector, then, is to consider how the output is affected when the load resistance is varied above and below its mean operating value. Figure 7 shows the result of varying R, while all other parameters, including the input signal, are held constant.
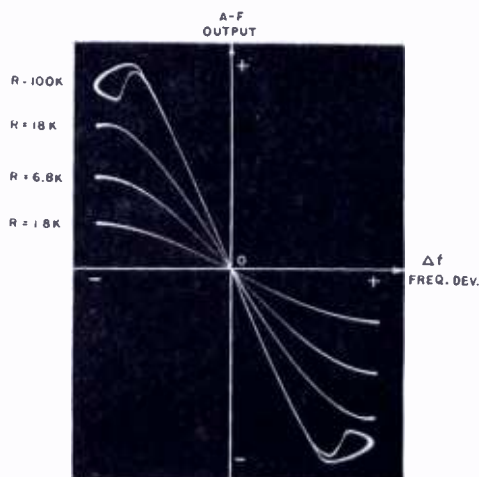
Fig. 7—Effect on the output of the ratio detector when the load resistance is varied. The curves were taken with the circuit shown in Figure 8.

If the rectified outputs $E_1 + E_2$ and $E_1 - E_2$ are measured, it is readily possible to determine whether the detector constants, the primary-secondary inductance ratio, the primary and secondary Q's, the coupling, the diode perveance, and the operating load resistance are such as to yield good amplitude rejection. If the circuit is designed properly, it will be found that, as R is varied, $E_1 - E_2$ will increase (or decrease) at the same rate as $E_1 + E_2$. In other words, $(E_1 - E_2)/(E_1 + E_2)$ must be independent of R and hence independent of the rectified current. If $(E_1 - E_2)/(E_1 + E_2)$ is independent of the rectified current, then it follows that the ratio E_1/E_2 must also be independent of the rectified current.

To take a specific example, suppose R is increased so that, for a fixed deviation, $(E_1 - E_2)/2$ increases to twice its original value.

Then $E_1 + E_2$ will also double. The input signal may therefore be reduced to one half its original value and the a-f output will then be the same as it was before the change in R and the reduction in input signal. In practice, when a battery or a large condenser is used across the load resistors, any variation in the input signal automatically causes the equivalent load resistance to vary in such a way as to keep the a-f output constant, provided of course that the detector circuit parameters are properly related.

The amount of downward amplitude modulation which can be rejected, that is, the extent to which the signal can fall below its initial value without causing the output to change, is an important characteristic. The limiting factor here is that, if the input signal drops to too low a value, the voltages across the primary and secondary are not sufficient to cause the diodes to conduct. Effectively, the diodes are biased off by the stabilizing voltage and the detector becomes inoperative until the signal rises to a level sufficiently great to cause the diodes to conduct.

It is desirable to design the ratio detector so that the signal can fall to as low a value as possible without the diodes being cut off. This is accomplished, in general, by using a high value of secondary Q and by using relatively low values of diode load resistance so that the operating Q of the secondary is on the order of 25 per cent of its unloaded Q. Other considerations are also involved, but the extent to which the operating Q is smaller than the unloaded Q is the principal factor in determining the maximum percentage of downward amplitude modulation which can be rejected without the diodes being cut off.

The limitation of the diodes being biased off by the stabilized rectified voltage does not exist as far as upward modulation is concerned. In general, the ratio detector can reject higher percentages of upward modulation than it can downward modulation.

Ratio Detector Receivers

Receivers using the ratio detector have characteristics which differ from limiter and locked-oscillator receivers in a number of respects. Since the rectified voltage across the long-time-constant load circuit of the ratio detector automatically adjusts itself to the input signal level, there is no fixed threshold, and the a-f output and the stabilizing voltage (which may be used for automatic-volume-control (a-v-c)) are proportional to the input signal. Less i-f gain is required since the ratio detector in typical designs will provide appreciable amplitude rejection with as little as ten to fifty millivolts of input signal to the grid of the ratio-detector driver tube. As a result, receivers using

this type of detector tend to be quiet between stations. When a-v-c is used, the selectivity of the receiver is maintained for strong as well as weak signals.

The tuning characteristic of a receiver using the ratio detector is characterized by comparatively low side responses. This results, in part, because the high degree of amplitude modulation which an off-resonant f-m signal acquires as it is modulated up and down the steep i-f selectivity curve produces relatively little output from the ratio detector. The extent to which the side responses will fall below the main response depends upon the amount of a-v-c, the i-f selectivity, and the ratio-detector peak separation.

TYPICAL RATIO DETECTOR

The circuit and performance data for a ratio detector circuit oper-

Fig. 8—A ratio-detector circuit using a balanced phase shift transformer feeding a 6AL5 double diode. The closely coupled tertiary winding L_T is wound over the $B+$ end of the primary to provide impedance matching and improved sensitivity.

ating at a center frequency of 10.7 megacycles is shown in Figure 8. In order to improve the sensitivity, a form of impedance matching is used between the high impedance of the driving pentode and the relatively low impedance which the diodes reflect across the winding that injects the primary voltage into the diode circuit. This is, of course, the winding L_t which is wound over the cold end of the primary winding L_p and is tightly coupled to the primary. The phase of the voltages across L_p and L_t is therefore substantially the same. The voltages across L_t and L_s are in quadrature (at the center frequency) and in accordance with the action which has been previously described, the demodulated f-m output is taken off through a connection to the secondary winding.

The construction of the transformer is evident from the photograph in Figure 9. Slug tuning is used for both primary and secondary windings. Since a bifilar construction is used for the secondary winding, the slug penetrates each half of the winding to essentially the same degree, and hence variation in the position of the slug does not unbalance the two halves of the secondary winding. Even where the secondary is capacitively tuned, this bifilar construction is desirable because it provides close coupling between the two halves of the secondary and uniform coupling of each half of the secondary to the primary winding.

As shown in Figure 8, the major part of the rectified output voltage is stabilized by means of the 8-microfarad condenser C_3. This, in con-
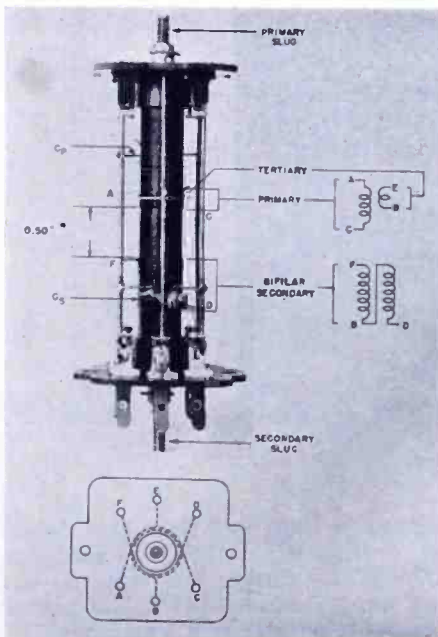
FORM: 13/32″ O.D. ⅜″ I.D. Bakelite XXX

SHIELD CAN: 1⅜″ Aluminum, Square

TUNING SLUGS: Stackpole G-2, SK-124

PRIMARY: 24 Turns #36E close wound

TERTIARY: 4½ Turns #36E close wound on layer paper electrical tape (0.004) over B + end of primary

SECONDARY: Bifilar, 18 Turns (total) #28. Form double grooved 20 TPI. Length of winding = 0.45″

All windings counter clockwise starting at far end

* *Measured adjacent to side rod E*
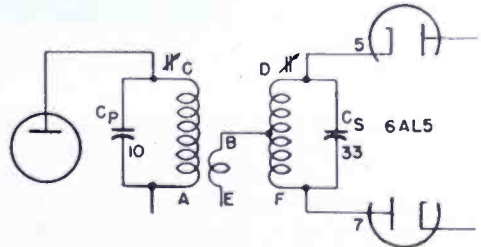
Fig. 9—Details of construction of the ratio-detector transformer used in the circuit of Figure 8. The bifilar secondary connections are brought out symmetrically to the vertical rods to prevent unbalance.

junction with the two diode load resistors R_1 and R_2, gives a discharge time constant of approximately 0.1 second. The rectified voltage drop across R_3 and R_4 is not stabilized against changes in diode current. This permits minimizing the residual balanced component of amplitude modulation (See Figure 21) for this particular circuit design. The fact that the two resistors R_3 and R_4 are not equal in value makes it possible to produce a compensating unbalanced component which cancels the unbalanced component which could otherwise appear in the output (see Figure 22). This unbalance is principally due to the variation in the dynamic input reactance of the diodes and is not

necessarily an indication that the circuit itself is unbalanced in any way. The 47-ohm resistor R_5 modifies the peak diode currents and further reduces the unbalanced a-m component, particularly at high signal levels.

The condenser C_4 bypasses the secondary system to ground at the intermediate frequency. The conventional deemphasis circuit which is conveniently placed at this point provides further filtering against i-f getting into other circuits and causing feedback. A 39,000-ohm resistor and a 0.002-microfarad condenser are suitable values for the deemphasis circuit.

The alignment procedure for this detector consists of applying an unmodulated i-f signal to the ratio-detector driver tube and peaking

— 350 kc —
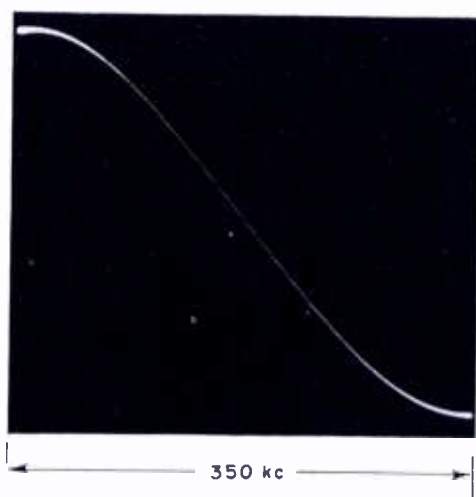
Fig. 10—Output characteristic and performance data for the ratio detector shown in Figure 8. Input signal = 100 millivolts; Rectified voltage = 6 volts; A-V-C voltage = 2.5 volts; A-F output (75-kilocycle deviation) = 0.7 volt root-mean-square; Distortion (100 per cent modulation) = 2.5 per cent root-mean-square; Distortion (30 per cent modulation) = 0.7 per cent root-mean-square; Maximum downward amplitude modulation = 70 per cent.

the primary so that maximum rectified voltage is obtained, as indicated by a d-c voltmeter connected to the a-v-c takeoff point (Figure 8). The secondary tuning is then adjusted for zero voltage as indicated by a d-c voltmeter connected to measure the voltage at the audio take-off point. It will be noted that the alignment procedure is essentially the same as for a balanced discriminator. Because the primary and secondary windings are below critical coupling, there is negligible interaction between the adjustments.

The output characteristic of this detector is shown in Figure 10, along with the data giving the audio recovery and rectified voltage for 100 millivolts input to the last i-f tube, i.e., to the ratio-detector

driver tube. Both the rectified output voltage and the a-f voltage are closely proportional to the average signal input.

One way of showing the amplitude-rejecting properties of this detector is by means of the output characteristic curves shown in Figure 11. These are taken with a battery across the stabilizing condenser to hold its voltage constant at the normal value which was present just before the battery was applied. The input signal is then reduced in strength until the diodes are cut off. Note that the output remains essentially constant over a band of more than 150 kilocycles while the signal is reduced to one-third of its initial value. The peak separation, however, is reduced as the input signal is reduced.

Another more convenient way of showing the amplitude rejection is to use an f-m signal which is simultaneously amplitude modulated.
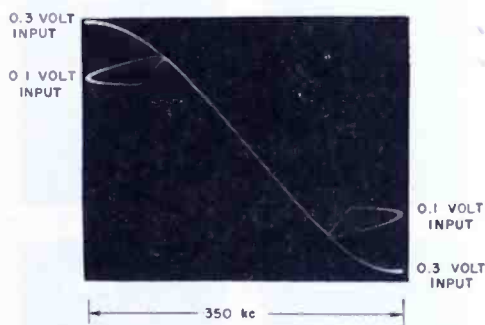
Fig. 11—Effect of reduction in the input signal. The stabilizing voltage is held constant at a level corresponding to the 0.3-volt input signal. Note the reduction in peak separation for decreasing input signal.

When this type of signal is applied, no stabilizing battery is required since the stabilizing condenser will maintain the rectified voltage constant for a-m frequencies above about 100 cycles. As explained in detail later, the extent to which the characteristics in Figure 12 differ from a line, indicates the relative amount of residual amplitude modulation in the f-m output.

In arriving at the design of this detector (Figure 8), a number of circuit parameters, in addition to those previously mentioned, are involved. These include the unloaded and loaded values of primary and secondary Q, the per cent of critical coupling between primary and secondary, and the grid to plate gain under various conditions. They are tabulated below:

Primary: Unloaded $Q = 70$
    Operating Q (with diode loading) $= 40$

Secondary: Unloaded $Q = 89$.
    Operating Q (with diode loading) $= 21$

Half-secondary/tertiary voltage ratio: 0.65

Coupling: 0.50 of critical. (This includes the effect of the capacitance unbalance due to the difference between the input capacitances of the two diodes.)

Grid-to-plate gain: The normal gain is 100. (Under the conditions yielding maximum gain, i.e., with downward amplitude modulation off the center frequency, the grid-plate gain rises to 130.)

CIRCUIT ANALYSIS

The analysis of the ratio detector is more difficult than that of the
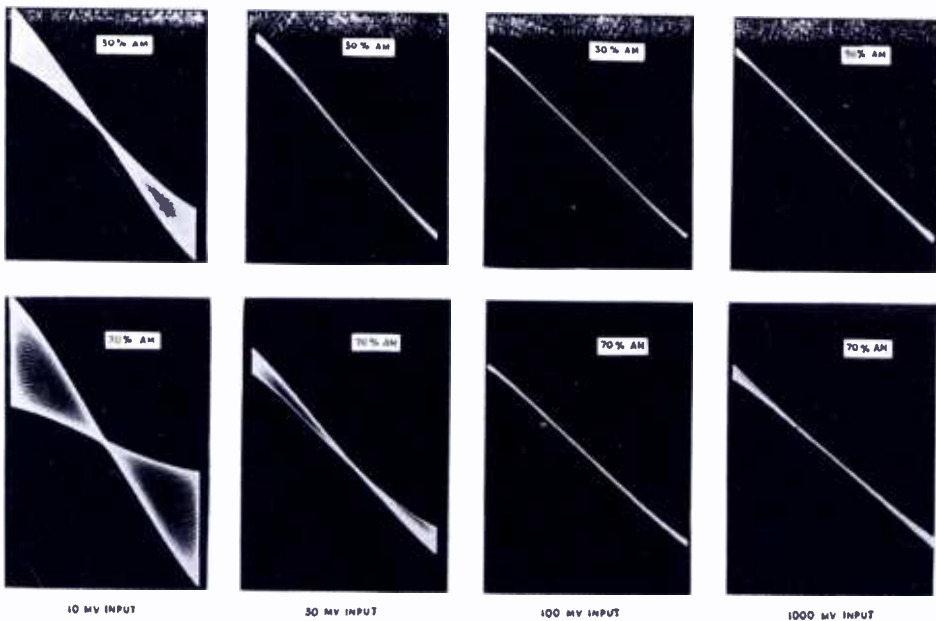
Fig. 12—The demodulated output when an f-m signal, 75 kilocycles deviation, having simultaneous a-m modulation, is applied to the ratio detector in Figure 8. The f-m modulation is at 400 cycles; the a-m modulation is at 250 cycles. The width of the detector characteristic indicates the residual a-m output.

balanced discriminator primarily because of the variation in equivalent load resistance during the a-m cycle as well as during the f-m cycle. In addition, the problem is complicated by the complex impedance characteristics of the frequency-sensitive driving circuit, the non-linearity of the diode characteristics, and the input reactance variations of the diodes which tend to modify the frequency characteristic of the driving circuit. A productive method of attack is to consider first the equivalent circuit and to develop an expression for the ratio of primary and secondary voltage. This expression is impor-

tant because the degree of a-m rejection and the peak separation are closely related to this ratio.

Equivalent Circuit

The effect of the diodes on the ratio detector circuit can be simulated, as shown in Figure 13, by placing a resistance $R/4\eta$ across the primary and a resistance R/η across the secondary. This is the same relationship which applies to the balanced discriminator circuit.

From Figure 13(b) it is clear why some form of impedance matching is of great importance if good sensitivity is to be obtained. It is not uncommon for R to have values of the order of 10,000 ohms or less, since R must be low enough to reduce the secondary Q to about one-

(a) BASIC RATIO DETECTOR (b) EQUIVALENT CIRCUIT
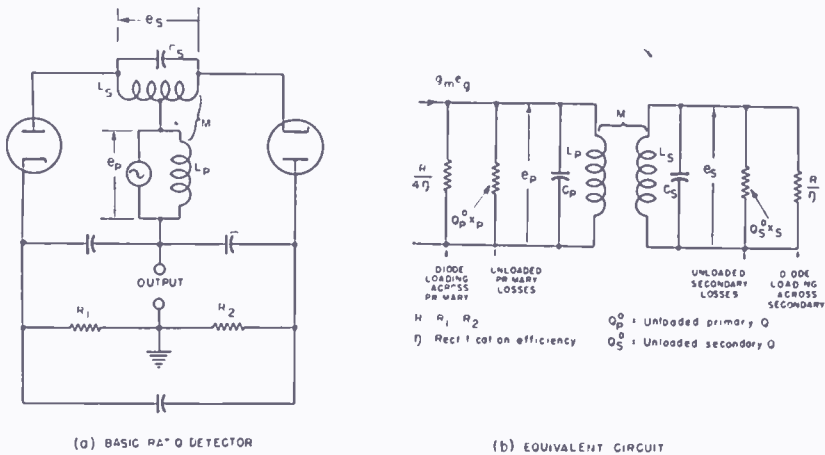
Fig. 13—The equivalent circuit for a basic phase shift ratio detector shows that the diodes reflect an equivalent shunt resistance $R/4\eta$ across the primary and a resistance R/η across the secondary.

fourth of its unloaded value. This would result in a load impedance of 2500 ohms which is too low to provide good energy transfer from a pentode.

A typical circuit using a tapped primary to obtain impedance matching has already been described. The equivalent circuit for this arrangement is shown in Figures 14 and 15. This circuit differs from Figure 13 in that the diode loading is across the tertiary and appears across the primary as a resistance n^2 times as great.

Referring to Figures 14 and 15, it is shown in the Appendix that

$$\frac{S}{P} = \alpha \sqrt{1 + \frac{n^2 Q_s^1}{4a Q_p^0}} \qquad (1)$$
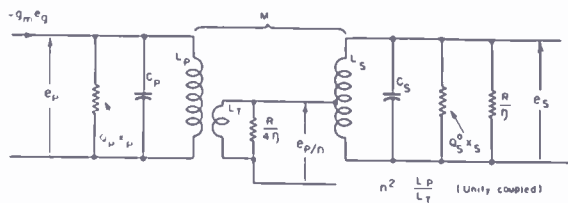
(a) TAPPED PRIMARY RATIO DETECTOR
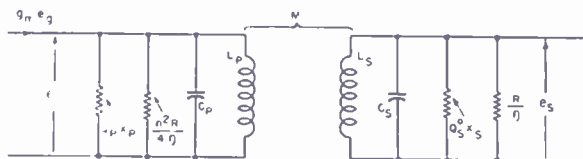
(b) EQUIVALENT CIRCUIT FOR DIODE LOADING

Fig. 14—The equivalent circuit for a ratio detector using a closely coupled tertiary winding (Figure 8) or a tapped primary to obtain impedance matching.

where S = half secondary voltage at the center frequency

P = "primary" (i.e. tertiary) voltage effective in the diode circuit, at the center frequency

$100\,\alpha$ = per cent of critical coupling existing between L_p and L_s

a = ratio of primary and secondary inductance = L_p/L_s

n = ratio between the primary and tertiary voltages, which corresponds approximately to the primary being tapped at $1/n$ turns

Q_s^1 = operating Q of the secondary, taking into account the diode loading

Q_p^0 = unloaded Q of the primary

The assumption is made in deriving this expression that the oper-
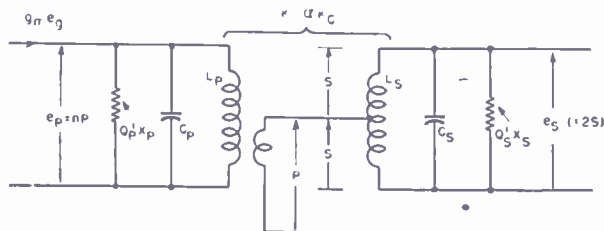
Q_P^1 = Operating Q of primary

Q_S^1 = Operating Q of secondary

$100\,\alpha$ = Per cent critical coupling $\left(\kappa_C = \dfrac{1}{\sqrt{Q_P^1 Q_S^1}}\right)$

Fig. 15—A further simplification of the equivalent circuit of Figure 14, showing the voltages P and S which are applied to the rectifier circuit.

ating Q of the secondary (Q_s^1) is small in comparison with the unloaded Q (Q_s^0). This assumption is usually justified and accounts for the factor R/η not appearing in the equation. Q_p^0 appears in the equation because it cannot usually be assumed that the loaded primary Q will be small in comparison with the unloaded primary Q.

It is shown in the Appendix that the half-secondary voltage S is given by

$$S = g_m\, \omega L_s\, Q_s^1\, n\; \frac{1}{4\,\sqrt{1 + \dfrac{n^2\, Q_s^1}{4a\, Q_p^0}}}\; \frac{\alpha}{1 + \alpha^2} \qquad (2)$$

or

$$S = \frac{g_m\, \omega L_s\, Q_s^1\, n}{4}\; \left(\frac{P}{S}\right)\; \frac{\alpha^2}{1 + \alpha^2}. \qquad (3)$$

The expression for S is put in this form because in general S/P will not be an independent variable but will be fixed by considerations which determine the amplitude rejection and the peak separation.

Effect of Varying S/P

Before discussing the significance of these equations, it is desirable to show the dependence of peak separation and a-m rejection on the value of S/P. For convenience, constant primary voltage is assumed; this simplifies the analysis and provides a basis for obtaining a solution when the primary voltage is not constant. In this connection, whether the primary voltage variation is due to external amplitude modulation, or whether it is due to the primary selectivity makes no appreciable difference in the analysis.

The curves in Figure 16 were taken with constant primary voltage. As indicated, the a-f output characteristic is plotted for several values of S/P, P being held constant at the same value for all curves. The output characteristics are shown with and without the rectified voltage being stabilized. In addition, the variation in the rectified voltage is shown for each value of S/P. The same voltage scale is used throughout for the a-f output and the rectified voltage variation.

From Figure 16 it is clear that as S/P is increased, the peak separation increases. This is true whether the rectified voltage is stabilized or not; that is, it is equally true for the balanced discriminator or for the ratio detector. When the rectified voltage is stabilized, how-

ever, the effect of the stabilization is much more pronounced when S/P is large than when S/P is small. The reason for this effect is apparent from a consideration of the rectified voltage variation. As shown in Figure 16 this variation is much greater when S/P is large than when S/P is small. It follows that the effect of stabilizing the rectified voltage and removing the variations referred to above will be greater when S/P is large. Furthermore, since $E_1 - E_2$ and $E_1 + E_2$ (Figure 16) tend to fall as the deviation increases, the effect of stabilizing the rectified voltage is to produce an increase in the peak separation.
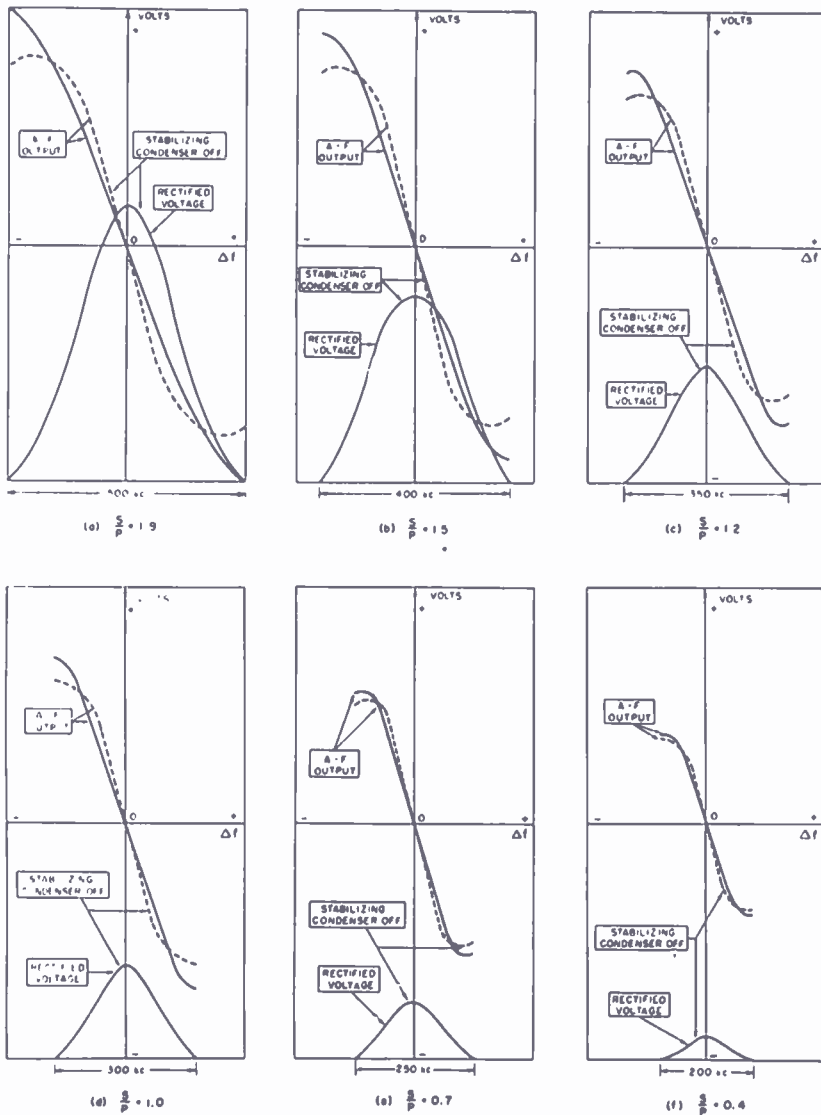
Fig. 16—The output of a ratio detector as a function of the ratio between the secondary and primary voltage, the primary voltage being held constant. The rectified output voltage variation, when the stabilizing condenser is removed, and the corresponding a-f output are also shown for each value of S/P.
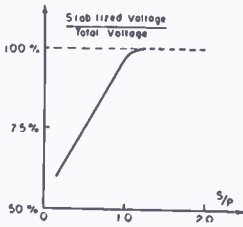
Fig. 17—The fraction of the total rectified voltage which must be stabilized to reduce the residual balanced amplitude modulation is a function of S/P. For values of S/P greater than about unity, the a-m in the output increases if less than the full rectified voltage is stabilized.

The a-m rejection is a matter of primary interest. To determine the effect of S/P on the a-m rejection, amplitude modulation was applied for each of the conditions shown in Figure 16. As shown in Figure 17, a threshold value of S/P exists, and for values of S/P greater than this it is not possible to obtain good a-m rejection. At this critical value, which is approximately unity, the full rectified voltage must be stabilized. As the value of S/P is decreased below this value, good a-m rejection will be obtained provided a particular fraction of the full rectified voltage is stabilized. The lower the value of S/P, the smaller the fraction of the rectified voltage which must be held constant. The ratio of unloaded to loaded secondary Q is four to one for the curve shown in Figure 17. A 6AL5 double diode was used.

Stabilizing the Rectified Voltage

Two general methods for controlling the desired percentage of the rectified voltage which is stabilized are shown in Figure 18. In (a), a resistor is added in series with the stabilizing condenser. In (b), the same effect is obtained by adding resistors R_a and R_b in series with the load resistance which is shunted by the stabilizing condenser.

If these circuits are to be equivalent, then a change $\triangle I$ in the d-c rectified current must result in the same change in rectified voltage for each of the two circuits.
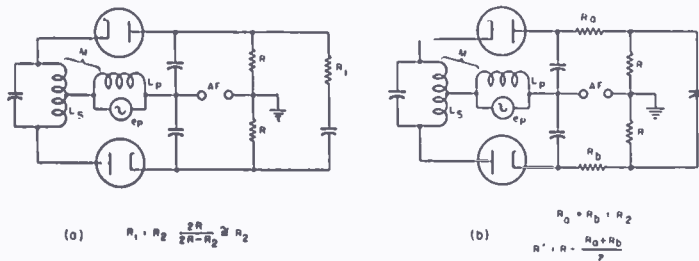
Fig. 18—Two methods of stabilizing any desired fraction of the rectified output voltage. In each case the fraction of the output voltage stabilized is approximately equal to $2R/(2R + R_1)$.

For circuit (a), $\Delta E = \Delta I \dfrac{2R}{2R + R_1} \cdot R_1$

For circuit (b), $\Delta E = \Delta I \, (R_a + R_b) = \Delta I \cdot R_2$

$$\therefore \ \Delta i \cdot R_2 = \Delta I \dfrac{2RR_1}{2R + R_1}$$

or $R_1 = R_2 \dfrac{2R}{2R - R_2} \cong R_2 \quad$ provided $R_2 << 2R$

Both circuits provide equal diode loading since the total load resistance is the same. When the desired variation in the rectified output voltage is small, then $R_1 = R_2$ as shown above.

Factors Affecting S/P

Consider the expression for S/P given by Equation (1). If $Q_p{}^0$ is large enough so that the primary Q is determined solely by the diode loading, it is clear that

$$\dfrac{n^2 Q_s{}^1}{4a \, Q_p{}^0} << 1 \qquad \text{and} \qquad \therefore \dfrac{S}{P} = \alpha$$

This gives the useful result that for this condition the ratio S/P is independent of the ratio between the primary and secondary inductance, and also independent of the number of turns in the tertiary winding. For this condition, then, S/P is dependent only on the per cent of critical coupling and is equal to α.

When the diode damping of the primary is comparable to the primary losses, S/P is greater than α as indicated by Equation 1. The extent to which the primary is damped by the diode rectifiers is of interest since the amount of downward amplitude modulation that can be handled depends, among other factors, on the primary diode damping. The greater the amount of damping, the greater will be the rejection of downward amplitude modulation because downward amplitude modulation is accompanied by an increase in the effective load resistance and hence an increase in the effective primary Q. This action increases the gain and helps to offset the drop in signal level.

Referring again to Equation (1), it is desirable to determine the extent to which the damping on the primary can be increased without decreasing the value of S/P which must be maintained at approxi-

mately unity. Since α will be fixed within relatively narrow limits by considerations which will be discussed later, the only variable part in the expression for S/P is $n^2 Q_s^1/4a Q_p^0$. Assuming that Q_s^1 is as large as practicable, consistent with the unloaded secondary Q being several times the loaded secondary Q, this leaves the factor $n^2/4a Q_p^0$. This factor must have a particular value, depending on α, in order to make S/P approximately unity. The question arises as to whether there is any advantage in making n^2 large and $a Q_p^0$ proportionately large, or in keeping n^2 small and making $a Q_p^0$ proportionately small.

To determine the manner in which the primary damping varies for particular values of n^2 and corresponding values of $a Q_p^0$, consider the ratio of the shunt damping resistance introduced by the diodes and the equivalent shunt resistance of the undamped primary. This ratio is equal to

$$\frac{n^2 R}{4Q_p^0 X_p} \propto \frac{n^2}{Q_p^0 a X_s} \propto \frac{n^2}{a Q_p^0}$$

since X_s is not a variable here. Comparing this expression with Equation (1), it follows that the relative amount of diode damping on the primary does not change with any change in n, Q_p^0, or a, provided these changes are made in such a way as to keep constant both the ratio S/P and the percent of critical coupling. Of course, the sensitivity will change, increasing with increases in n, a, and Q_p^0. The grid-plate gain of the driver tube will also increase as n is increased.

It has just been demonstrated that the primary damping cannot be controlled by varying L_p/L_s, the unloaded primary Q, or the relative number of tertiary turns, if the ratio S/P is to be maintained. From Equation (1) it is clear that if the primary damping is to be increased, it must be accompanied by an increase in α, in order to maintain the ratio S/P constant. This increase in α is frequently undesirable, as discussed below.

Consider Equation (2) which gives the value of S. Again if P/S is held constant at approximately unity for optimum a-m rejection, the gain to the secondary increases with increasing values of Q_s, n and α. For values of α between 0.4 and 1.0, S increases rapidly with α, as shown in Figure 19. The implication of this, so far as design for handling maximum downward amplitude modulation is concerned, is that other things being equal, the initial per cent of critical coupling should be approximately 50. This means that as Q_p and Q_s increase with downward modulation, the resultant increase in the per cent of critical coupling will cause the greatest changes in the gain to the secondary.

Fig. 19—Relative amplification from the
driver grid to the secondary as a function
of the per cent of critical coupling, where
the change in the per cent of critical
coupling takes place as a result of
changes in the primary or secondary Q.
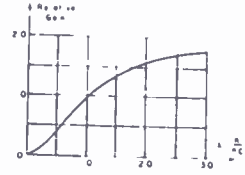
Circuit Impedance Ratio

The ratio detector circuit may be put in the form shown in Figure
20. Normally the input signal voltages e_1 and e_2 will follow the
approximate variation shown in Figure 5. These voltages may be
derived from a phase-shift circuit, from side-tuned circuits, or from
other suitable means. A large number of circuit variations are
possible.

If the circuit is analyzed from an impedance standpoint, it is found
that the rectified voltages are in the same ratio as the input voltages,
provided the circuit impedances z_1 and z_2 are in the same ratio as the
input voltages e_1 and e_2.

This can be demonstrated as follows. The diode currents flow in
short pulses, assuming ideal diodes, and therefore the fundamental
a-c component of each diode current is nearly equal to twice the d-c
component. Since the d-c components are equal, it follows that the
fundamental frequency a-c components will also be equal.

$$i_1 = i_2 = i; \qquad E_1 = k\,(e_1 - iz_1) \qquad \text{and} \qquad E_2 = k\,(e_2 - iz_2)$$

$$\therefore \frac{E_1}{E_2} = \frac{e_1 - iz_1}{e_2 - iz_2} = \frac{e_1\left(1 - i\dfrac{z_1}{e_1}\right)}{e_2\left(1 - i\dfrac{z_2}{e_2}\right)}$$
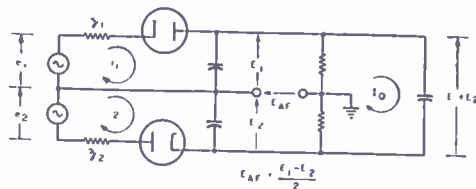
Fig. 20—The ratio-detector circuit in a more general form. The voltages
e_1 and e_2 may be produced in various ways, including the phase-shift circuit
and side-tuned circuits.

$$\frac{E_1}{E_2} = \frac{e_1}{e_2} \qquad \text{provided that} \qquad \frac{z_1}{e_1} = \frac{z_2}{e_2}$$

Since an arbitrary value of direct current was assumed, it follows that if $z_1/e_1 = z_2/e_2$, then E_1/E_2 will equal e_1/e_2 independently of the value of I_0.

If now $E_1 + E_2$ is stabilized, then it is evident that a-m rejection is obtained because E_1 and E_2 remain constant as the input signal amplitude is varied.

If only a fraction of $E_1 + E_2$ is stabilized, then the condition for zero a-m output will depart from the relation $e_1/e_2 = z_1/z_2$.

In the case of the balanced phase-shift circuit, useful relationships between the circuit parameters can be more easily obtained by the methods used in the preceding paragraphs. In other circuit variations, an attack based on the impedance relationships may be expedient.

DESIGN CONSIDERATIONS

In this section the general principles governing the design of a ratio detector are described. These are based on the analysis in the preceding section. Although illustrations and specific discussions of circuit constants are based on a center frequency on the order of 10 megacycles and a peak separation on the order of 350 kilocycles, the principles are quite general and apply at other frequencies.

Diode Characteristics

Good ratio detector performance can be obtained with either high-perveance diodes such as the 6AL5 or medium-perveance diodes such as the 6H6. Diodes having a perveance lower than the 6H6 give less satisfactory performance in the ratio detector because the residual balanced component of amplitude modulation becomes appreciably large. In general, better performance has been obtained with ratio detectors using the 6AL5 than with those using the 6H6.

The circuits used with low and high perveance diodes will differ in the extent to which the rectified output voltage is held constant. They will also differ with respect to the compensation used to minimize the residual unbalanced component of amplitude modulation in the output. This unbalance is the result of the input reactance variation of the diodes exerting a detuning effect on the secondary. The magnitude of this effect tends to be less for low-perveance diodes.

The rectification efficiency and hence the diode circuit loading vary with signal level. For this reason, optimum a-m rejection is obtained

at a particular signal level. Above and below this level, a balanced a-m component is present. As indicated in Figure 12, the magnitude of the residual amplitude modulation is not large except at low levels where the diode perveance is low. The level at which optimum a-m rejection is obtained may be varied by altering the circuit constants, particularly the fraction of the total rectified voltage which is stabilized, or the ratio of secondary and tertiary voltages.

Secondary Inductance

It is desirable to make the secondary inductance-capacitance (L/C) ratio as high as possible, consistent with keeping the secondary tuning capacitance high enough so that stray capacitances and variations in tube capacitances do not have an excessive effect on the tuning. Using a high L/C ratio has the advantage of increasing the sensitivity and at the same time tends to reduce the peak diode currents. At a frequency on the order of ten megacycles these considerations point toward the use of a secondary tuning capacitance on the order of 25 to 75 micromicrofarads. Higher values result in lower sensitivity for the same amount of a-m rejection without any significant advantage as far as stability of tuning and independence of tube replacement are concerned.

The advantage of making the secondary a bifilar winding has been described. If a single center-tapped winding is used instead of a bifilar winding, it is desirable to use a fixed slug to obtain the same coupling between the two halves of the secondary and the primary. Another circuit variation involves the use of two equal fixed condensers across the secondary to obtain an i-f center-tap.

The secondary Q should, in general, be as high as possible, consistent with the desired peak separation. At frequencies on the order of ten megacycles, this will mean a Q on the order of 75 to 150. Use of the higher values of Q will result in improved sensitivity for a given a-m rejection. The peak separation, however, will be lower than if smaller values of secondary Q were used.

Load Resistors

The value R of the diode load resistors will depend on the amount of downward amplitude modulation to be handled which in turn depends upon the i-f selectivity characteristic, the amount of multipath transmission anticipated, and the importance of obtaining the maximum sensitivity. In general, R will be selected so as to reduce the operating secondary Q to a value approximately one-fourth or less of its unloaded value.

The lower the value of R, the greater will be the ratio between the unloaded and loaded values of the secondary Q. This means that when the diode current decreases during downward amplitude modulation, the Q of the secondary is able to rise considerably and to compensate for the decrease in input signal by effectively raising the sensitivity of the detector. The greater the extent to which the Q can rise when the input signal drops, the greater will be the downward modulation capability of the detector. In addition, the value of R affects not only the operating Q of the secondary, but also the operating Q of the primary. As a result of both of these factors, using lower values of load resistance increases the extent to which the signal can drop below its average value without the diodes being biased to cutoff by the stabilizing voltage.

If the i-f passband preceding the ratio-detector driver tube is not flat over a range equal to the maximum frequency swing, the amplitude modulation introduced by this selectivity must be removed by the ratio detector. As a result of this, the more the i-f selectivity characteristic deviates from a relatively flat top, the lower are the load resistance values which must be used.

If it is expected that a receiver using a ratio detector will be used under conditions of multipath reception, it follows that the detector must be capable of removing the amplitude modulation which results from the partial cancellation of the direct signal by the delayed signal which reaches the receiver over a longer path. Experience with multipath reception indicates that it is desirable for the detector to be able to reject more than 50 per cent downward amplitude modulation to reduce distortion as much as possible. Where very severe multipath is encountered, the phase modulation distortion which accompanies it becomes appreciable even if all of the a-m distortion is removed.

Sensitivity is also involved in the choice of load resistors. The greater the value of load resistance R, the greater will be the sensitivity and the less the downward modulation-rejecting capability.

Primary L/C Ratio and Q

The primary L/C ratio should be as large as possible in order to obtain the greatest sensitivity. The limiting factor is the maximum stable gain between the grid and plate of the ratio detector driver tube. When determining this maximum gain, it should be kept in mind that the gain may increase during downward amplitude modulation, particularly on either side of the center frequency.

If the primary Q is high enough so that the operating Q of the primary is determined essentially by the diode loading, the grid-plate

gain will rise to a higher value during the a-m cycle. This increase in grid-plate gain is desirable from the viewpoint of increasing the ability of the detector to reject downward amplitude modulation, so that in practice the primary Q is made as high as possible, consistent with obtaining the required peak separation and not exceeding the maximum allowable grid-plate gain during downward amplitude modulation.

Primary Impedance Variation

During the a-m cycle two opposing effects take place which alter the primary impedance and hence affect the gain between grid and plate of the driver tube. When the input signal falls, for example, the impedance coupled into the primary by the secondary increases because the Q of the secondary rises. This tends to lower the gain from the grid to the plate of the driver tube. On the other hand, the diode loading across the primary decreases and this effect tends to raise the gain from the grid to the plate. From the viewpoint of rejecting the maximum downward amplitude modulation, it is desirable that the circuit parameters be so related that the net change in gain be such as not to result in a decrease in gain to the primary when the signal level falls.

Coupling

The value of coupling used, along with the relative number of turns used in the tertiary winding, is the principal factor in determining the ratio S/P. The importance of maintaining this ratio in the vicinity of unity, and the effect of varying the ratio by changing the coupling, or by any other means, has been described. In general, the coupling should be adjusted to be approximately one-half critical. Since the absolute coefficient of coupling which corresponds to critical coupling is itself dependent upon the load resistance and on the tertiary inductance, the final coupling adjustment must be made after the other parameters are fixed because the per cent of critical coupling is affected by changes in these.

Tertiary Inductance

In the notation used here, the tertiary inductance is specified in terms of the parameter n where the tertiary voltage is equal to $1/n$ times the primary voltage. With a specified value of coupling in mind, usually about 0.5 critical, the number of turns on the tertiary is adjusted so that the required S/P ratio is obtained. If the required S/P ratio is obtained with too few turns on the tertiary so that the

grid-plate gain is high, this condition can be remedied by reducing the primary inductance.

Residual Amplitude Modulation in Output

In general the ratio detector will not completely reject all of the applied amplitude modulation. Where the effect of the applied amplitude modulation is to cause the slope of the detector characteristic to vary, the output of the detector will appear as shown in Figure 21. The output amplitude modulation may be either in phase with the applied modulation, or out of phase, i.e., the slope of the detector characteristic may either increase or decrease slightly with increasing values of input signal, depending upon the circuit constants and the signal level. Where the output characteristic appears as shown in Figure 21, when simultaneous amplitude and frequency modulation are applied, the output is said to be balanced in that, just as in the
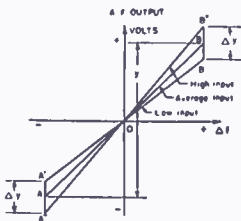
Fig. 21—Effect of amplitude modulation on the output of a balanced detector. If $100M = \%$ amplitude modulation of the input signal, then $\triangle y = yM$, and $\triangle y/y = M$. This is referred to as a balanced a-m component.
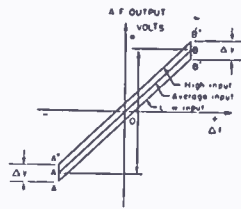
Fig. 22—Effect on the output of a balanced detector when amplitude modulation causes a detuning of the secondary. This is referred to as an unbalanced a-m component.

balanced discriminator, there is a center frequency at which the output is insensitive to applied amplitude modulation. With proper design, the amplitude modulation in the output, as indicated by the slope variation in Figure 21, will be very much less than the amplitude modulation in the input signal. This is indicated by the oscillograms in Figure 12.

The output of a ratio detector will not appear completely balanced as shown in Figure 21, unless the circuit is compensated to remove amplitude variations which result from the fact that the effective input capacitance of the diodes varies with the average diode current and therefore varies during the a-m cycle. The detector output characteristic in Figure 22 shows the output characteristic which is obtained when an unbalance is present in the circuit; this may be due not only to variations in the input capacitance of the diodes, but

Fig. 23—When unbalance is present, the effect is to cause the crossover or point of zero a-m response to be at other than the center frequency. This type of characteristic has both a balanced component of a-m (Figure 21) and an unbalanced component (Figure 22).
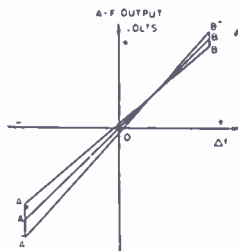
may also be due to unbalance in the transformer, diodes, or circuit constants.

Where the output of a detector contains both balanced and unbalanced components, it will appear in general as shown in Figure 23. As would be expected, the effect of the unbalance is to shift the crossover from the center frequency.

Reducing Residual Amplitude Modulation

It is convenient to consider separately the means for reducing the residual balanced component and the residual unbalanced component of amplitude modulation in the output. Basically, the magnitude of the balanced component depends upon the ratio S/P at the mean carrier level. This may be visualized if the effect of a change in the secondary Q on the ratio E_1/E_2 in Figure 4 is considered; not only does the secondary Q and hence the phase angle of the secondary current change with diode loading during the a-m cycle, but the relative amplitudes of the primary and secondary voltages also change. There is thus a complex relationship which governs the extent to which E_1/E_2 is independent of diode loading, and this relationship is clearly a function of S/P. Thus, it is to be expected, as shown in Figure 24, that there should exist an optimum value of S/P for which E_1/E_2 is

(a) $\frac{S}{P}$ < OPTIMUM   (b) $\frac{S}{P}$ = OPTIMUM   (c) $\frac{S}{P}$ > OPTIMUM
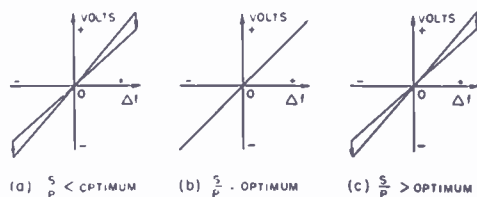
Fig. 24—On either side of the optimum value of S/P for which the balanced component of a-m is zero, there is a reversal in the phase of the a-m in the output. Since, for a given transformer, the value of S/P changes with coupling, the figure shows that for a loose coupling the output is 180 degrees out of phase with the input a-m, while the two are in phase for close coupling.

independent of diode loading and hence for which the balanced component of amplitude modulation in the output is a minimum. It will be noted in Figure 24 that the phase of the output amplitude modulation with respect to the input amplitude modulation undergoes a 180-degree reversal at the critical value of S/P. Since the principal effect of varying the coupling is to change the ratio S/P, Figure 24 also shows that for a given set of circuit constants, there exists a particular value of coupling for which the balanced component of amplitude modulation is zero.

Reducing Unbalanced A-M Component

The residual unbalanced component in the output may be reduced by several different means. The ratio detector circuit shown in Figure 8 contains two methods for reducing the unbalanced component. One of these consists of making the two resistors R_3 and R_4 unequal. By this means, it is possible to cancel the existing unbalance. This cancellation takes place because the differential drop across these resistors, which varies with a-m modulation, feeds into the a-f output. In practice, R_3 and R_4 are adjusted so that the unbalanced component as observed when frequency and amplitude modulation are applied simultaneously, goes to zero. During this adjustment the sum of R_3 and R_4 remains essentially constant since this sum depends upon the ratio S/P rather than upon any unbalance which may be present. In addition, a resistor R_5 is used in series with the tertiary winding common to both diode circuits. This modifies the peak diode currents and, particularly at high signal levels, has the effect of appreciably reducing the unbalanced a-m component.

Another method which may be used to reduce the unbalanced component is to use diode load condensers which have appreciable reactance at the intermediate frequency. At 10 megacycles, the values of load capacitance which are effective will range from about 50 micromicrofarads to several hundred micromicrofarads. In general, the greater the perveance of the diodes used in the ratio detector, the smaller will be the value of diode load capacitance which is required to eliminate the unbalanced component.

Still another method for reducing the unbalanced component is to vary the effective center-tap on the secondary winding slightly from the nominal center position.

Single-ended or Unbalanced Circuit

All of the circuits which have been described thus far have been of the balanced type, with the a-f take-off point at ground potential

when the input signal is applied at the center frequency. It is possible, however, to ground one side of the rectified output, as shown in Figure 25. In this case, the voltage available for a-v-c purposes is twice as great as in the balanced circuit case. There is no change in the a-f output.

Where only one diode load condenser is used, as in Figure 25(b), its capacitance should be twice as large as that used in Figure 25(a). This follows because in (a) the two condensers are effectively in parallel at the intermediate frequency, while in (b) since there is only one condenser its value must be twice as great. This relationship is of particular interest where the unbalanced a-m component is reduced by using a critical value for the diode load capacitance, as previously described.

In connection with unbalanced circuits, it may be noted for the circuit shown in Figure 8, it is not necessary that the center of the
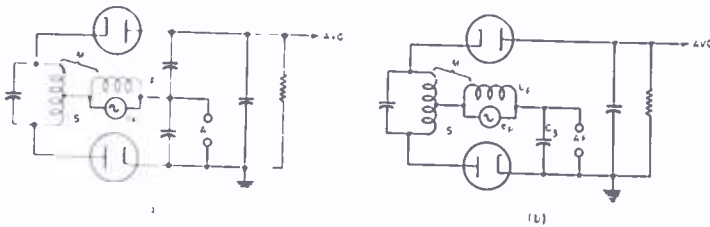
Fig. 25—Either one or two diode load condensers may be used in the ratio-detector load circuit. To obtain the same effective diode load capacitance in (b) as in (a), C_3 must be equal to the sum of C_1 and C_2.

load resistor be grounded; the a-m rejection will be essentially the same if any point along the load resistor bypassed by the stabilizing condenser is grounded. This statement is not true, however, at frequencies which are so low that the stabilizing condenser does not effectively hold the voltage across its terminals constant.

Time Constant of Stabilizing Voltage

At low audio frequencies, the a-m rejection of the ratio detector depends upon the time constant of the stabilized rectified voltage. The same considerations which determine the time constant in an a-v-c circuit can also be applied to the determination of the time constant of the stabilizing voltage. In general, the discharge time constant of the stabilizing voltage, formed by the load resistance and the stabilizing capacitance should be about 0.2 second. Time constants larger than this have an undesirable effect on the tuning characteristic which is similar to the effect of too long a time constant in the a-v-c circuit of a receiver.

The manner in which the a-m rejection of a ratio detector varies with the frequency of the amplitude modulation is shown in Figure 26. This detector (see Figure 8) has a time constant of 0.1 second. The characteristics apply (a) to a balanced detector with the center of the load resistor grounded and (b) to the unbalanced form of the circuit which is the same as Figure 8, but with one end of the stabilizing condenser grounded. It should be noted that for the same time constant, the balanced circuit gives much better rejection of low audio frequencies. This is to be expected because in the case of the balanced circuit, fluctuations in the stabilizing voltage do not cause any disturbance in the output, whereas in the case of the unbalanced
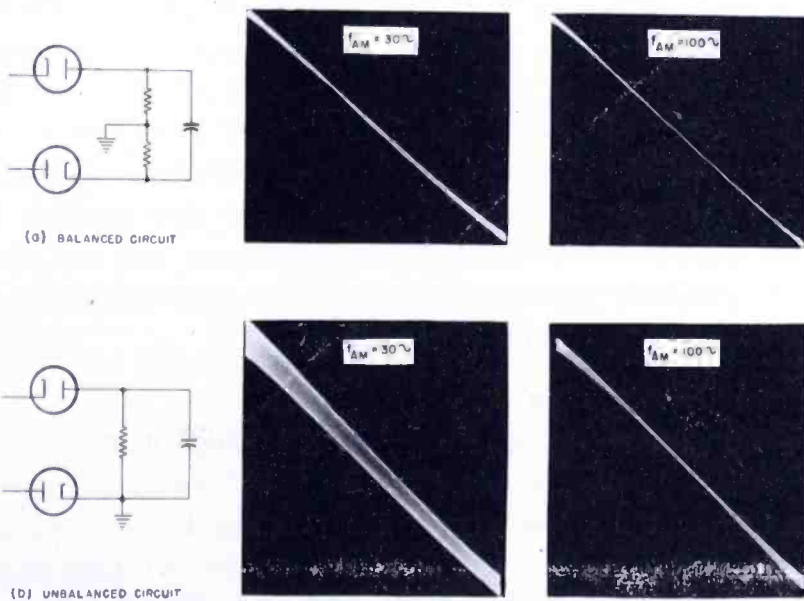
Fig. 26—A comparison of balanced and unbalanced circuits with respect to their effectiveness in rejecting low-frequency amplitude modulation. The time constant of the load circuit is the same for both.

circuit they do contribute to the output. For a given value of time constant in the stabilizing voltage, then, it follows that the balanced circuit will give better rejection of low-frequency amplitude fluctuations.

Tolerances

In general, the ratio detector circuit will require more attention to tolerances than is necessary for a balanced discriminator. The principal factor which must be controlled closely is the effective coupling between the primary and secondary winding, since this controls the ratio between the secondary and tertiary voltages, which in turn affects the a-m rejection. This coupling is determined not only

by the separation between the primary and secondary, but also by the capacitance unbalance from either end of the secondary to ground.

The ratio detector is essentially a balanced circuit and from its method of operation it is evident that the degree of a-m rejection will depend upon the two diodes having substantially the same characteristics. If the diodes differ materially from each other, the principal effect will be the production of an unbalanced a-m component in the output. The effect on the peak separation and f-m sensitivity is usually negligible. If the detector is tested with an f-m signal which is also amplitude modulated, so that oscillograms similar to those in Figure 12 are obtained, unbalanced diodes will have the effect of broadening the output characteristic which is indicative of an unbalanced a-m component in the output.

MEASUREMENTS

The measurements necessary in the design of a ratio detector and in checking its performance are described in this section. These include the unloaded and loaded values of primary and secondary Q, the per cent critical coupling, the ratio of the secondary and tertiary voltages, and amplitude modulation rejection.

Primary and Secondary Q's

To measure the unloaded primary Q, the double diode is removed from its socket and the secondary is detuned. The primary Q is then determined from the selectivity of the primary tuned circuit. The loaded primary Q is measured in the same way but with the diodes in the circuit so that the normal diode loading is reflected across the primary through the tertiary winding.

To measure the secondary Q, the primary winding is heavily loaded by shunting a resistance across it. The secondary Q is then determined from the selectivity of the secondary winding as indicated by the rectified voltage variation with frequency. When measuring the unloaded secondary Q, the diode load resistance should be replaced with high values of resistance, on the order of a megohm. When measuring the loaded secondary Q, the normal load resistors should be used. For these measurements the centertap of the secondary should be disconnected from the high side of the tertiary winding, so as to prevent the tertiary voltage from contributing to the rectified voltage.

Coupling

The per cent of critical coupling can be measured by noting the

change in primary voltage as the secondary is varied from a tuned to a detuned condition. With all circuit conditions normal, and the signal applied at the center frequency, the primary voltage is noted. With the same input signal level, the secondary is detuned so that the primary voltage rises. The per cent critical coupling can then be expressed in terms of the ratio between the primary voltage with the secondary tuned and detuned. For example, if the signal at the plate rises 25 per cent when the secondary is detuned, the coupling is 50 per cent of critical.

Ratio S/P

The ratio between the secondary and tertiary voltages can be measured indirectly in terms of the rectified output voltage which is obtained (a) with the secondary tuned and (b) with the secondary detuned. In both cases the input signal is adjusted so that the primary voltage remains constant. If the ratio between the voltages read in (a) and (b) is r, that is, if

$$\frac{\text{Rectified voltage (secondary tuned)}}{\text{Rectified voltage (secondary detuned)}} = \frac{\sqrt{P^2 + S^2}}{P} = r$$

then

$$\frac{S}{P} = \sqrt{r^2 - 1}$$

Signal Generator

In checking the performance of ratio detectors it is convenient to have available a signal generator which is capable of being simultaneously frequency and amplitude modulated. The advantage of using this type of modulation is that it provides graphically a complete picture (Figure 12, for example) of the f-m response of the detector and at the same time shows the a-m rejection under dynamic conditions at every frequency within the range of the detector.

It is important that the signal generator used to check ratio detectors be free of spurious modulation. In particular, it is essential that when the signal generator is amplitude modulated, no frequency modulation be produced as a result of the amplitude modulation. If frequency modulation takes place when the generator is amplitude modulated, the resultant output will be construed as being due to faulty a-m rejection whereas it is actually the normal f-m response of the detector.

Alignment Procedure

The ratio detector may be aligned by using either an unmodulated signal at the center frequency and a d-c vacuum-tube voltmeter, or by using an f-m signal generator and an oscilloscope.

If an unmodulated signal generator is used, the procedure is to set the signal generator to the center frequency. With the d-c vacuum-tube voltmeter connected to measure the rectified output voltage (this is usually at the a-v-c take-off point), the primary tuning is adjusted for maximum voltage.

The procedure used for adjusting the secondary tuning depends upon whether the center-tap of the stabilizing voltage is grounded or whether one end is grounded. If the center-tap is grounded, the secondary tuning is adjusted so that the d-c voltage at the audio take-off point is equal to zero; the d-c vacuum-tube voltmeter is shifted to the audio take-off point for this measurement. If the stabilizing voltage is grounded at one end (see Figure 25) rather than at the center, the secondary tuning is adjusted so that the d-c voltage at the audio take-off point is equal to half the rectified voltage.

If sweep alignment is used, the primary can be accurately aligned by using a comparatively low deviation and adjusting it for maximum amplitude on the screen. The secondary may be adjusted by using a deviation such that the total frequency swing (twice the deviation) is equal to the peak separation. This procedure makes it possible to adjust the secondary tuning so that a symmetrical detector characteristic is obtained.

Peak Separation

The separation between the peaks on the f-m output characteristics of a ratio detector may be measured most simply by applying an f-m signal and increasing the deviation until the response is just observed to flatten at the peaks. When this is done, the peak separation is equal to twice the deviation.

If an attempt is made to measure the peak separation by plotting the output characteristic point by point, the peak separation obtained will usually be considerably less than is obtained under dynamic conditions with the output voltage stabilized. The f-m detector characteristic may be plotted point by point provided a battery of the proper voltage is connected across the stabilizing condenser. The voltage of this battery must be equal to the rectified voltage which exists at the center frequency. In practice it is convenient to use a 7.5-volt C-battery and to adjust the signal input so that the condenser-stabilized voltage at the center frequency is equal to the battery voltage.

Measurement of A-M Rejection

The measurement of a-m rejection can be carried out by means of a signal generator which can be simultaneously frequency and amplitude modulated. The type of pattern obtained when there are residual balanced and unbalanced components of amplitude modulation in the output has been described in connection with Figure 23. Typical oscillograms are shown in Figure 12.

The measurement of the a-m rejection of a ratio detector can be described in terms of the pattern obtained for a given frequency deviation, i.e., for a given per cent of frequency modulation, and for a given per cent of amplitude modulation. Ideally the pattern obtained should remain a diagonal line regardless of the presence of the amplitude modulation. The extent to which this pattern departs from a straight line indicates to what extent the detector fails to reject amplitude modulation. While it would be desirable to be able to quote a single figure of merit to indicate the a-m rejection, it is essential to check the performance at various levels and to interpret the wedge-shaped patterns which are obtained so as to determine the extent of the residual balanced and unbalanced components of amplitude modulation in the output.

In addition to the method of using a signal which is simultaneously frequency and amplitude modulated, it is possible to make a-m rejection measurements by using a generator which is only frequency modulated. To measure a-m rejection using this method, an f-m signal is applied at full deviation corresponding to 100 per cent modulation, and a battery equal in value to the rectified output is shunted across the stabilizing condenser. This battery will have negligible effect on the f-m output. Now the input signal is reduced in value until the f-m output becomes distorted as a result of the diodes being biased by the stabilizing voltage, and the f-m output drops to zero. The ratio between the initial input signal and the minimum input signal for which the f-m output becomes distorted is then a measure of the amount of downward modulation that the detector can reject. For example, if this ratio is r, then the per cent downward modulation which can be handled is $100 \ (r-1)/r$. The performance of a typical ratio detector as measured by this method has been shown in Figure 11. To determine the rejection of the detector for upward amplitude modulation, the same setup is used, and the change in the output is noted as the input signal is increased.

Since the amplitude of the input signal is not varied dynamically, this method will not indicate any unbalanced component which may

be present in the output. The latter is more conveniently measured by using simultaneous frequency and amplitude modulation as previously described.

APPENDIX

Formulas for S/P and S

The fundamental circuit under consideration is shown below in (a).

(a)   (b)
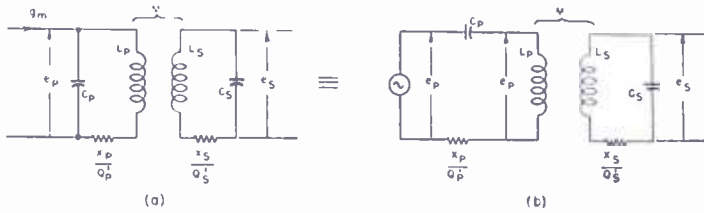
By Thévenin's theorem it is equivalent to (b), where

$$e_p{}^1 = i X_p = g_m X_p$$

At the center frequency,

$$i_p = \frac{e_p{}^1}{\dfrac{X_p}{Q_p{}^1} + \dfrac{\omega^2 M^2 Q_s{}^1}{X_s}}$$

But $\omega^2 M^2 = K^2 X_p X_s = \dfrac{K^2}{K_c{}^2} K_c{}^2 X_p X_s$

$$\omega^2 M^2 = \alpha^2 \frac{X_p X_s}{Q_p{}^1 Q_s{}^1}$$

$$\therefore i_p = \frac{g_m X_p}{\dfrac{X_p}{Q_p{}^1} + \alpha^2 \dfrac{X_p}{Q_p{}^1}}$$

$$i_p = \frac{g_m Q_p{}^1}{1 + \alpha^2}$$

$$e_s{}^1 = \omega M i_p$$

$$e_s^1 = \alpha \sqrt{\frac{X_p X_s}{Q_p^1 Q_s^1}} \frac{g_m Q_p^1}{1 + \alpha^2}$$

$$e_s = Q_s^1 e_s^1$$

$$e_s = g_m \sqrt{X_p X_s} \sqrt{Q_p^1 Q_s^1} \cdot \frac{\alpha}{1 + \alpha^2}$$

$$e_p = i_p X_p = \frac{g_m Q_p^1 X_p}{1 + \alpha^2}$$

$$\therefore \frac{e_s}{e_p} = \alpha \sqrt{\frac{X_s Q_s^1}{X_p Q_p^1}}$$

To find Q_p^1, the operating Q of the primary, refer to Figure 14.

$$Q_p^1 = \frac{Q_p^0 \cdot \dfrac{n^2 R}{4}}{Q_p^0 X_p + \dfrac{n^2 R}{4}}$$

$$Q_p^1 = \frac{n^2 R}{4a \cdot \dfrac{X_p}{a}} \cdot \frac{1}{1 + \dfrac{n^2 R}{4a Q_p^0 \cdot \dfrac{X_p}{a}}} \qquad \text{where } a = \frac{X_p}{X_s}$$

$$Q_p^1 = \frac{n^2 Q_s^1}{4a} \cdot \frac{1}{1 + \dfrac{n^2 Q_s^1}{4a Q_p^0}}$$

$$\therefore \frac{e_s}{e_p} = \alpha \left\{ \frac{L_s}{a L_s} \cdot \frac{4a}{n^2} \left(1 + \frac{n^2 Q_s^1}{4a Q_p^0} \right) \right\}^{\frac{1}{2}}$$

Since $S = \dfrac{e_s}{2}$ and $P = \dfrac{e_p}{n}$

$$\frac{S}{P} = \alpha \sqrt{1 + \frac{n^2 Q_s^1}{4a Q_p^0}}$$

To find S, substitute in the expression for e_s

$$S = \frac{g_m}{2} \left\{ a X_s \cdot X_s \frac{n^2 Q_s^1}{4a} \cdot \frac{1}{1 + \frac{n^2 Q_s^1}{4a Q_p^0}} \right\}^{\frac{1}{2}} \frac{\alpha}{1 + \alpha^2}$$

$$= \frac{g_m X_s Q_s^1 n}{4} \cdot \frac{1}{\sqrt{1 + \frac{n^2 Q_s^{11}}{4a Q_p^0}}} \cdot \frac{\alpha}{1 + \alpha^2}$$

But $\dfrac{S}{P} = \alpha \sqrt{1 + \dfrac{n^2 Q_s^1}{4a Q_p^0}}$

$$\therefore S = \frac{g_m X_s Q_s^1 n}{4} \left(\frac{P}{S} \right) \frac{\alpha^2}{1 + \alpha^2}$$

NEW TECHNIQUES IN SYNCHRONIZING-SIGNAL GENERATORS*†

By

Earl Schoenfeld, William Brown, and William Milwitt

Industry Service Laboratory, RCA Laboratories Division,
New York, N. Y.

Summary—A generator of synchronizing and blanking signals has been developed in which the important pulse edges are established by means of a "stop watch", consisting of a terminated artificial transmission line carrying brief 31.5-kilocycle trigger impulses. The number of equalizing and vertical-synchronizing pulses appearing during each framing interval is determined by an electronic counter. The locked-in relationship between line and field scanning frequencies makes use of the cascaded-binary type of frequency divider wherein the divisor is established by the circuit connections rather than the value of a circuit element. The resulting apparatus lacks most of the screwdriver adjustments which usually have been associated with equipment of its type.

INTRODUCTION

APPARATUS for generating, monitoring, and utilizing television signals has been described by various writers before the start of World War II. Since then, events have occurred which indicate the desirability of a new approach to that part of the equipment which generates synchronizing and blanking signals. First, the formulation of more nearly complete specifications of the television signal[1] has been announced. Second, the appearance of automatic-frequency-control circuits for receiver scanning has underlined the importance of extremely close tolerance in the phase constancy of synchronizing-signal leading edges. Third, war-born developments have indicated the desirability of replacing circuits containing adjustable elements with others in which passive elements or stable electronic circuits can establish a phase for a leading edge or a pulse time duration without reference to a continuously variable element; i.e., screwdriver adjustment.

In the light of the above requirements, new techniques for obtaining synchronizing and blanking signals have been devised. The desired

---

* Decimal Classification: R583.13.
† Presented before the New York Section of the I.R.E. on May 7, 1946.
[1] FCC Proposed Standard Television Synchronizing Waveform, Appendix I.

pulses are generated in circuits triggered by a selection of impulses whose timings are established by an artificial transmission line.

To avoid confusion in the following text, the term "pulses" is reserved for the desired output signals generated by the apparatus. The much briefer signals used to trigger component circuits are called "pips".
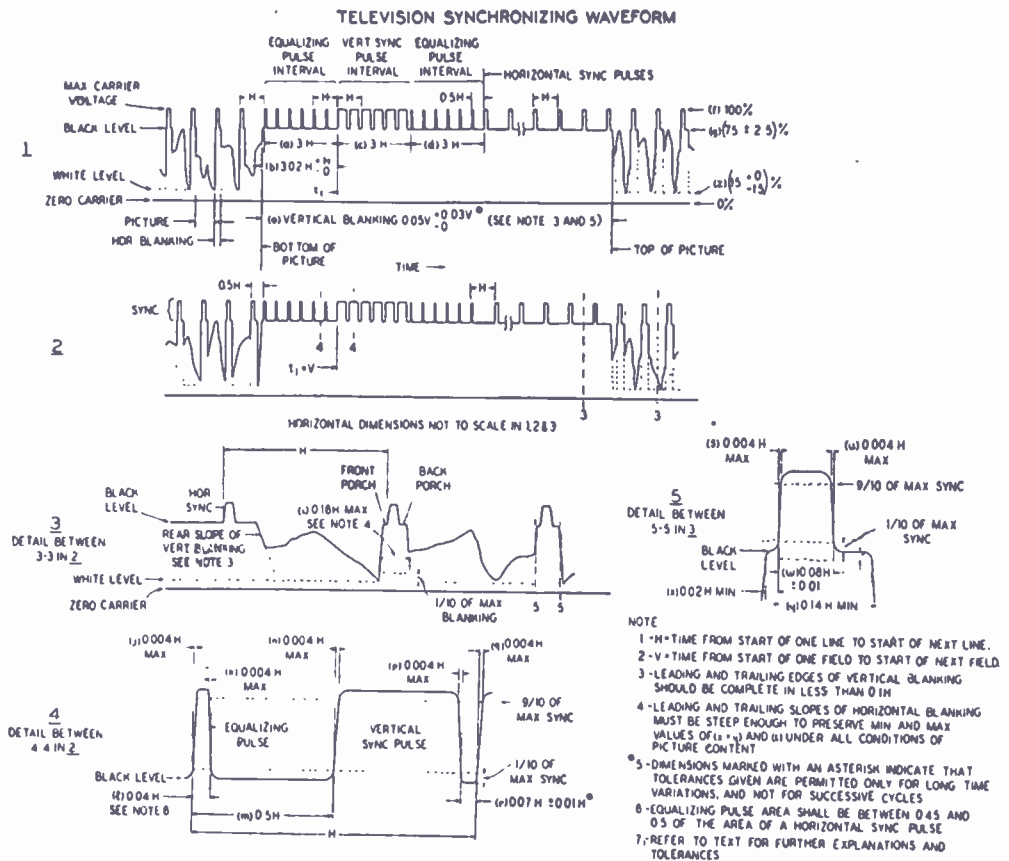
Fig. 1—FCC proposed standard television synchronizing waveform.

I. THE TIMER

The waveform of the 525-line interlaced television signals used in the United States is shown in Figure 1. Most generators of synchronizing and blanking signals which adhere to these standards develop as an intermediate step a 31,500-cycle (twice line frequency) wave. In addition they utilize a 60-cycle pulse whose frequency is synchronized with 1/525th that of the 31,500-cycle wave. It is the function of the "timer" to maintain this relationship.

A casual consideration of this problem might indicate a choice of two principles of timer operation. In the first, the 60-cycle pulse is

derived from the 31,500-cycle wave by the use of a frequency divider. In the second, the 31,500-cycle wave would be derived from the 60-cycle pulse by means of a frequency multiplier. Previous writers[2] have explained why only the first of these principles is successful.

Heretofore it has been considered desirable (although not essential) that the 60-cycle timer output be synchronized accurately with the main power system of the community being served by the transmitter. The prospect of nationwide network broadcasting will detract from the advantages of such power-system synchronization, since portions of the audience will obtain power from unsynchronized sources. Receivers intended for general sale should be sufficiently free from the objectionable effects of inadequately-filtered power supplies and stray alternating-current fields to perform satisfactorily under these conditions. If the receivers which will be sold to the public have this quality, there would remain but little reason for the continuation of "locked-in" operation by the transmitter, and advantages to be gained by other methods could be considered.

Control of synchronizing-pulse frequency from a highly stable oscillator has appealed to some engineers. The resulting freedom from the effects of power-systems phase variations would open new avenues for the development of inexpensive automatic-frequency-control scanning circuits for receivers. The present apparatus offers a choice of either locked-in or crystal control operation.

After considering several applicable frequency dividers, the triggered cascade binary[3] type was selected. This choice was based on its superior stability. Normal variations in resistance, capacitance, and tube characteristics are insufficient to affect the operation of the cascade binary divider. This results from the fact that the order of division is determined by the choice of circuit, and unlike most other dividers, may not normally be varied by manipulation of a circuit parameter. This divider is, therefore, devoid of controls to adjust the order of division.

II. SYNCHRONIZING-SIGNAL GENERATOR

The synchronizing signals are identified as the portion of Figure 1 extending above the blanking pedestals. If the synchronizing signals are viewed alone on an oscilloscope with linear horizontal deflection

---

[2] A. V. Bedford and J. P. Smith, "A Precision Television Synchronizing Signal Generator", *RCA REVIEW*, Vol. V, No. 1, pp. 51-68, July, 1940.

[3] I. E. Grosdoff, "Electronic Counters", *RCA REVIEW*, Vol. VII, No. 3, pp. 438-447, September, 1946.
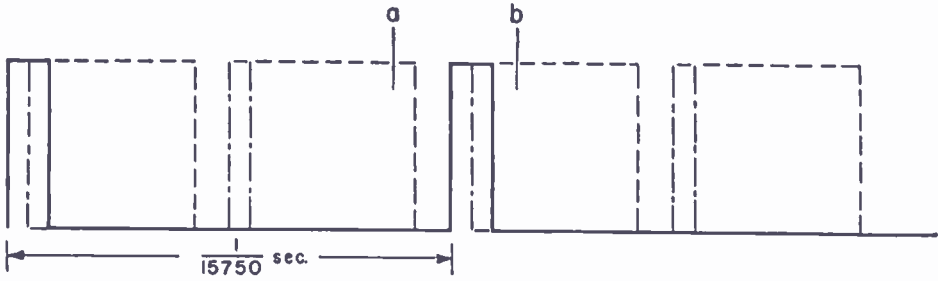
Fig. 2—Oscillogram of synchronizing signal.

at one-half line frequency (7875 cycles), the pattern of Figure 2 would be seen. The horizontal-synchronizing pulses would be delineated by a brilliant trace, while the less-frequently-swept equalizing and vertical-synchronizing pulses would be discerned as barely-visible lines.

If the interval a-b is examined, as in Figure 3, it is seen that all of the leading and trailing pulse edges occur within an elapsed time of less than 10 microseconds.

The "stop watch" which determines these four critical times (as well as others) is a terminated artificial transmission line of approximately 10 microseconds electrical length, through which pass sharp 31.5-kilocycle pips to the terminating resistor, with but negligible attenuation or distortion. By making taps at appropriate points along this line, several phases of pip voltages are obtained, each phase being determined precisely and stably by the amount of preceding delay line. A selection of these pips, serving as triggers, establish leading and trailing edges for all synchronizing pulses.
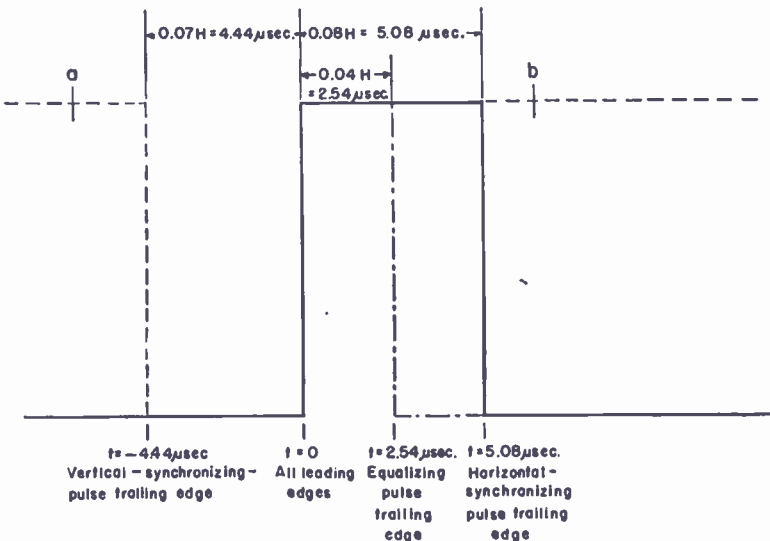
Fig. 3—Enlargement of section a-b of Figure 2.

Fig. 4—Preliminary form of kinescope-synchronizing signals.
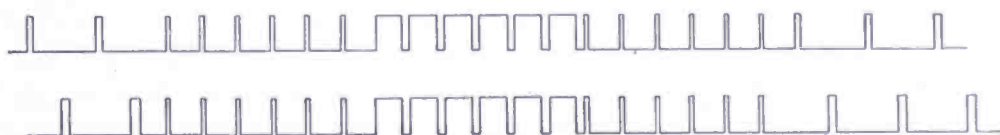
Fig. 5—Kinescope synchronizing signals.

The kinescope-synchronizing signals are generated first in the preliminary form of Figure 4, where they have the prescribed number of equalizing and vertical-synchronizing pulses, but twice too many horizontal pulses. The unwanted horizontal-synchronizing pulses are then deleted, leaving the desired wave of Figure 5.

The first step, generation of the preliminary waveform of Figure 4, is performed with the triggered multivibrator MV-5 of Figure 6. The behavior of the two-tube circuit of MV-5 is such that pips introduced at the leading edge trigger terminal cause the transfer of conduction current only from the first tube to the second. Similarly pips appearing at the trailing-edge terminal can only cause the restoration of conduction from the second tube back to the first.

The leading-edge trigger terminal is supplied with the 31.5-kilocycle
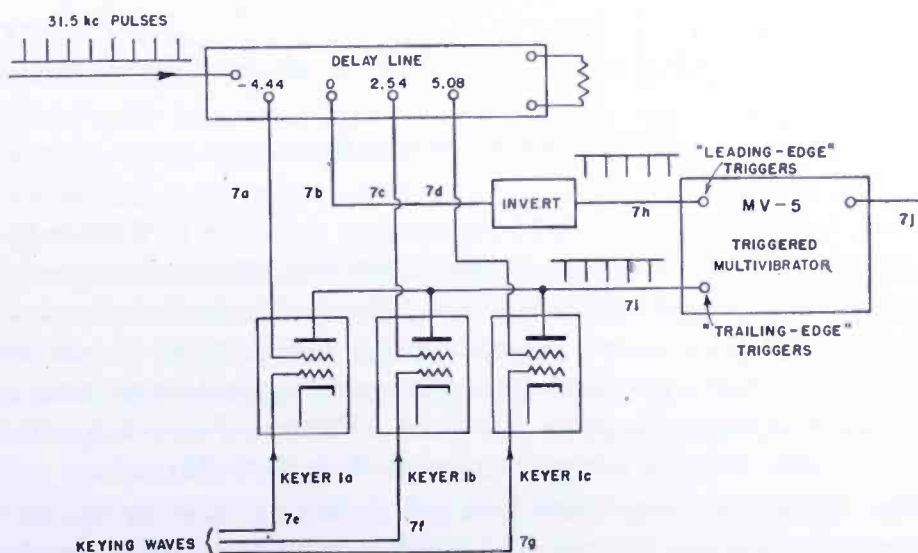
Fig. 6—Block diagram of multivibrator MV-5 and trigger generator.

pips of constant phase shown in Figure 7(h). The trailing-edge trig-
ger terminal is fed with the pips of Figure 7(i), whose phase (or
timing) is successively varied among three fixed values. These cor-
respond with the trailing edges of the desired horizontal, equalizing,
and vertical-synchronizing pulses.

Figure 6 shows how the trigger pips are selected. The delay-line
taps are labelled in terms of microseconds delay from the "O" tap,
whose pips establish the leading edges. Following taps then supply
pips with positive delays, and preceding taps with negative. The
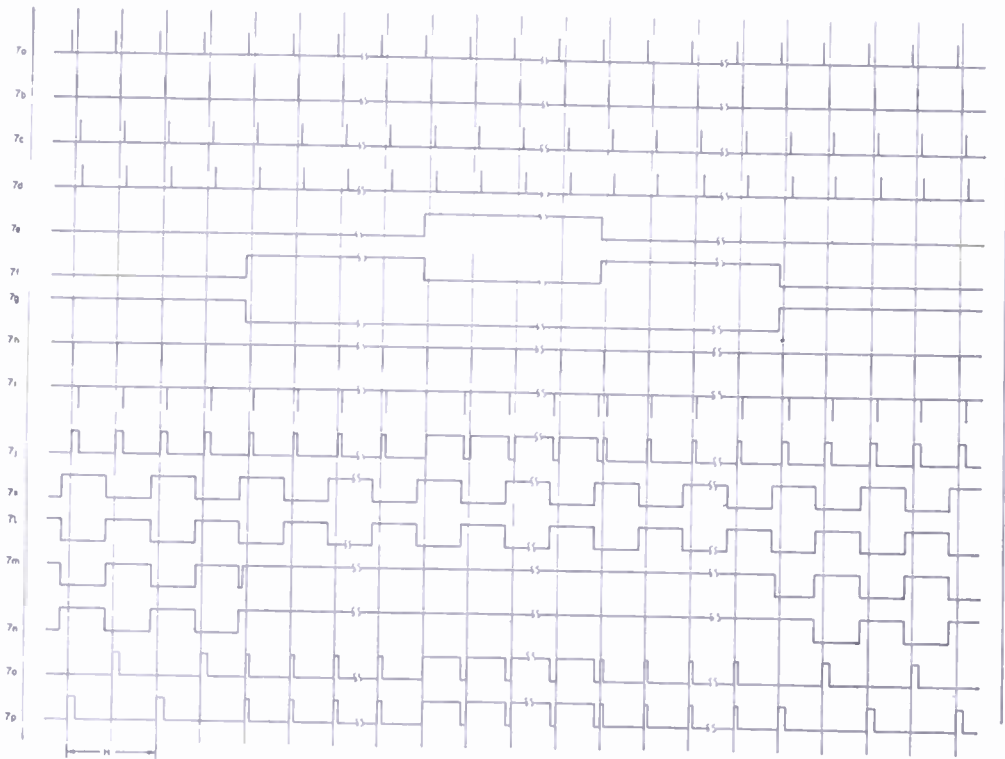
Fig. 7—Shaper voltage waves.

interval, 4.44 microseconds, between the first two taps is 7 per cent of
H, and corresponds with the serration between two vertical-synchro-
nizing pulses. The intervals, 2.54 and 5.08 microseconds, between the
second and third taps, and the second and fourth taps, respectively,
are 4 per cent and 8 per cent of H, corresponding with equalizing and
horizontal-synchronizing-pulse durations. Figures 7(a), 7(b), 7(c),
and 7(d) show relative phases of pips at these four line taps.

The "O"-phase pips, after polarity inversion, are as shown in
Figure 7(h) and are impressed on the leading-edge trigger terminal
of MV-5. They thereby establish a leading edge of invariant phase

for all kinescope-synchronizing pulses, horizontal, equalizing, and vertical.

The -4.44, 2.54, and 5.08 pip phases are sequentially keyed in by keyers 1a, 1b, and 1c, at whose common plate load appear the pips of Figure 7(i). These, introduced at the trailing-edge trigger terminal of MV-5, determine trailing edges for the pulses generated.

The keyers in Figure 6 require the keying waves of Figures 7(e), 7(f), and 7(g). The generation of similar waves for other pulse generators has been described by previous writers.[2] A study of Figure 7(i) will show that the principles of this pulse generator require accurate timing of the keying-wave edges. For instance, at the end of the vertical-synchronizing-pulse interval, the keying-wave trailing edge of Figure 7(e) must not occur too soon or it will exclude the last
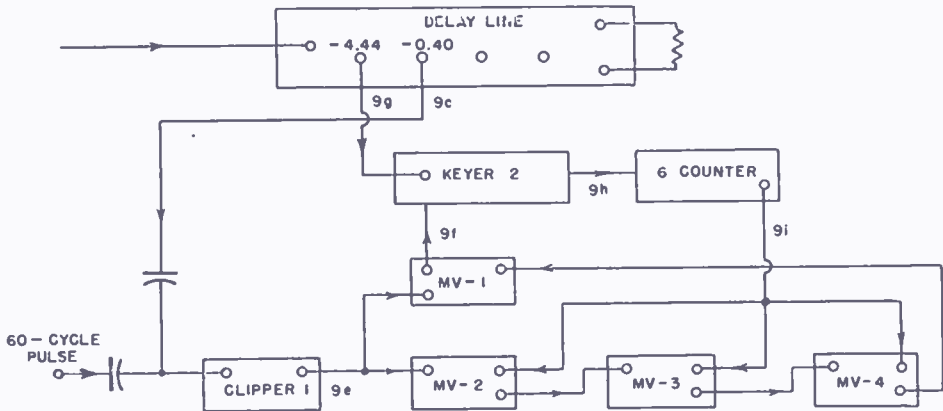
Fig. 8—Block diagram of keying-wave generator.

-4.44 pip which triggers off the sixth vertical-synchronizing pulse. On the other hand the second leading edge of Figure 7(f) (occurring simultaneously with the trailing edge of 7(e)) must take place within the ensuing 6.98 microseconds ($4.44 + 2.54$) to assure triggering off the equalizing pulse which follows immediately the vertical-synchronizing period.

A means for generating these waves with the necessary precision has been developed and is shown in the block diagram of Figure 8. Durations of the three significant intervals comprising the framing period are determined by an electronic counter, counting off six of the 31.5-kilocycle pips per interval. The operational details of this circuit section are explained with reference to Figures 8 and 9.

The elements MV-1, MV-2, MV-3 and MV-4 are triggered multivibrators (flip-flop circuits). MV-2 is flipped during the preceding equalizing-pulse interval (t_1-t_2, Figure 9(j)). MV-3 is flipped during

the vertical-synchronizing-pulse interval (t_2-t_3, Figure 9(k)). MV-4 is flipped during the succeeding-equalizing-pulse interval (t_3-t_4, Figure 9(l)). MV-1 is flipped during the interval (t_1-t_4, Figure 9(f)) which embraces the three above mentioned intervals.

Figure 9(a) shows a rectangular 60-cycle pulse obtained from the timer. A differentiation produces the wave of Figure 9(b) which, when combined with the pips of Figure 9(c), yields the wave of Figure 9(d). One of these pips is seen to rise to a higher positive voltage than the others, enabling Clipper 1 of Figure 8 to select only this one pip at its output. This triggers MV-1 and MV-2, thereby establishing t_1.

Pips of suitable phase, Figure 9(g), are fed to one grid of Keyer 2. The wave of Figure 9(f) from MV-1 goes to the other grid, so that
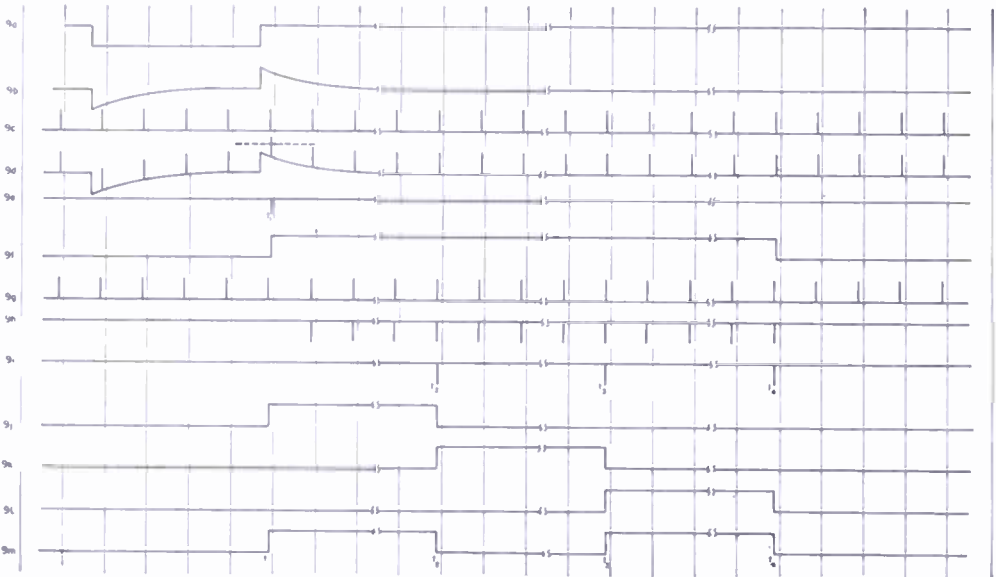
Fig. 9—Voltage waves in keying-wave generator.

only the 18 pips of Figure 9(h) pass through Keyer 2 to the 6-counter input. The 6 counter produces an output pip coincident with each 6th input pip, and thereby establishes t_2, t_3, and t_4, as shown in Figure 9(i).

The three trigger pips generated by the 6 counter are introduced to MV-2, MV-3, and MV-4. Just before the occurrence of each pip, one of the foregoing multivibrators will be found to have its conduction in the normally-cut-off triode. The trigger pip causes this one multi-vibrator to restore its conduction to the normally-on triode.

At time t_2 the restoration of current in MV-2 produces a trigger which results in conduction transfer in MV-3. Similarly at time t_3 the restoration of current in MV-3 triggers the conduction transfer in MV-4. At t_4 the trigger released by current restoration in MV-4

causes restoration to occur also in MV-1. This stops the passage of pips through Keyer 2 to the 6 counter.

The circuits of Figure 8 have then completed the cycle of events for one field, and remain dormant until the time t_1 of succeeding field.

The period t_1 to t_4 is seen to contain 18 half-line intervals, following each of which a pip is led to the 6-counter input. Since the 6 counter must count off these 18 intervals in terms of pips to establish the t_1-t_4 period, it is important that no pip should get through Keyer 2 at the *start* of the first interval. This is precluded by selecting the phase of the Figure 9(c) pips, which establish t_1, to be slightly later than that of the Figure 9(g) pips, which energize the 6 counter.

Both counter-type and cascade-binary frequency dividers have been used successfully for the 6 counter. The cascade binary divider chosen for this apparatus is similar to that of the timer section. The 6 counter has the additional feature of an asymmetry which insures that during the time immediately preceding t_1, tube current will flow in the triodes intended to be normally conducting, so that counter elements will be polarized properly when the framing cycle starts at t_1.

Deletion of Unwanted Horizontal-Synchronizing Pulses

An Eccles-Jordan trigger circuit is triggered from the 31.5-kilocycle pips, thereby producing a 15.75-kilocycle square wave. This voltage, shown in Figures 7(k) and 7(l) for successive fields, is mixed with the plate voltage of MV-1 (Figure 7(g)) in a multigrid tube, whose plate-voltage wave is shown in Figure 7(m) and 7(n) for successive fields.

This, in turn, is applied to the grid of a triode mixer tube, on the cathode of which is impressed the preliminary kinescope-synchronizing pulses of Figure 7(j). This tube then deletes the unwanted alternate horizontal-synchronizing pulses, so that its plate voltage is the desired kinescope-synchronizing wave which is shown for successive fields in Figures 7(o) and 7(p).

Usually it is desirable to amplify the signal thus generated in preparation for its delivery to another piece of apparatus via a low-impedance transmission line.

III. Auxiliary Signals from Generator

The additional signals most likely to be required from a generator of this type include the kinescope-blanking signal, camera-tube driving signals, and camera-tube blanking signals. The techniques for generating these waves are modifications or extensions of the principles

outlined above for the generation of the more complex synchronizing signals. Additional taps from the same "stop-watch" transmission line are utilized to establish precisely the critical front edges of pulses occurring at line frequency, and also the rear edges of the horizontal-driving pulses. It has been found possible to allow multivibrator time constants to determine the rear edges of the kinescope- and camera-tube-blanking signals with adequate precision. However, if desired, these can also be obtained from the delay line by merely extending its length.

The front edges of the vertical-driving and blanking signals are all derived from the sixty-cycle square wave made in the timer unit. The widths of these field-frequency waves are determined by multi-vibrator time constants.

The requirements for and methods of generating the respective waves are outlined below.

Kinescope-Blanking Signal

Details of the desired kinescope-blanking waves and their relations to the synchronizing waves are shown in Figures 10(n) and 10(o), which present these waves in successive fields. A block diagram of the kinescope-blanking-signal generator is shown in Figure 11. The blanking signals originate in two separate generators, one for making the horizontal- and the other the vertical-blanking waveshapes. The outputs are added and clipped, thereby obtaining the desired complete signal.

The horizontal-blanking generator is a single-stroke-multivibrator circuit. In this type of multivibrator, pips introduced at one terminal cause current conduction to be transferred from a normally conducting tube to a normally cut-off tube. However, after a chosen time has elapsed, as determined by a resistance-capacitance time constant of the circuit itself, this condition of current conduction again abruptly reverses, so that the tubes resume their original normal functions. These are maintained stably until another pip occurs, at which time the process is repeated.

The pips which are used for triggering occur at line frequency (15.75 kilocycles) and at a time phase of approximately —2 microseconds, which is in accordance with the specification that the front porch be a minimum of 1.6 microseconds. The pips are obtained from a delay-line tap, which means they occur at double-line frequency. Therefore, it is necessary to delete alternate pips before injecting them into the multivibrator. This deletion is achieved by making use of the wave shown in Figures 10(c) and 10(d), which is obtained from the same
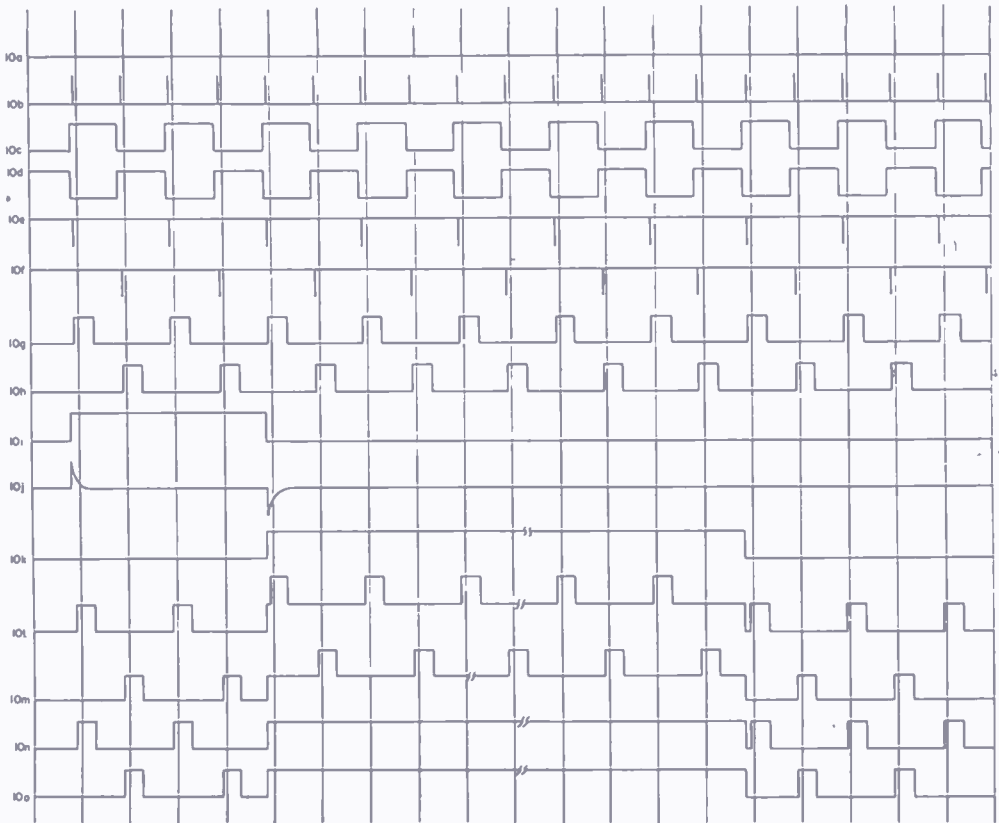
Fig. 10—Voltage waves in kinescope-blanking-signal generator.

source as the waves of Figures 7(k) and 7(l). These, it will be recalled, were generated to delete unwanted kinescope-horizontal-synchronizing pulses.

Figure 10(a) shows the zero-phased 31.5-kilocycle pips (to serve as
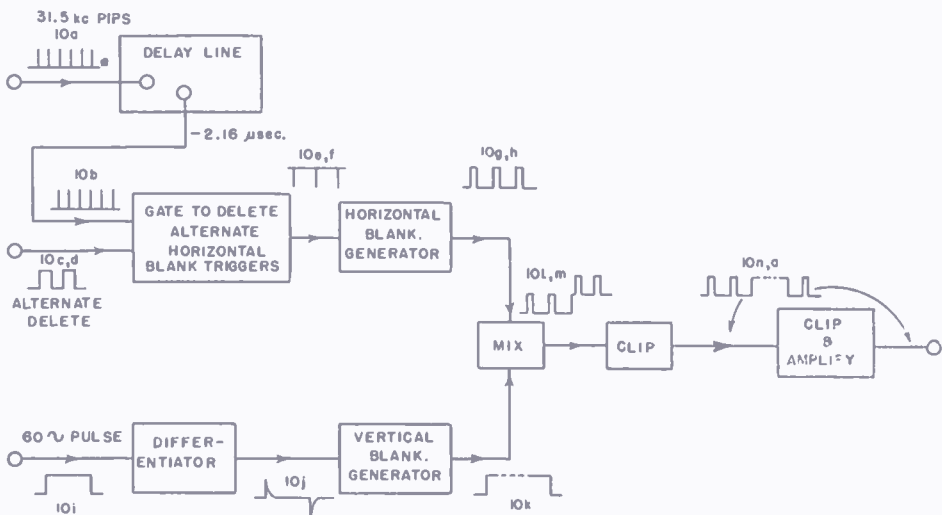
Fig. 11—Block diagram of kinescope-blanking-signal generator.

a reference) while Figure 10(b) shows the phasing of pips which are used for horizontal-blanking triggers. By feeding the pips of Figure 10(b) to one grid, and the wave of Figures 10(c) and 10(d) to another grid of a multigrid tube, the desired triggering wave of Figures 10(e) and 10(f) can be obtained at the plate. The horizontal-blanking wave is shown in Figures 10 (g) and 10(h).

Generation of the vertical-blanking waves is performed in a manner similar to that for the horizontal. Again a single-stroke multivibrator of the type just described is used. The triggering pip is secured by differentiating a 60-cycle pulse from the timer unit. As pointed out earlier in the report the phasing of this pip is essentially invariant with respect to the 31.5-kilocycle pips. The 60-cycle wave, before differentiation, is shown in Figure 10(i) and the differentiated wave appears as Figure 10(j). The negative kick triggers the vertical-blanking-signal generator. As in the case of the horizontal-blanking generator, the time elapsed before the tube current conduction reverses again is determined by a resistance-capacitance time constant in the generator. By inserting a small amplitude of 31.5-kilocycle pips into this generator, an additional desirable feature is added. The vertical-blanking signal always ends at the same time with respect to the horizontal-blanking signal. This does away with a tendency for jitter at the beginning of the top line of each field that is sometimes present in older equipment.

Mixing outputs of the horizontal and vertical-blanking signal generators yields the voltage wave of Figures 10(l) and 10(m). A clipper tube then produces the desired blanking signal of Figures 10(n) and 10(o).

Camera-Tube Driving Signals

The driving signals are generated so that the respective leading edges occur coincidentally with those of the horizontal- and vertical-kinescope-blanking signals. They are derived as shown in the block diagram of Figure 12. These signals are generated separately, one generator making the horizontal and the other the vertical signals.

The horizontal-driving-pulse generator is functionally the same as the multivibrator used for making the kinescope-synchronizing signals —that is, there are two triggering terminals, one for the leading edge and one for the trailing edge. The triggering pips are again supplied from the delay-line taps. It is necessary to delete alternate pips from each of these taps to have the horizontal-driving pulses occur at line frequency. This is done by using two keying tubes and feeding one grid of each with the wave of Figures 10(c) and 10(d) respectively.
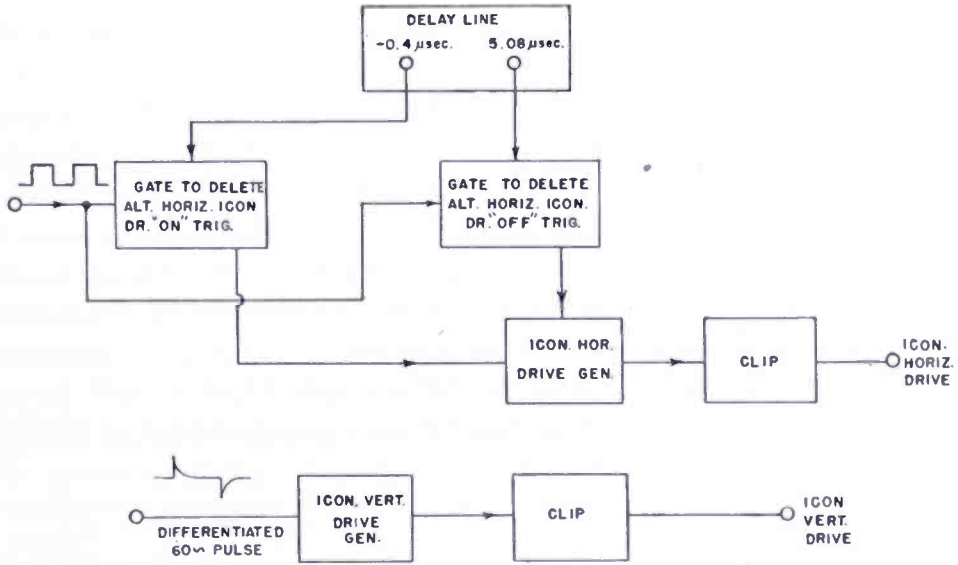
Fig. 12—Block diagram of iconoscope-drive-signal generator.

If the horizontal driving signals are to be fed over cables long enough to cause appreciable delays, as may be the case in supplying a distant pick-up tube, it is possible to change the settings of the leading and trailing edges by moving the taps on the delay line from which the triggers are secured.

The vertical drive generator is a single-stroke-multivibrator circuit of the same type as described previously. It is triggered from the same differentiated 60-cycle wave which triggers the kinescope-vertical-blanking generator. The width of the vertical-driving pulse is determined by means of a resistance-capacitance time constant.

Camera-Tube Blanking Generator

A block diagram in Figure 13 shows how the camera-tube-blanking
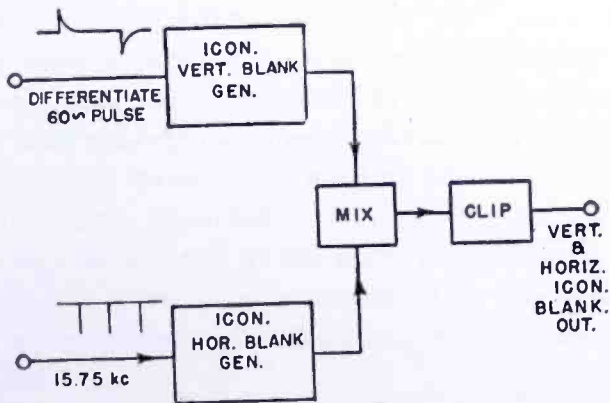
Fig. 13—Block diagram of iconoscope-blanking-signal generator.

signals are obtained. Again, two generators are used, one each for the horizontal and vertical blanking waves.

The generators are both single-stroke multivibrators. The triggers for the horizontal-blanking signals are the same 15.75-kilocycle pips used to trigger the kinescope-horizontal-blanking generator. (Figures 10(e) and 10(f)). The trigger used for the vertical-blanking pulse is the differentiated 60-cycle pulse. The trailing edges of both horizontal and vertical-iconoscope-blanking waves are determined by resistance-capacitance time constants in each generator. Both the horizontal- and vertical-iconoscope-blanking waves are added and clipped in the same manner as previously described for the kinescope-blanking signals.

THE RADIO MIKE*

By

J. L. HATHAWAY AND RALPH KENNEDY

Engineering Department, National Broadcasting Company, Inc.,
New York. N. Y.

Summary—*Miniature pre-war transmitters called "Beermugs" have proven themselves useful in a number of specialized broadcast applications. Redesign, using improved circuits and components, has made possible a new transmitter, called the Radio Mike, which is half the physical size of the "Beermug", lighter in weight, and gives superior performance. Various considerations leading to the present design are outlined and the present transmitter is described. Operating characteristics and a series of field tests are discussed.*

MINIATURE radio transmitters have been used by the National Broadcasting Company for a number of years for short distance pick-up work. Since their development in 1935, these have been known as "Beermugs", because of their physical shape. Each transmitter included a built-in power supply, microphone, modulator, crystal-controlled radio-frequency generator, attached antenna rod and side handles for carrying. They were, in effect, the "grandaddies" of the walkie-talkie units which became so well known during the war.

Broadcasting has found a wide range of applications for these transmitters because of their small size and light weight. One was strapped on a jockey in a horse race, permitting him to broadcast his own version of the race. Numerous conventions have considered them invaluable, since they could be carried on the convention floor to the different delegates wishing to speak. The difficulties of long microphone cords were eliminated, and announcers could move freely about in large crowds, interviewing celebrities with ease. Championship trotting races were broadcast directly from the racing sulkies. Golf matches, parades, and many horse shows have also been covered. In fact, wherever long microphone lines would be required, the "Beermug" has offered a solution through the medium of radio.

Recently, it became apparent that redesign was desirable in order to reduce size and weight and at the same time increase output power. These improvements have been incorporated in a new design utilizing improved circuit components and the new unit is appropriately termed the "Radio Mike."

---

* Decimal Classification: R355.14.

Necessary Characteristics

The physical size and weight of a broadcaster's Radio Mike should be as small as possible, since it must often be supported by one hand while speaking, without undue strain. It should, however, permit easy maintenance and provide sufficient radiation for reliable operation over a distance of several hundred yards. Battery life should permit continuous transmission for at least three hours or intermittent operation for at least ten hours total transmission time. Necessary frequency stability is determined by Federal Communications Commission regulations on the carrier frequency employed. Audio gain control should be automatic since extra controls cause confusion and operational errors. The antenna must be short so that when carried in a room it will not strike the ceiling or low hanging protuberances. On the other hand, it should be long enough to realize a fair value of antenna efficiency.

Antenna length and efficiency point to utilization of the 152-megacycle frequency band. However, available channels in this region are so narrow that difficulty would be encountered in maintaining the required stability in a miniature transmitter. It probably would be necessary to use a very stable crystal oscillator followed by frequency multipliers which, with the necessary power supply would be unduly large.

The remote pickup frequencies around 2 megacycles offer little in this application, because of the insignificant antenna efficiency possible and also because of the severe interference encountered in some sections.

By the process of elimination, the 26-megacycle band appears at present to offer the only practical operating frequency for the broadcaster's miniature transmitter. Here, the transmitting apparatus is quite simple and the antenna radiation efficiency reasonably good. The only major difficulty is interference caused by diathermy apparatus and automobile ignition. However, experience shows that if transmission is not attempted over too long a distance, the received signal is strong enough to override the interferences.

Power Supply

Power supply considerations are most important in a miniature transmitter. Unless great care is exercised in this respect, the final unit may have 75 per cent or more of its total weight concentrated in the power supply. Storage batteries and vibrators were studied but were not adopted because of weight. Instead, a special battery which was manufactured by the Burgess Battery Company for the "Beermug"

transmitters has now been improved and modified. With this battery, the power supply accounts for slightly less than 50 per cent of the total weight.

PRESENT DESIGN

The "Radio Mike" pictured in Figure 1 (which shows the microphone grill), weighs 6 pounds including battery and antenna, and is housed in a lightweight case of aluminum and Dow metal, measuring $4\frac{1}{2} \times 3\frac{3}{8} \times 10$ inches. This represents a reduction of 50 per cent in volume and 20 per cent in weight from the pre-war "Beermug" trans-
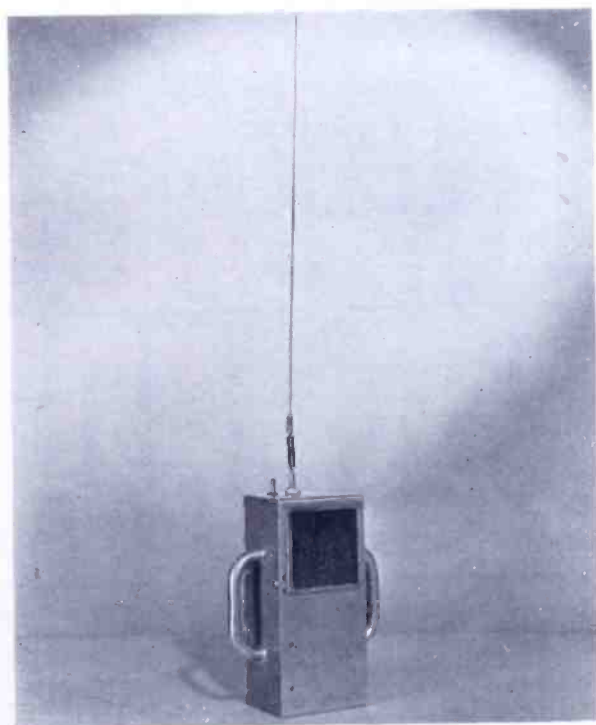
Fig. 1—Front view of Radio Mike showing microphone grill.

mitters. Output power into an electric light bulb resistive load is 250 milliwatts, and slightly greater than 100 per cent positive modulation is possible without excess distortion.[1] Thus appreciably greater effective power is available from this transmitter than from the earlier models. A complete schematic is shown in Figure 2. The carrier is crystal controlled to within .015 per cent of the assigned frequency. Automatic audio gain control is incorporated to assure proper modulation even though sound intensity varies widely. The antenna is a 20-inch length of 0.1-inch dural rod attached to the transmitter through a spring loading coil. This arrangement not only increases electrical loading

---

[1] J. L. Hathaway, "Effect of Microphone Polarity on Percentage Modulation", *Electronics*, October, 1939.

but safeguards the steatite lead-through insulator in the event that the antenna is bumped. Tests show that neither longer antennas nor top-loading arrangements are advisable since the increase in radiation does not compensate for the added mechanical hazard. Operation is intended in the 25- to 28-megacycle frequency band and the tuning range is approximately 23 to 30 megacycles. With correct tuning the battery gives 10 hours of operation at 2 hours per day discharge. Several more hours of operation are possible if taken only one hour per day, following the initial 10 hour discharge. The power switch, located on top of the transmitter has three positions: "Off", "Low",
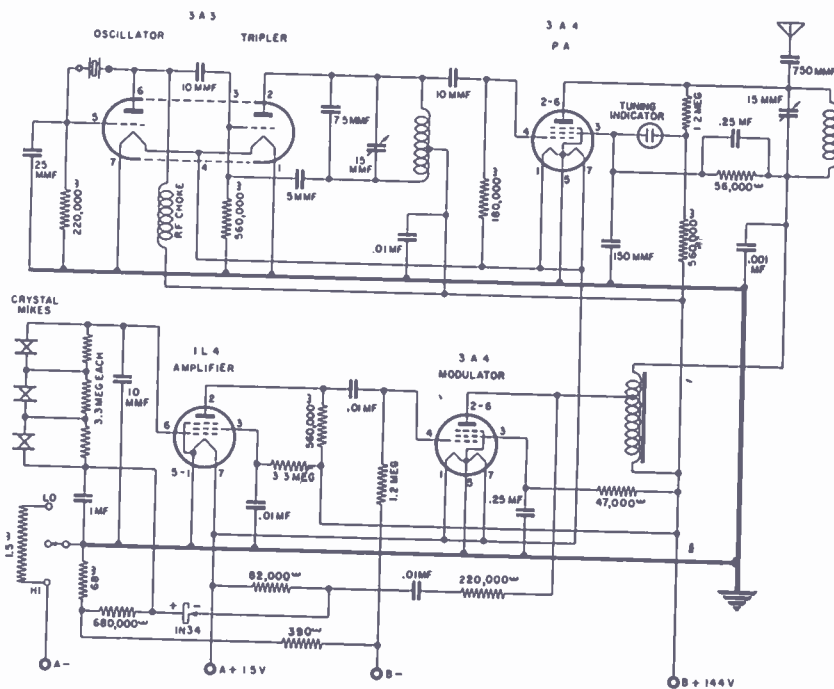
Fig. 2—Schematic diagram of Radio Mike.

and "High." In the low position, the filament voltage applied to the tube filaments is 1.1 volts with a new battery and in the high position the full A-battery voltage is applied to the filaments. Because of reduced plate and filament drains on the low power position, this is used whenever higher output power is not required, as for example, in a convention hall.

AUDIO CIRCUIT

Three crystal microphones are operated in series, each with an individual shunt resistor. This arrangement gives approximately 10

decibels higher voltage level than a single microphone thus obviating an extra amplifier stage. A single voltage amplifier and the modulator provide a voltage gain of 73 decibels, sufficient to modulate the transmitted fully on moderately loud sound intensities. The modulator operates with a high screen voltage and high bias in order to conserve plate current and at the same time allow for high upward modulation. The asymmetry of most human voices is such that peaks are about twice as high in one phase as in the reverse. Consequently the microphones are phased to place maximum peaks negative on the voltage amplifier grid, corresponding to positive on the modulator grid. After phase reversals in this tube and the modulation transformer, these excessive peaks modulate the carrier upward. Thus, greater than 100 per cent modulation actually can be accomplished without distortion.

Audio gain is varied automatically as a function of sound level, high sound intensity at the microphone causing it to drop. This reduced amplification is accomplished by shifting bias on the input
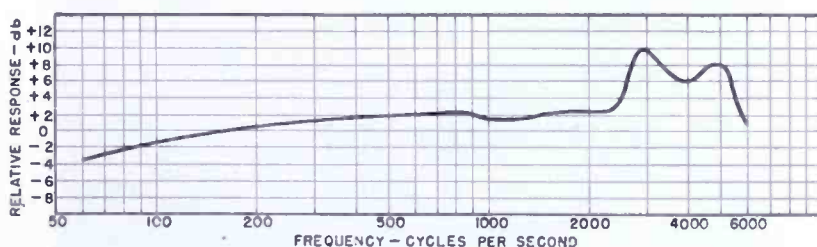
Fig. 3—Overall frequency response curve.

amplifier at a rate which prevents overload and at the same time does not introduce audible distortion or excessive audible thump. Frequency response of the audio system is essentially flat from 100 through 6000 cycles. Overall frequency response of the transmitter, including microphones, is shown in Figure 3.

The modulation transformer is of the auto-transformer type with optimum step-up ratio. It is extremely small and light in weight, this being possible because the d-c magnetizing currents are almost completely balanced out. This transformer, the tubes and the crystal are shown in Figure 4. This also pictures the battery occupying the lower compartment.

RADIO FREQUENCY CIRCUITS

The radio frequency section of the transmitter includes a crystal controlled oscillator, a frequency tripler, and a radio-frequency amplifier. The oscillator is of the Pierce type and uses a small high precision BT quartz crystal. This circuit is employed since it does not require

tuning controls. The tripler functions in a slightly over-neutralized condition in order to obtain maximum possible output. The final amplifier is a pentode, plate- and screen-grid modulated and the antenna is coupled to the plate through a blocking condenser. Variable air condensers are used across each of the plate circuit coils for tuning and a single small neon lamp acts as an indicator.

The indicator is connected between screen and plate of the radio-frequency amplifier. When the power switch is in the "Off" position,
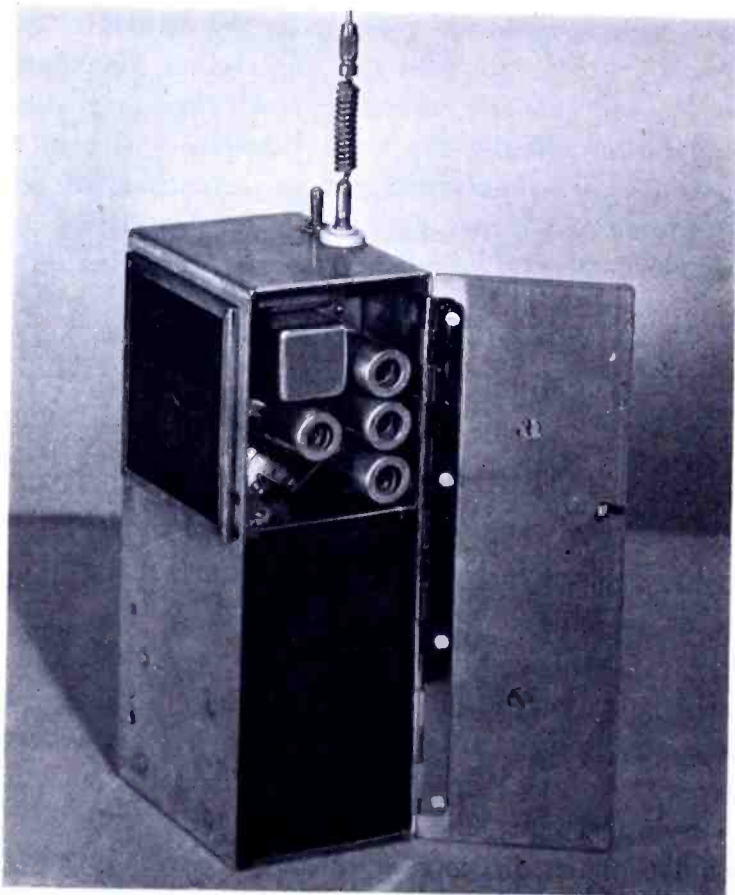
Fig. 4—Side view of Radio Mike showing transformer and battery.

no current flows, the screen and plate are at the same potential, and the lamp is out. With the power switch on, the screen voltage drops through the screen dropping resistor, thus igniting the lamp on direct current only, assuming both circuits are out of tune. As the tripler is brought into tune, however, more bias results on the radio-frequency amplifier grid. Consequently, the screen grid potential increases and the lamp dims. Next, the radio-frequency amplifier plate circuit is tuned. As this is brought into resonance, the radio-frequency potential at the plate increases, causing the lamp to increase in brilliance.

If these two adjustments are carefully made, no readjustments are necessary. Since the tripler tuning results in lamp dimming, this circuit is most readily tuned if the final tank is completely out of tune. The neon bulb is a great improvement over the system used in the early model transmitters, wherein a meter was plugged into the various circuits. The jacks caused noise and at the same time tuning was not quite optimum because the meter and leads altered the antenna loading. In this respect, it should be noted that exact tuning of the final plate
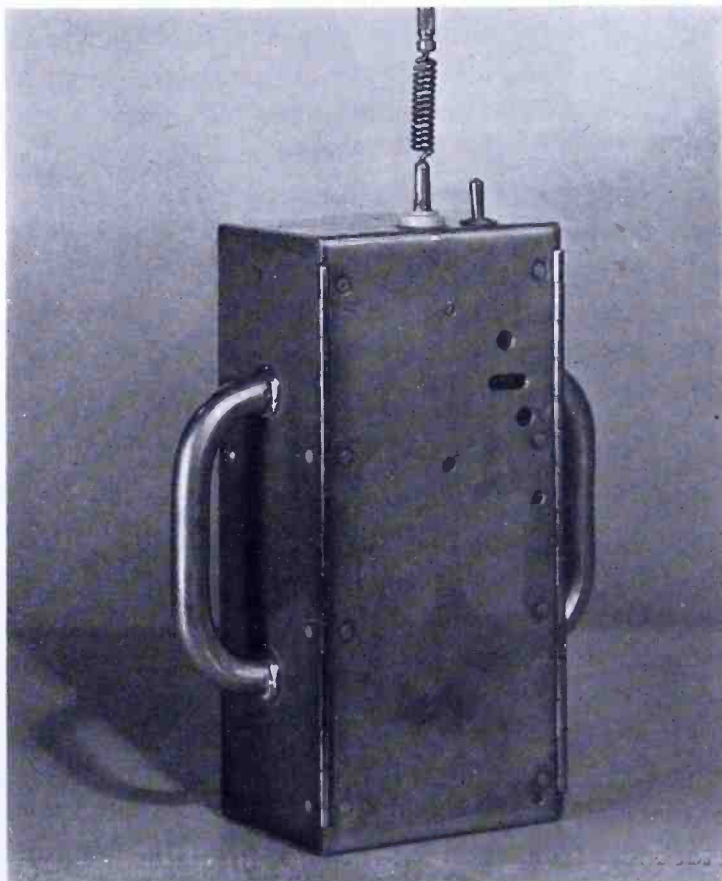
Fig. 5—Rear view of Radio Mike showing tuning holes and viewing slot.

can be effected only for the condition under which it is tuned. Thus, if the unit is to be carried, it should be held free of ground for this final circuit tuning. The tuning holes and a slot for viewing the indicator are visible in Figure 5.

OPERATIONAL TESTS

Numerous field tests under a wide variety of conditions have been conducted on the new transmitter in New York City with gratifying results. The first was from the 85th floor of the Empire State Building

to the roof of the RCA Building, a distance of about ¾ mile, direct line-of-sight. The received signal was strong and no interference was observed. Tests were then conducted at ground level in Central Park up to distances of ½ mile with excellent results. The receiving location was beside a roadway and ignition noise from passing autos caused no interference. Another test was made with the transmitter located across the Hudson River from New York City and a receiver at the Empire State Building. The distance was 3½ miles and the received signal was of broadcast quality. Tests have been conducted along a number of crowded city streets and reception has been very good. The audio system was sufficiently sensitive to pick up background effects such as whistles and automobile horns. One transmission was made carrying the unit around a New York City block of large steel reinforced concrete buildings and at no point was fading severe enough to lose the signal, and about 90 per cent of the time the reception was excellent. In another test, the transmitter was carried into a large steel building, through corridors, and up five flights in an elevator. Reception, at a location across the street was good at all times even from within the elevator.

FUTURE MODIFICATIONS AND APPLICATIONS

Several minor modifications are being incorporated in the transmitters now being manufactured. The unit pictured is a developmental model, without finish or frills. The manufactured transmitters are styled for pleasing appearance and at the same time will be slightly smaller physically. In order to carry the equipment easily in an ordinary brief case, the antenna rod is being shortened while maintaining the same effective total length. This is accomplished by mounting the loading spring on a short section of tubing so that less length is required above it. The rod is detachable from the spring and the tubing is detachable from the feed-through insulator.

When these units are available broadcasters and other services should find them invaluable in many applications. Sidewalk interview broadcasts and telecasts can be facilitated and improved, participants in sporting events picked up with ease, and sudden disasters presented to the audience which would be impossible if microphones lines were required. Use in conjunction with the "Pocket Ear" for transmission of instructions has been mentioned.[2] Police and Fire Departments, rescue teams, construction companies and others should find that these Radio Mikes improve their efficiency.

---

[2] J. L. Hathaway and William Hotine, "The Pocket Ear", *RCA REVIEW*, Vol. VIII, No. 1, pp. 189-146, March, 1947.

CIRCULARLY-POLARIZED OMNIDIRECTIONAL ANTENNA*

By

George H. Brown and O. M. Woodward, Jr.

Research Department, RCA Laboratories Division,
Princeton, N. J.

Summary—This paper describes a circularly-polarized antenna which has been developed specifically for ground station use in airport-to-airplane communication. After briefly considering the necessary field conditions in space to bring about circular polarization, a combination of a vertical dipole and a horizontal loop antenna is treated theoretically. An equivalent arrangement using four dipoles is also studied and a number of factors influencing the performance are displayed.

The theoretical treatment is followed by a description of an antenna which was constructed according to the principles outlined. Test results show that the antenna produced a substantially circularly-polarized wave over a rather wide frequency range without readjustment.

Introduction

EXPERIENCE in airport-to-airplane communication has indicated a need for more reliable communication, free from random polarization changes caused by banking of the aircraft and from amplitude variations due to ground reflections. It has been suggested that a circularly-polarized antenna at the ground station would help to stabilize signal transmission, and permit maximum freedom of choice of antenna location on the aircraft.

The antenna described in this paper is the result of an extensive investigation which included experiments with slotted cylinder radiators, dipole and loop combinations, and spiral radiators.

Theoretical Considerations

(a) A Circularly-Polarized Wave

A circularly-polarized wave may quite properly be considered as made up of a vertically-polarized wave imposed on a horizontally-polarized wave with both waves traveling in the same direction. At any chosen point, the fields of the two waves are in time quadrature with one another.

The electric field intensity of the vertically-polarized wave is represented by the expression

$$e_V = A \cdot \sin \omega t \qquad (1)$$

This field intensity component is vertical.

---

* Decimal Classification: R320.

The electric field intensity of the horizontally-polarized wave has the same peak value, but differs in phase by 90 degrees. This component, which is horizontal, is given by $\quad e_H = A \cdot \cos \omega t \quad$ (2)
At any given instant of time, the resultant field intensity vector has a magnitude equal to $\sqrt{e_V^2 + e_H^2} = A$, and this vector makes an angle

α with the horizontal where $\qquad \tan \alpha = \dfrac{e_V}{e_H} = \tan \omega t \qquad$ (3)

The field intensity vector is seen to be constant in magnitude and rotates in the plane of the wave at synchronous speed.

When the observer looks in the direction of travel of the wave and sees the vector rotating clockwise, the wave is said to be right-hand circularly polarized. When the vector rotates counterclockwise, the wave is left-hand circularly polarized.[1]

(b) *The Combination of a Vertical Dipole and a Horizontal Loop*

A horizontal loop antenna, with a vertical half-wave dipole piercing the center of the loop, may be used to produce a circularly-polarized wave.

At a remote point in the horizontal plane, the vertical half-wave dipole produces a vertical electric field given by

$$E_V = \frac{j60 I_V}{r} \epsilon^{-jkr} \qquad (4)$$

The horizontal loop produces a horizontal electric field at the same point.

$$E_H = \frac{-60\pi kR \cdot J_1(kR)}{r} I_H \epsilon^{-jkr} \qquad (5)$$

where I_V = the current at the center of the dipole,

I_H = the current in the loop,

λ = the wavelength, $\qquad\qquad k = 2\pi/\lambda$,

r = the distance from the antenna to the remote point,

---

[1] Standards on Radio Wave Propagation, (Definition of Terms—p. 2), Institute of Radio Engineers, New York, N. Y., 1942.

$R =$ the radius of the loop,

$J_1(kR) =$ the Bessel function of the first kind and first order.

It may be seen from equations (4) and (5) that the vertical and horizontal fields are in phase quadrature, when the currents in the loop and the dipole are in phase.

To make the two field components be equal to achieve circular polarization, the following relation must be satisfied:

$$I_V/I_H = \pi kR \cdot J_1(kR) \qquad (6)$$
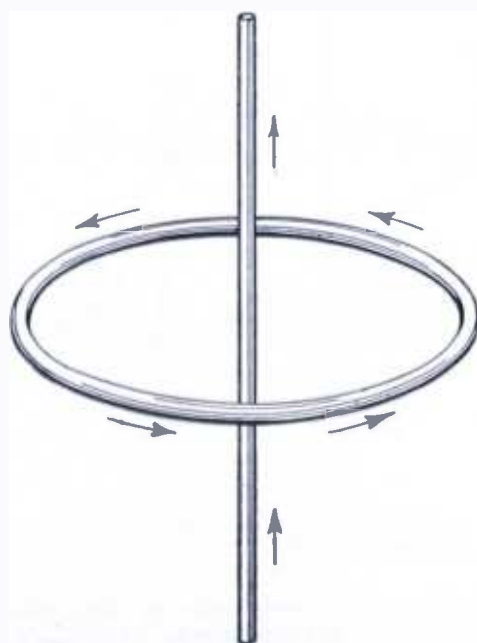
Fig. 1—Current flow relationships in a horizontal loop and a vertical dipole which radiate a right-hand circularly-polarized wave.

Typical values of this ratio, as a function of the radius of the loop, are given below:

R/λ	I_V/I_H
0.05	0.152
0.10	0.587
0.15	1.25
0.20	2.02
0.25	2.8

When the currents in the loop and dipole flow as shown in Figure 1, the resultant wave is right-hand circularly polarized.

While this combination of a loop and a dipole appears to be a simple arrangement, one soon finds that the necessary plumbing to achieve the proper current division while maintaining the currents in phase is quite elaborate and the adjustments are critical. This is particularly true when a wide band of frequencies is used.

(c) *An Equivalent Arrangement*

An arrangement which produces the same result but which is not difficult to attain has been proposed by Lindenblad.[2, 3] His plan may be described best in two steps. First, several vertical dipoles are disposed uniformly about the periphery of a circle which lies in the
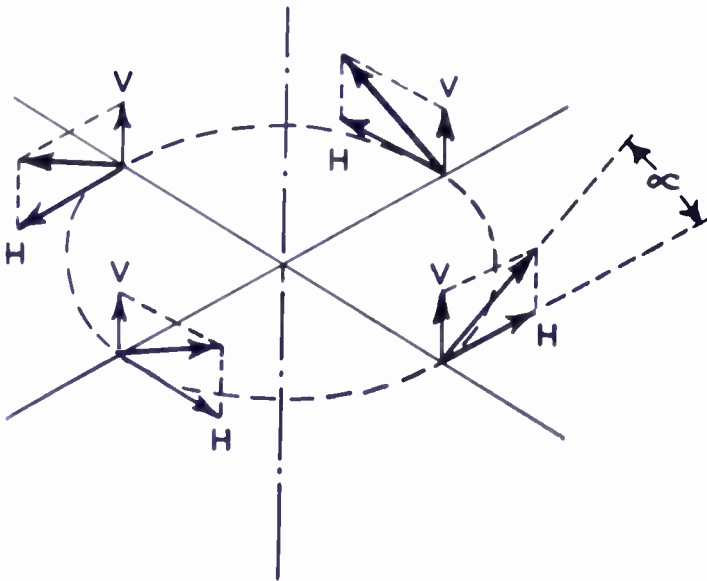
Fig. 2—The effective-current components in the slanted-dipole antenna arrangement.

horizontal plane. Then each dipole is rotated about its center point, with the rotation taking place in a vertical plane which is tangent to the imaginary circle. Each dipole is rotated in the same angular direction. Figure 2 may help to clarify the description. Here four dipoles are used and the heavy arrows represent the direction of current flow in the dipoles. The vertical components of these currents are shown, all pointing upward and acting somewhat as a single vertical radiator. The horizontal components may be seen to flow just as the currents in a continuous loop antenna flow.

---

[2] N. E. Lindenblad, "Antennas and Transmission Lines at the Empire State Television Station", *Communications*, Vol. 21, No. 4, pp. 13-14, April, 1941.

[3] N. E. Lindenblad, U. S. Patent 2,217,911.

Figure 3 shows the plan view with the vertical current components all in phase, and the lower part of the same diagram shows the plan view for the horizontal current components.

PLAN VIEW-VERTICAL POLARIZATION
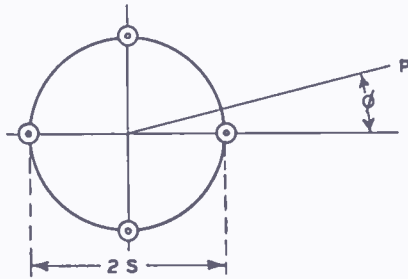
PLAN VIEW-HORIZONTAL POLARIZATION
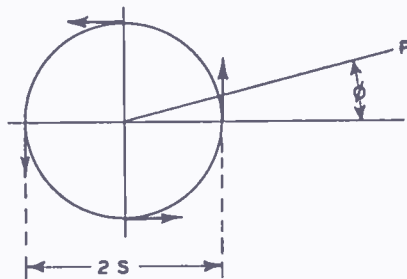
Fig. 3—Plan views showing the relative disposition of the vertical and horizontal components of antenna current.

Using the four radiators shown in Figures 2 and 3, we may write the expressions for the vertical and horizontal components of electric field at a remote point P thus:

$$E_V = j \frac{120\, I \epsilon^{-jkr}}{r} \cdot \sin \alpha \cos \theta \left[\cos (kS \cos \phi \cos \theta) \right.$$

$$\left. + \cos (kS \sin \phi \cos \theta) \right] \qquad (7)$$

and

$$E_H = \frac{-120\, I \epsilon^{-jkr}}{r} \cdot \cos \alpha \left[\cos \phi \sin (kS \cos \phi \cos \theta) \right.$$

$$\left. + \sin \phi \sin (kS \sin \phi \cos \theta) \right] \qquad (8)$$

where $S =$ the radius of the circle on which the antennas are located

$\alpha =$ the angle between each radiator and the horizontal plane

$\phi =$ the angle that locates the point P in the horizontal plane

$\theta =$ the angle which locates the point P in the vertical plane. (When this angle is zero, the point lies in the horizontal plane.)

$I =$ the current in each radiator.

The symbols k and r have been defined earlier in this paper.

Digressing for a moment, the case is considered where the dimension S is very small compared to a wavelength. Then the following approximations may be used:

$$\cos (kS \cdot \cos \phi \cos \theta) \doteq 1$$

$$\cos (kS \cdot \sin \phi \cos \theta) \doteq 1$$

$$\sin (kS \cdot \cos \phi \cos \theta) \doteq kS \cdot \cos \phi \cos \theta$$

$$\sin (kS \cdot \sin \phi \cos \theta) = kS \cdot \sin \phi \cos \theta$$

and (7) becomes
$$E_V = j \frac{120 \, I \epsilon^{-jkr}}{r} \cdot 2 \sin \alpha \cos \theta \qquad (9)$$

while (8) takes the form

$$E_H = \frac{-120 \, I \epsilon^{-jkr}}{r} \cdot \cos \alpha \, [kS \cos^2 \phi \cos \theta + kS \sin^2 \phi \cos \theta]$$

$$= \frac{-120 \, I \epsilon^{-jkr}}{r} \cdot kS \cos \alpha \cos \theta \qquad (10)$$

Equations (9) and (10) show that, for small values of S, both the vertical and horizontal components of electric field are independent of the angle ϕ. In other words, the radiation pattern is uniformly circular. Both vertical patterns vary simply as $\cos \theta$. Hence, if we satisfy the

condition
$$2 \cdot \sin \alpha = kS \cos \alpha$$

or
$$\tan \alpha = kS/2 \qquad (11)$$

the radiated field will be circularly polarized at all points in space.

When the dimension S is not sufficiently small, perfect circular polarization will not be achieved at all points. However, elliptical polarization which closely approaches circular polarization may be

readily obtained. For example, if it is desired to insure true circular polarization in the horizontal plane at positions corresponding to values of ϕ equal to 0, 90, 180, and 270 degrees, it is merely necessary to satisfy the relation

$$\sin \alpha \, [1 + \cos \, (kS)] = \cos \alpha \, \sin \, (kS)$$

or
$$\tan \alpha = \tan \, (kS/2) \qquad (12)$$

To obtain circular polarization at points corresponding to ϕ equal to 45, 135, 225, and 315 degrees, it is necessary to satisfy the relation

$$\tan \alpha = \frac{1}{\sqrt{2}} \tan \left(\frac{kS}{\sqrt{2}} \right) \qquad (13)$$

The relation between the tilt angle of the dipoles and the dimension S may be seen in the following tabulation.

S (wavelengths)	kS (degrees)	α (degrees) From equation (12)	From equation (13)
0	0	0	0
0.0833	30	15°	15° 22′
0.166	60	30°	32° 55′
0.25	90	45°	55°

DESCRIPTION OF A CIRCULARLY-POLARIZED ANTENNA

An antenna has been constructed, following the basic design principles established by Lindenblad, and is shown in Figure 4. The antenna consists of four in-phase dipoles arranged on the circumference of a circle having a diameter of approximately one-third wavelength. Hence kS is 60 degrees, so from Equation (12) it is found necessary to incline each dipole at an angle of 30 degrees from the horizontal plane.

Each of the four dipoles is fed with a RG-11U solid-dielectric coaxial cable placed inside one of the two tubular support legs, with the cables each one-quarter wave in length at the mid-band frequency of operation. The inner conductor of the cable extends through a protecting end seal to the end of the other support leg, providing a balanced feed to the dipole. This method of securing balanced feed is illustrated in Figure 5.

The impedance offered to the transmission line at this point consists of the antenna impedance shunted by the inductive reactance of
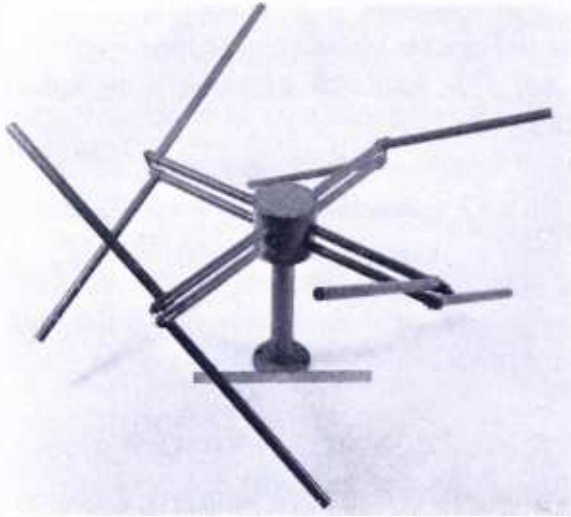
Fig. 4—The development model designed to operate over the frequency range from 110 to 132 megacycles. (This model radiates a left-hand circularly-polarized wave.)

the parallel-bar support legs. The dipoles are made somewhat less than a half wave, so the antenna impedance consists of a resistive component and a capacitive reactance. The dimensions were so chosen that the inductive reactance of the support legs just parallel-resonated the dipole. In addition, at resonance the resistance of the combination is 100 ohms. The RG-11U cable has a characteristic impedance of 72 ohms. Hence, the impedance looking into the quarter-wave section which feeds the dipole is approximately 52 ohms. It is of interest to
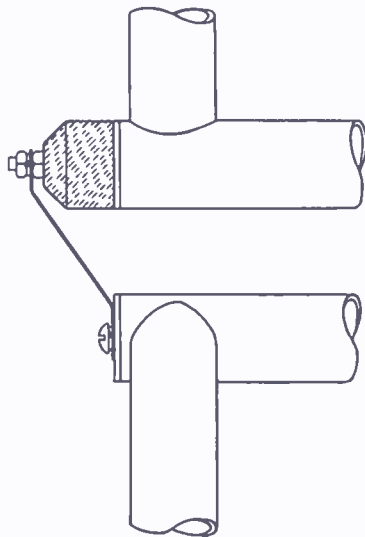
Fig. 5—The method used to secure balanced feed of the dipole from a concentric transmission line.

note that the velocity in this solid-dielectric cable is two-thirds of the velocity of radio waves in free space so the quarter wavelength of cable has an actual physical length of one-sixth of a free-space wavelength and thus just reaches from the end-seal of the dipole to the center of the large cylinder shown in Figure 4. The four cables join in this cylinder. Since they are all in parallel, they offer a resistance of 13 ohms. A quarter-wave transformer with a characteristic impedance of 26 ohms is contained in the central vertical support post. This transformer steps the 13-ohm resistance up to 52 ohms. Thus an impedance match is offered to the 52-ohm feed line which leads from the transmitter to the antenna. The result is a well-matched
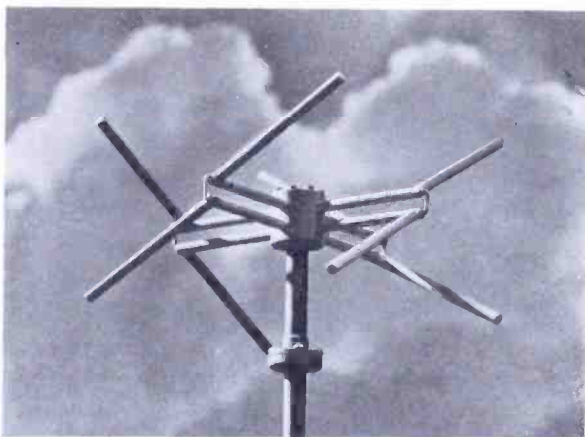
Fig. 6—A very small model of the circularly-polarized antenna. (This model radiates a right-hand circularly-polarized wave.)

antenna radiating a substantially circularly-polarized wave. Equal currents in the dipoles, all in phase, are obtained simply from the symmetrical construction and depend in no way upon the method of securing an impedance match.

While it is true that the central support pole lies in the field of the antenna, tests proved that it was not necessary to use a quarter-wave sleeve around the support pole to secure the desired radiation characteristics.

The weight of the completed antenna is less than 30 pounds, exclusive of the mounting pole and feed line.

An inspection of Figures 1 and 4 reveals that the antenna shown in Figure 4 will radiate a left-hand circularly-polarized wave. A small model of this type of antenna is shown in Figure 6. This model is constructed to yield a right-hand circularly-polarized wave.
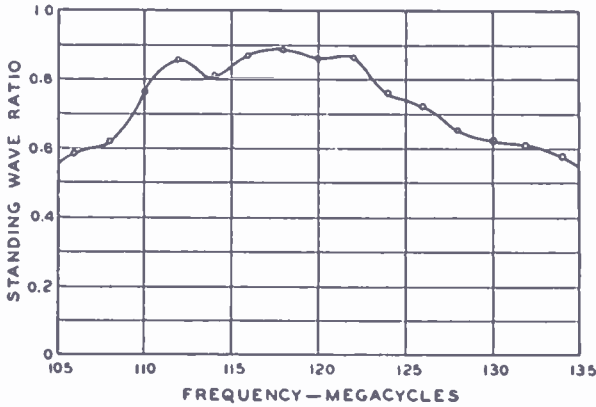
Fig. 7—The measured standing-wave ratio as a function of frequency.

TEST RESULTS

The antenna was designed to cover a band of frequencies lying between 110 and 132 megacycles. The standing-wave ratio on the main feed line, as a function of frequency, is shown in Figure 7. It may be seen that the standing-wave ratio is better than 0.5 over the entire band.

To learn how well circular polarization had been achieved, a transmitter was connected to the antenna and a dipole at the receiver was rotated on a horizontal axis. This test was made at many points around the antenna and at several frequencies. Figure 8 shows typical results. A possible explanation of the departure of the measured curve from a perfect circle is the slight shading or shielding effect experienced by
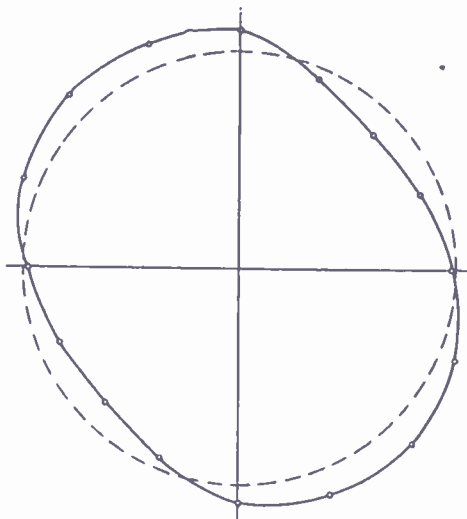
Fig. 8—Experimental data showed the close approach to a true circularly-polarized wave.

the radiators or portions of radiators farthest from the receiver, behind the central pipe support and cable connector box.

Vertical radiation patterns were found to obey the cos θ law rather well throughout the band of frequencies.

Radiation patterns in the horizontal plane were measured at a number of frequencies. The patterns were found to be essentially circular for all frequencies in the band. Typical measurements taken at 122 megacycles are shown in the tabulation below. The theoretical values were calculated from Equations (7) and (8).

Angle ϕ (degrees)	Horizontally-polarized field		Vertically-polarized field	
	Theoretical	Measured	Theoretical	Measured
0	1.0	1.0	1.0	1.02
22.5	1.05		0.992	
45	1.095	1.015	0.976	1.042
67.5	1.05		0.992	
90	1.0	0.98	1.0	1.042
135	1.095	1.015	0.976	1.065
180	1.0	1.0	1.0	1.075
225	1.095	1.015	0.976	1.052
270	1.0	0.98	1.0	1.032
315	1.095	1.015	0.976	1.032

CONCLUSION ·

The antenna described in this paper produces a substantially circularly-polarized wave over a rather wide frequency range without readjustment. In fact, the initial adjustments are far from critical.

The signal radiated by this antenna may be received on a dipole or loop antenna. The receiving antenna may be oriented in any position, with the reservation that the receiving antenna does not have a null in its pattern at this position. For example, a dipole could be rotated about a horizontal axis and receive a substantially constant signal if this axis coincides with the line from the transmitter to the receiver. However, if the rotation were such that the receiving antenna assumed a position which coincided with the axis mentioned above, no signal would be received.

If a circularly-polarized antenna is used to receive the circularly-polarized wave, it is necessary that both antennas be capable of pro ducing a right-hand circularly-polarized wave or that they both be capable of producing a left-hand circularly-polarized wave. For example, if the transmitting antenna were the one shown in Figure 4 and the receiving antenna similar to the antenna of Figure 6, the receiving antenna would be blind to the transmitter.

PHASE-FRONT PLOTTER FOR CENTIMETER WAVES*†

By

HARLEY IAMS

Research Department, RCA Laboratories Division,
Princeton, N. J.

Summary—In the centimeter-wave range it is not unusual to have an antenna, dish, or horn across which the phase of the radiation should be constant, or should vary in some predetermined manner. To test such behavior a machine was evolved which is capable of recording on a sheet of paper lines showing the regions in space which have the same phase.

This plotter can be used to test centimeter-wave antennas, to demonstrate principles of physical optics, or to measure the refractive index of dielectrics. The recordings are equivalent to pictures of radio waves.

D IRECTIONAL patterns of antennas are determined by both the amplitude and phase of the radiated energy. The need for improved methods of measuring relative phase across apertures many wavelengths wide arose in connection with the testing of rapid-scanning antennas for centimeter waves. A machine was developed to record on a sheet of paper lines showing the regions in space having the same phase. This device has proved useful for many purposes in addition to the one for which it was originally built.

One of the uses of the phase-front plotter is the making of pictures of radio waves as they pass through space. These pictures can be used by an antenna designer to determine the electrical center of a horn, to observe the relative phase at different parts of a structure, and to study the operation of a new antenna. Workers in the field of propagation can observe refraction, diffraction and reflection of radio-frequency energy. Another use is the measurement of the refractive index of dielectrics at radio frequencies; this does not require the preparation of special specimens nor involved computation.

OPERATION

The principle of operation of the plotter may be explained with the aid of Figure 1, which is a photograph of one form of the device. A centimeter-wave transmitter (not shown) keyed at audio frequency

---

* Decimal Classification: R246.
† Presented at the 1947 I.R.E. National Convention in New York, N. Y. on March 6, 1947.

supplies power to the horn H, which is being tested. The small movable probe A picks up some of the radiated energy, which is transferred by means of wave guides and rotary joints to the crystal detector D. Some of the transmitter power is also conveyed directly to the detector through a wave guide and an attenuator R (which is used to control the amplitude of this reference signal). The signals which reach the detector over the two routes may or may not be in the same phase, depending upon the position in which the probe is placed. The detector output is a maximum when the phase is the same, and a minimum when it differs by 180 degrees. This output is carried by cable E to an amplifier, the output of which is connected to stylus S placed directly below the probe. A sheet of current-sensitive paper on which the stylus rests is darkened in proportion to the detector output.
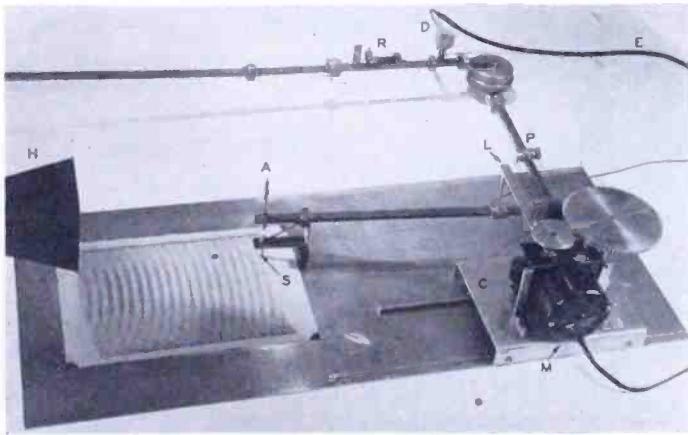
Fig. 1—Automatic plotter.

A motor M causes the probe to scan the area in front of the horn; through link L the waveguide is rocked back and forth, and it is moved in a second direction by the motion of carriage C.

In a few minutes a complete record is made, showing which parts of the scanned area have the same phase. The degree of darkening is an indication of the amplitude. Such a record may be said to be a picture of the radio waves; a photograph of ripples on a pond is also a record of the regions which vibrate in the same phase. By means of "line stretcher" P (in Figure 1) a line of maximum darkening of the paper can be made to pass through any desired point; this corresponds to the selection of the time at which water waves are photographed.

Wavelengths in the neighborhood of one centimeter are particularly suitable for phase-front plotting, since they are short enough to include a number of wavelengths in even a small scanned area and

long enough that the construction of models of typical antennas is not difficult. The use of $1\frac{1}{4}$-centimeter wavelength in the plotter of Figure 1 led to the selection of a combination of rigid wave guides and rotary joints to transfer the radio-frequency energy to the detector. At this wavelength there is, as far as it is known, no suitable transmission line or flexible wave guide which does not change its electrical length when flexed. Fortunately, the rotary joints which were tested proved very satisfactory in this respect.

When numerical data are to be taken, as is sometimes necessary in testing an antenna, the position of the phase fronts can be determined most accurately by moving the probe by hand, following lines along which the detector output is a minimum. To record the posi-
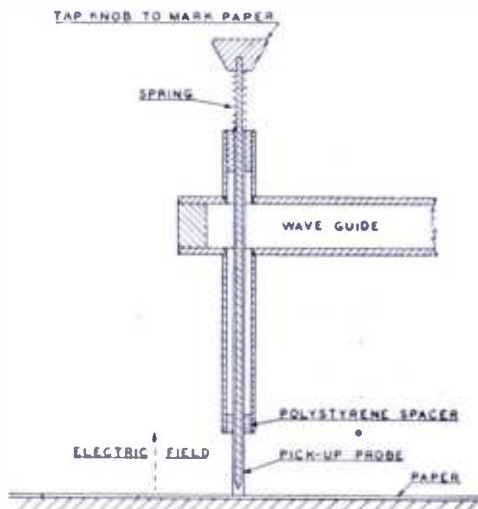
Fig. 2—Self-plotting probe.
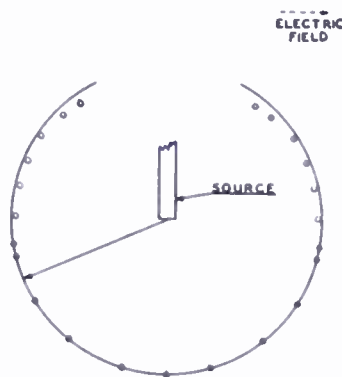
Fig. 3—Phase front near the open end of a waveguide.

tions, a self-plotting probe such as the one shown in Figure 2 is very convenient. When care is taken, it is possible to repeat readings to within ± 0.010 inch, which is ± 1/50 of a wavelength at the frequency used. A sample of such a plot is given in Figure 3.

When records are to be made at longer wavelengths than those mentioned it may be desirable to reduce the scale at which the plotting is done. This can be done by moving the stylus or plotting device by means of a pantograph attached to the probe, or by using a facsimile recorder synchronized with the motion of the probe.

APPLICATIONS

An example of the testing of a "pillbox" antenna is given in
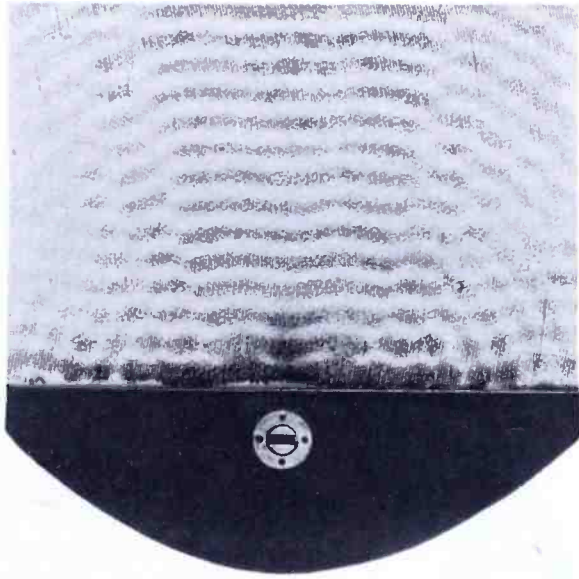
Fig. 4—Phase fronts from a "pillbox."

Figures 4 and 5. Such an antenna focuses the radiation from a wave guide by reflecting it from a parabolic surface; the emerging waves should be straight. As Figure 4 shows, one such "pillbox" did produce nearly straight phase fronts — and some curved ones, as well. An examination of the curved waves shows that they are centered in the area masked by the wave guide. They are the result of the masking; one explanation is that the interrupted part of the wave could also have been produced by energy from another transmitter, equal in
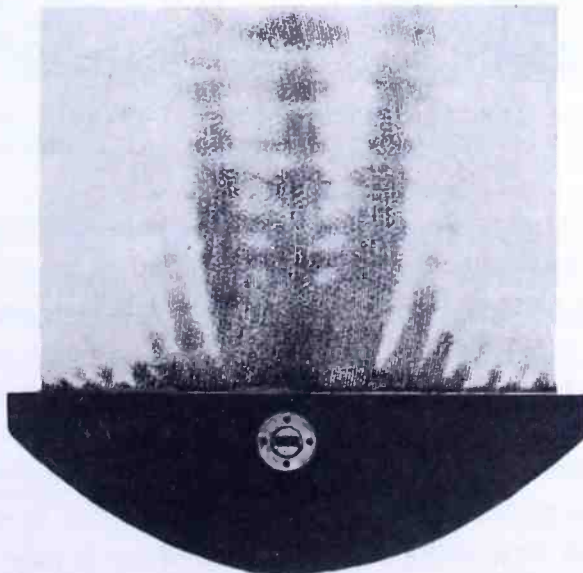
Fig. 5—Intensity pattern near a "pillbox."

amplitude and opposite in phase to the energy supplied in this region by the reflector. Figure 5 is an intensity pattern from the same "pillbox" recorded by cutting off the reference signal. It shows how the interference between the straight and curved phase fronts acts to produce side lobes. Because the recording was made near the antenna the lobes have not assumed their final angular positions.

The phase fronts can be recorded in a series of layers when it is desired to obtain information in three dimensions. Also, the plane
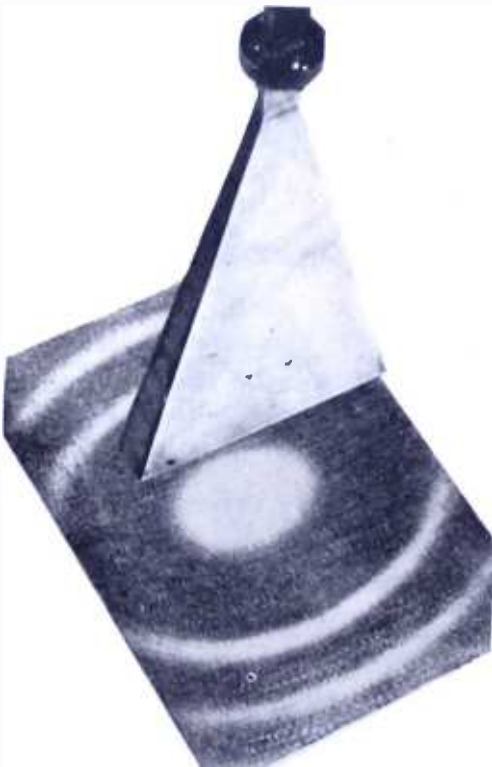
Fig. 6 — Phase fronts at right
angles to horn axis.
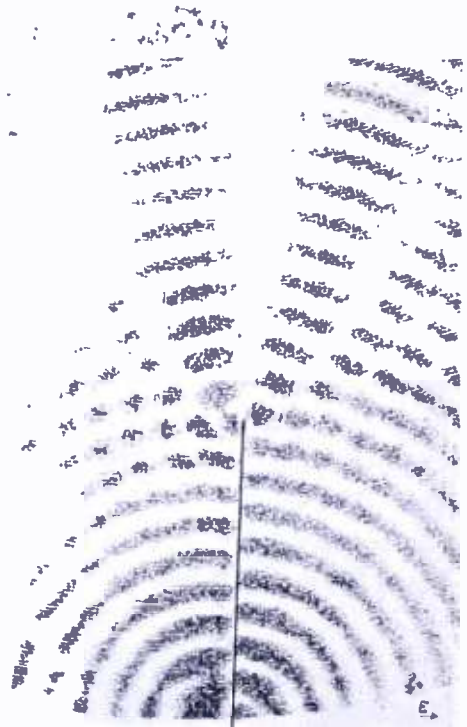
Fig. 7—Waves from a long-wire
antenna.

which is scanned may be at right angles to the direction of propagation, as it was in Figure 6. A plot of this kind is, to a first approximation, a contour map of the lens which would be required to focus the radiation into a parallel beam.

Models of antennas usually used at longer wavelengths can also be tested. Figure 7 shows the recording which was made by scanning in a plane just grazing a single wire antenna about ten wavelengths long.

Problems in physical optics can be investigated in similar fashion. Figure 8 shows how radiation was focused by a pair of polystyrene lenses. While these lenses were not designed to give perfect focus,

the recording is illustrative of the limit to attainable spot size which is set up by the wavelength and angle of convergence of the radiation.
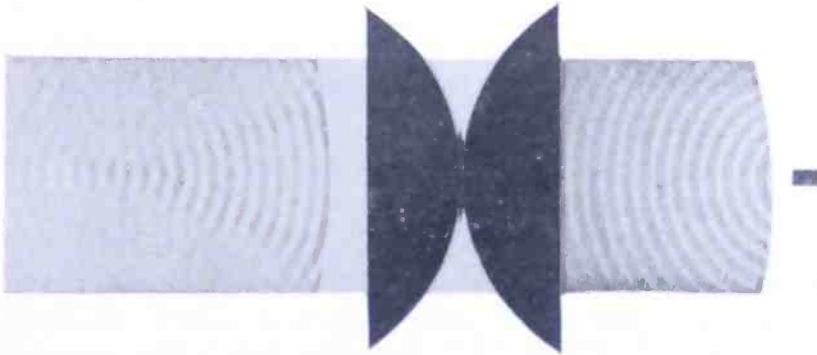
Fig. 8—Waves focused with lenses.

The refractive index of a dielectric (which is the square root of its dielectric constant) can be measured very easily. A sheet of the material is placed between the source and the probe, and the resulting displacement of a phase front is measured. The refractive index is $1 + S/T$, where S is the added phase delay and T is the thickness of the sample. When care is used in making the adjustments, it is possible to observe even the small phase shift resulting from interposing a sheet of paper, or blowing one's humid breath into one of the wave-guides.

ACKNOWLEDGMENTS

---

[1] *Engineering Experiment Station News*, Ohio State University, Vol. XVIII, No. 5, December, 1946.

PRECISION DEVICE FOR MEASUREMENT OF PULSE WIDTH AND PULSE SLOPE*

By

H. L. MORRISON

formerly with

Engineering Products Department, RCA Victor Division,
Camden, N. J.

Summary—A device for measuring pulse widths directly in microseconds, in terms of dial rotation necessary to move a marker-dot along the trace of the waveform on an oscilloscope, is described. The dial system used provides an effective scale length of fifty feet, with a nominal calibration factor of 0.0132 microseconds per dial division for pulses having a repetition rate corresponding to the horizontal scanning frequency in present-day commercial television equipment. A limitation is the fact that the unit is essentially a single-frequency device, and its applications are therefore restricted to television and other equipment in which the pulses to be measured have the same repetition rate, or integral multiple thereof.

INTRODUCTION

ONE of the problems which has always been somewhat difficult and tedious in television measurement technique[1,2] is that of determining accurately and rapidly the slope and duration of waveforms.

It is of interest to outline earlier methods used to measure pulses. One method depends on having a linear horizontal sweep on the oscilloscope which is used for making the measurement. The wave to be measured is applied to the vertical amplifier of the oscilloscope, and the horizontal sweep rate is adjusted to give one or two complete traces. By direct measurement, the width of a pulse can be determined as the ratio between the length of the pulse being studied and the total length of the complete trace cycle. It is apparent that the linearity of the horizontal sweep directly influences the accuracy of the measurement. It is also apparent that, as the width of the pulse becomes small compared with the total cycle width, the precision of measurement becomes inherently poor. The convenience of making pulse-width measurements in this manner is offset by the resultant inaccuracies.

A better method which has inherently high accuracy and which is not influenced by deflection linearity in the oscilloscope is that of applying a synchronized, high-frequency sine wave to the control grid of

---

* Decimal Classification: R583 × R200.

the cathode-ray tube so that the observed trace is formed by a series of dots.[1,2] Knowing that the time interval between adjacent dots equals the reciprocal of the frequency applied to the grid, the width of a pulse applied to the vertical amplifier is obtained by counting the number of dots which form the pulse. For example, if a 10-megacycle signal is applied to the grid of the cathode-ray tube, the interval between any two marker-dots is 0.1 microseconds. If a pulse being measured persists for 50 dots, it is thus known to be five microseconds wide. This method is subject to three annoying features: it is tedious and difficult to count a large number of dots without making an error in the counting; with pulses having steep edges, it is difficult to estimate intervals in terms of fractions of a dot; and it is often difficult to synchronize the marker-dots with the wave being measured. Without synchronization, the dots either disappear in a blur or else "jitter" back and forth so that they cannot be counted accurately.

Because of these difficulties, a circuit has been developed which generates a narrow marker-pulse whose phase can be controlled with respect to the wave being measured, and whose repetition rate is the same as the wave. The narrow marker-pulse is applied to the grid of the cathode-ray tube with such a polarity as to cut off the electron beam. Therefore, a single black dot appears at some point on the trace. The phase of the marker-pulse is controlled by means of a calibrated handwheel. The wave to be measured is applied to the vertical amplifier of the oscilloscope, and the handwheel is rotated to move the marker-dot between any two desired points on the wave. The interval, in microseconds, between the two points is found by noting the number of dial divisions traversed by the handwheel and multiplying by a fixed calibration factor. For example, in the unit to be described, 4800 dial divisions represent 360 degrees of phase shift at the frequency used for horizontal scanning in commercial television equipment — 15.75 kilocycles. A repetition rate of 15.75 kilocycles corresponds to a repetition time of 63.492 microseconds. Therefore, each dial division corresponds to 0.0132 microseconds.

APPLICATIONS

Applications of this device to measurements of pulse-width and rise-time are quite evident. Such measurements can be made accurately

---

[1] R. A. Monfort and F. J. Somers, "Measurement of the Slope and Duration of Television Synchronizing Impulses", *RCA REVIEW*, Vol. VI, No. 3, pp. 370-389, January, 1942.

[2] R. D. Kell, A. V. Bedford and H. N. Kozanowski, "A Portable High-Frequency Square-Wave Oscillograph for Television", *Proc. I.R.E.*, Vol. 30, No. 10, pp. 458-464, October, 1942.

and rapidly with very little chance of error. Another application is the measurement of time-delay in a cable or a network. A pulse is applied to the sending end of the cable and the marker-dot is moved to one edge of the pulse. The input to the vertical amplifier of the oscilloscope is then transferred to the other end of the cable or network and the marker-dot is moved until it falls on the same edge of the pulse. The time-delay, in microseconds, in the cable or network equals the number of divisions the handwheel is rotated multiplied by 0.0132.

A picture of the unit is shown in Figure 1. The handwheel itself is marked with one hundred equally spaced divisions on its periphery. A Veeder counter, located directly above the handwheel, is geared to

Fig. 1—Photograph of the measuring device.

it, and moves one division for each revolution of the handwheel. The shaft of the handwheel is connected to the phase-shifting device by a worm-gear assembly that has a reduction of 48 to 1. The diameter of the handwheel is four inches, which makes the effective scale length for 4800 divisions equal to slightly over fifty feet. Backlash is reduced to a negligible amount by the use of a spring-loaded scissor gear in the reduction-gear assembly. The overall accuracy of the unit, and the reason for using the seemingly arbitrary value of 4800 divisions, will be discussed in a later section.

TECHNICAL DETAILS

A block diagram of the unit is shown in Figure 2. The waveforms existing in various sections of the circuit are also shown. The opera-

tion is explained briefly as follows. A driving pulse is applied to a sine-wave oscillator so as to lock it in with a television synchronizing generator at the horizontal scanning frequency, 15.75 kilocycles. The oscillator output is applied through a resonant filter to the grids of two separate amplifiers. The output of one amplifier is brought out to a coaxial connector labelled CRO SWEEP and provides a sine-wave horizontal sweep for the oscilloscope which is synchronized with the driving pulse. A sinusoidal sweep has certain advantages over a linear sweep when narrow pulses (25 per cent of the period or less) are to be examined. Providing that the sweep is so phased that the pulse occurs near the center of the sweep trace, the pulse is spread out 3.14 times wider than when using a linear sweep. The phase of the sine-
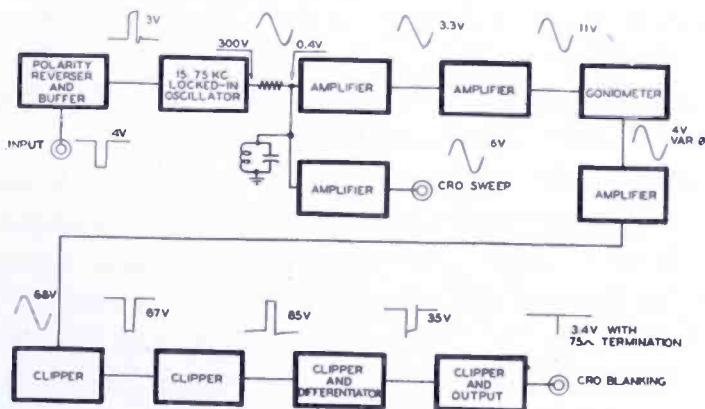
Fig. 2—Block diagram of the equipment.

wave sweep voltage supplied by the unit is such that any pulse whose phase corresponds to that of the driving pulse previously mentioned (which is usually the case in television work) will occur near the center of the sweep trace. The phase of the sweep can be varied over an angle of 60 degrees by adjusting the tuning of the locked oscillator, without losing synchronization.

The output of the second amplifier is used to drive a goniometer which is used as the phase-shifting device in this unit. The goniometer consists of two similar coils fixed mechanically at 90 degrees with respect to each other and excited by sinusoidal currents which are equal in amplitude and 90 degrees apart in phase. This much of the goniometer is similar to the armature of a two-phase alternating-current motor; therefore, a rotating magnetic field is produced. A third or pickup coil is so arranged that its angular position with respect to the first two coils can be varied. A sinusoidal voltage is induced

in this third coil by the rotating magnetic field. The phase of this voltage with respect to the output voltage of the amplifier which drives the armature coils of the goniometer is determined, in the ideal case, solely by the angular position of the pickup coil. Details of the method of obtaining the quadrature currents for armature excitation, and of the adjustment procedure, are discussed in the Appendix. In the unit shown in Figure 1, a small two-phase selsyn, the Bendix AY-120-D "Autosyn Resolver," is used as a goniometer. The two windings on the physical rotor are used for the armature windings, and one of the two coils on the stator is used as the pickup coil.

The resonant filter between the oscillator and amplifier is required to remove harmonic distortion in the output of the oscillator. The circuit used to provide the armature currents produces currents which are 90 degrees out of phase at only one frequency. Therefore, harmonics in the wave used to drive the goniometer must be greatly attenuated if variation in the calibration constant (0.0132 microseconds per division) is to be held to a minimum.

The output of the pickup coil of the goniometer is amplified and clipped in the following four stages to form a rectangular pulse as shown in Figure 2. Differentiation of this rectangular pulse is caused by a critically-damped inductance in the plate circuit of the fourth stage, and one of the two "spikes" resulting from the differentiation is clipped off in the grid circuit of the output stage. The resultant output voltage is therefore a single narrow spike of negative polarity, whose repetition rate is 15.75 kilocycles, and whose phase corresponds to the angular position of the goniometer rotor. The spike is approximately 0.15-microsecond wide at its base, and therefore contains harmonic components located in the band between 15 kilocycles and 5 megacycles. The output current is sufficient to develop 3.4 volts across a 75-ohm load.

The output of the pulse-measuring device is usually connected to the blanking amplifier in the oscilloscope by means of a terminated 75-ohm coaxial cable. The blanking amplifier should have a bandwidth of at least 4 megacycles if a narrow marker-dot is to be obtained. If the oscilloscope does not have a good blanking amplifier, the control grid of the cathode-ray tube can be connected to the output terminal through as short a length of cable as possible, and the termination on the cable made as low as possible without extinguishing the marker-dot. The marker-dot will be considerably wider when a large terminating resistance is used, but one edge of the dark space can be used as the reference point when making measurements.

With a good blanking amplifier, the apparent width of the marker-

dot is approximately 0.10 microsecond, which is about as narrow as can be accommodated on a five-inch oscilloscope with 15.75-kilocycle horizontal sweep. The apparent width of the marker-dot is of course dependent on the scanning speed of the cathode-ray beam, and appears to be much wider when it falls on the vertical edge of a pulse than when it falls on a horizontal portion of the same pulse. However, if the marker-dot were much narrower, it would be difficult to locate unless it did happen to fall on the edge of a pulse.

A schematic diagram is shown in Figure 3. The driving pulse which is used to synchronize the oscillator is usually the horizontal drive signal provided by a television synchronizing generator which
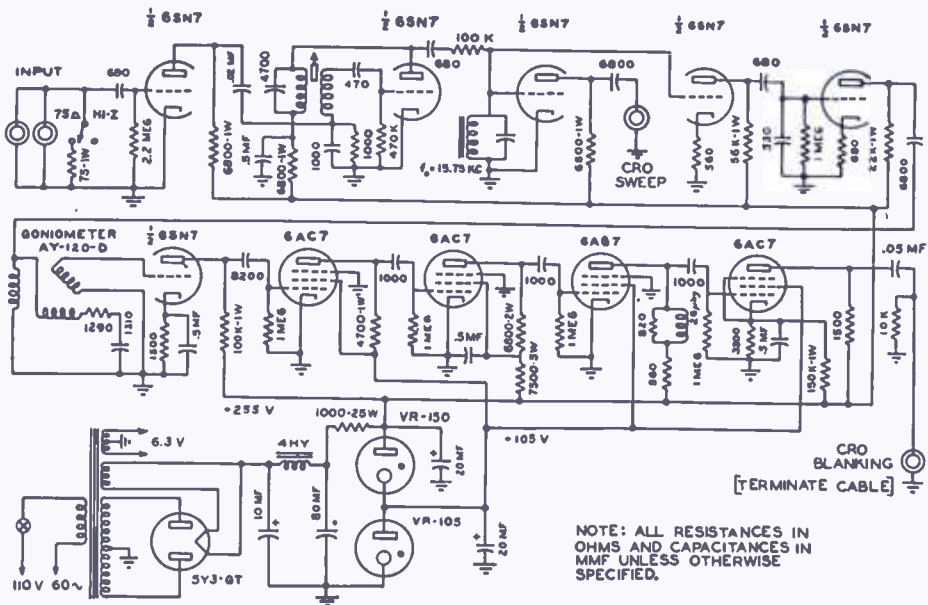
Fig. 3—Schematic diagram of the equipment.

produces standard RMA (Radio Manufacturers Association) synchronizing signals. A switch on the front panel selects the termination for the input terminals, for either bridging (high impedance) or terminated (75 ohms) operation. The first triode reverses the polarity of the input signal and provides isolation between the input circuit and the oscillator. A positive-polarity pulse is applied to the grid circuit of a conventional tuned-plate, grid-tickler type of oscillator for purposes of synchronization. As previously explained, a resonant filter is used to remove harmonic distortion in the oscillator output. A parallel-resonant circuit is used as the common input circuit for the two amplifiers following the oscillator. A 100,000-ohm resistor in series with the coupling capacitor causes high attenuation between

oscillator plate and amplifier grids at frequencies other than resonance. A tuned circuit having a very low inductance-capacitance ratio is used in order to obtain a sharply selective response characteristic.

The stages following the goniometer are conventional resistance-coupled amplifiers in which clipping occurs as a result of driving the grids beyond cut-off. The tube in the fourth stage following the goniometer, being a pentode, supplies rectangular pulses of current to its plate-load impedance. The rapid rate of change of current at each edge of the pulse develops a relatively large voltage across the inductance, which, with the associated shunt capacity contributed by the tubes and circuit components, has a self-resonant frequency of 6.5 megacycles. The two resistances in series and in shunt with the inductance critically damp this resonant circuit so that only a single half-cycle of oscillation occurs at each edge of the pulse. The series resistance also functions to produce a portion of the pulse itself in the plate circuit. Hence, the voltage which drives the grid of the output tube consists of a rectangular pulse having "overshoot spikes" on each edge. This waveform is illustrated in Figure 2. The purpose of such a waveform is to provide an easily-obtained pedestal for the positive-polarity half-cycle of oscillation, or spike. In the output stage, which is also a clipper, all but the positive-polarity spike falls below plate current cut-off on the tube's grid-voltage vs. plate-current characteristic. Hence, the voltage developed across the output-load resistance (which is usually a terminated cable) is a single spike of negative polarity. Regulated B voltages of 255 volts and 105 volts are obtained from a VR-150 and a VR-105 tube connected in series across the output of the self-contained power supply.

The circuit shown in Figure 3 represents only one of several methods that could be used to obtain the same or improved results. For example, the synchronized oscillator might be eliminated by forming sine waves directly from the input pulse. This could be done by limiting, integrating, and then passing the input pulse through several cascaded resonant filters. This would be advantageous in that phase variations of the input pulse could be accommodated, whereas they are not in the present arrangement. The effect of phase variations is discussed in the following section.

ACCURACY AND CALIBRATION

It has been stated that each dial division represents 0.0132 microseconds of marker-dot travel. In the ideal case this calibration factor does not vary; in the unit shown in Figure 1, the variation is shown

in Table 1. This variation is apparently due to mechanical asymmetry in the goniometer which causes the phase of the voltage induced in the pickup coil to differ from the exact angular position of the coil. This statement is made on the assumption that the armature of the goniometer is supplied with sinusoidal currents which are equal in amplitude and exactly 90 degrees apart in phase. Methods of obtaining this condition are discussed in the Appendix.

Before discussing the method of making the calibration, it should be pointed out that it is necessary to unlock the television synchronizing generator from synchronization with the 60-cycle power line when using or calibrating the device. Although the oscillator in the device is synchronized with the repetition rate of the input pulse, it cannot follow variations in the *phase* of the input pulse if such variations occur between consecutive pulses. To illustrate this point, suppose that it is desired to measure the width of the retrace or kick-back pulse in a horizontal deflection circuit, and horizontal-drive signal is used to synchronize the pulse-measuring device. With the kick-back pulse being measured applied to the vertical amplifier of an oscilloscope, and the output of the device connected to the blanking amplifier of the cathode-ray tube, the marker-dot is moved to the desired position on the trace by turning the handwheel. If the synchronizing generator is locked to the power line, the position of the marker-dot relative to the kick-back pulse under measurement will drift back and forth about the desired position because of variations in the phase of the master oscillator due to the action of the automatic-frequency-control circuit. On the other hand, when the synchronizing generator is unlocked from the line and the master oscillator left free-running (in the case of the latest-model synchronizing generators the master oscillator can be switched to crystal-control), the marker-dot remains stationary.

The second source of error in measurements made with this device, and one which cannot be eliminated by means of a calibration table, is that due to the effects of temperature on the resistance of the goniometer armature coils. From the equations and vector diagrams shown in the Appendix it can be seen that the constants of the resistance-capacitance circuit which provides the quadrature current depend upon the resistance of the armature coils. Therefore, if the coil resistance changes with temperature, the currents in the two armature coils will become unequal in amplitude and have a phase displacement different from 90 degrees. In the unit described, a one-hour warm-up period allows temperatures to stabilize sufficiently to use the calibration table with accuracy.

Table 1—Calibration Table.

Operating Frequency: 15.75 kc   Period: 63.49 μsec
Calibrating Frequency: 12 × 15.75 : 189 kc   Period: 5.291 μsec
Calibrating wave has 12 positive and 12 negative peaks:
                                          Period: 2.645 μsec/peak
One rotation of goniometer equals 4800 dial divisions. With 24 calibration peaks, the distance between peaks is 200 dial divisions under ideal conditions. Therefore, the nominal calibration factor is 2.645 ÷ 200: *.01322 μsec/division.*

Peak No.	Reading	Difference	μsec/division 2.645 ÷ difference	Measured width of 2.645 μsec pulse	μsec error
1.	05758				
		201	.01317	2.634	— .01
2.	05557				
		200	.01322	2.644	.00
3.	05357				
		194	.01364	2.728	+ .08
4.	05163				
		198	.01336	2.672	+ .03
5.	04965				
		200	.01322	2.644	.00
6.	04765				
		205	.01290	2.580	— .06
7.	04560				
		201	.01317	2.634	— .01
8.	04359				
		206	.01284	2.568	— .08
9.	04153				
		206	.01284	2.568	— .08
10.	03947				
		204	.01298	2.596	— .05
11.	03743				
		197	.01342	2.684	+ .04
12.	03546				
		202	.01310	2.620	— .03
13.	03344				
		203	.01303	2.606	— .04
14.	03141				
		210	.01260	2.520	— .13
15.	02931				
		204	.01298	2.596	— .05
16.	02727				
		204	.01298	2.596	— .05
17.	02523				
		198	.01336	2.672	+ .03
18.	02325				
		194	.01364	2.728	+ .08
19.	02131				
		185	.01430	2.860	+ .21
20.	01946				
		189	.01400	2.800	+ .15
21.	01757				
		196	.01350	2.700	+ .05
22.	01561				
		201	.01317	2.634	+ .02
23.	01360				
		200	.01322	2.644	.00
24.	01160				
		203	.01303	2.606	.04
1'	00957				

In the case of this unit, calibration was aided by the fact that the synchronizing generator (Type TG-1A) had a crystal-controlled master oscillator. The crystal frequency of this generator is six times that of horizontal deflection, or 94.5 kilocycles. A frequency doubler was constructed, the grid being connected to the plate circuit of the crystal oscillator, and the plate circuit resonated to 189 kilocycles. With the 189-kilocycle signal from the doubler connected to the vertical amplifier of an oscilloscope, and with 15.75-kilocycle sine-wave horizontal sweep obtained from the CRO SWEEP terminals of the measuring device, the trace will show twelve complete sine waves. Consequently there will be 24 peaks which serve as accurately known calibration points. The period of a 15.75-kilocycle wave is 63.492 microseconds. The spacing between adjacent peaks will be 1/24 of this, or 2.6455 microseconds. One of the advantages of having 4800 dial divisions now becomes apparent; with 24 calibration points the handwheel would be rotated exactly 200 divisions to move the marker-dot from one point to the next if the goniometer had ideal characteristics. The calibration factor (in microseconds per division) which applies to a given section of the dial is then found by dividing 2.645 by the number of divisions traversed in moving the marker-dot from one peak to another. The list of calibration factors is given in the fourth column of Table 1. A further advantage of using 4800 dial divisions is that precision gears with 48 teeth are standard items, whereas gears having 50 teeth are not. Since the goniometer is continuously rotatable, and since the position of the goniometer rotor repeats itself every 4800 divisions, it is necessary to have a three-place Veeder Counter in order to know to which group of 4800 divisions the calibration table applies. For example, the goniometer position corresponding to a dial reading of 05758 does not coincide with the position corresponding with dial readings 15758 or 25758.

CONCLUSION

The pulse-measuring device which has been described provides a method of measuring pulse widths and slopes which is rapid and convenient to use, which is independent of oscilloscope linearity, and which has an accuracy that is comparable with the best of former methods. The most serious limitation is that it is inherently a single-frequency device, and hence can measure only those pulses that have a repetition rate equal to the frequency for which it is designed, or integral multiple of that frequency. In television work, most of the waveforms encountered are synchronized with either the horizontal

or the vertical scanning rates and the limitation mentioned is not too serious.

APPENDIX

Method of Obtaining Quadrature Currents for the Armature of the Goniometer

From the theory of two-phase alternating-current machines it is known that a rotating magnetic field having constant angular velocity and uniform amplitude can be produced by exciting two mutually-perpendicular coils with sinusoidal currents which are equal in amplitude and displaced 90 degrees in phase from each other.

The goniometer armature is represented schematically in Figure 4. Resistances r_1 and r_2 represent the internal resistances of coils L_1 and L_2. An external resistance, R, and capacitance, C, are placed in series with the second coil, as shown in the Figure. The relation between the current in coil L_1 and line voltage, E, are illustrated in the vector diagram, Figure 5. Similarly, the relation between coil current and line voltage for the second coil is shown in Figure 6. Since the same line voltage is applied to both branches of the circuit, the two vector diagrams can be superimposed by making the vectors representing E coincide, as in Figure 7. From this figure it may be seen that the coil currents, I_1 and I_2, are equal in magnitude and 90 degrees apart when the constants of the circuit are such that the following relations hold:

$$I_1 X_{L_1} = I_2(R + r_2) \quad (1) \qquad I_1 r_1 = I_2 X_C - I_2 X_{L_2} = I_2(X_C - X_{L_2}) \quad (2)$$

When Equations (1) and (2) are true: $\qquad I_1 = I_2 = I \qquad (3)$

Therefore the currents on both sides of Equations (1) and (2) can be canceled. Since the two coils are similar:

$$X_{L_1} = X_{L_2} = X_L \quad (4) \qquad\qquad r_1 = r_2 = r \quad (5)$$

Solving Equation (1) for R and Equation (2) for X_C:

$$R = X_L - r \quad (6) \qquad\qquad X_C = r + X_L \quad (7)$$
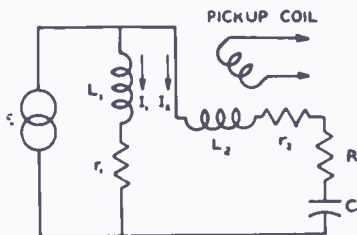
Fig. 4 — Schematic diagram of goniometer armature.
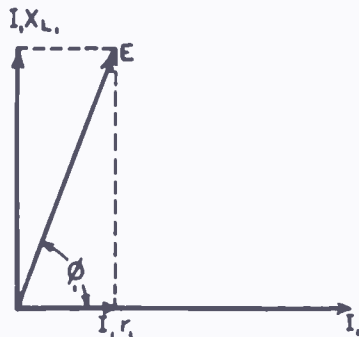
Fig. 5—Current and voltage relation in coil L_1.
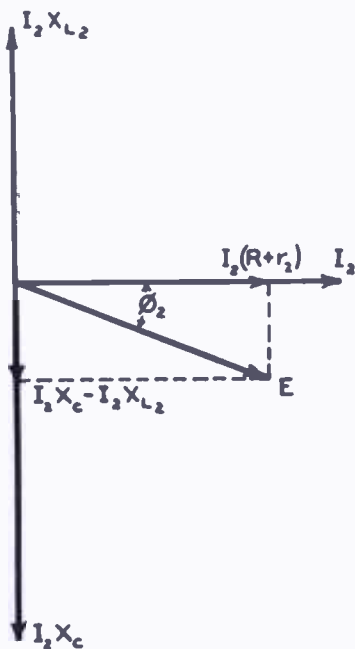
Fig. 6—Current and voltage relation in coil L_2.
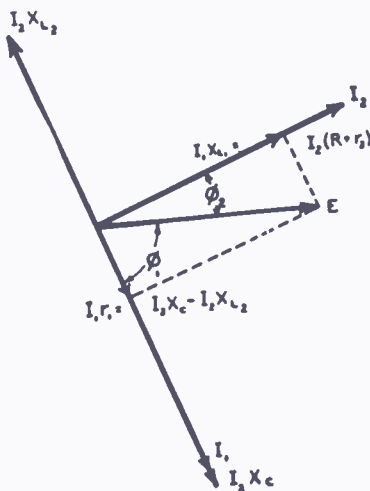
Fig. 7 — Superposition of Figures 5 and 6.

Experimental method of determining R and C.

Even with highly accurate initial measurements of X_L and r, a final experimental check of the correctness of the values for R and C as calculated by Equations (6) and (7) is practically mandatory because the constancy of the calibration factor is directly dependent upon the uniformity of amplitude and angular velocity of the rotating field.

These values can be checked experimentally by the following method. Horizontal sweep for an oscilloscope is taken directly from the plate of the tube which drives the goniometer. The pickup coil is connected to the input of the vertical amplifier in the oscilloscope. The reduction gear assembly is temporarily disconnected from the shaft of the goniometer. As the shaft is rotated, the pattern on the oscilloscope will be a changing Lissajou figure corresponding to the projection of two sine waves having the same frequency and a phase difference which varies between zero and 360 degrees; i.e., the trace will vary from the circular, to the elliptical, to the linear as the shaft is rotated. When R and C have the correct values, and if mechanical asymmetry in the goniometer is negligible, the voltage induced in the pickup coil (which corresponds to the vertical dimension of the trace) will remain constant as the shaft is rotated. Therefore, R and C are alternately varied in one direction and then the other until the vertical deflection remains as constant as possible as the goniometer is rotated through a full 360 degrees. During the course of adjustments it will be seen that the high and low points in the vertical deflection occur at varying locations along the horizontal axis as R and C are changed. By correlating these locations with the corresponding changes in R and C, the correct values can be arrived at more quickly than by merely using the straight trial-and-error method.

INPUT IMPEDANCE OF A FOLDED DIPOLE*†

By

W. van B. Roberts

Research Department, RCA Laboratories Division,
Princeton, N. J.

Summary—The folded dipole has become a familiar expedient to provide increased input impedance over that of a dipole antenna and permit more efficient transmission line matching. The input impedances of standard configurations, are well known; however there has been no convenient way of determining the actual input impedance in the general case of elements of arbitrary size, shape, number and arrangement. This paper presents an analysis which attempts to provide necessary formulas and a physical picture of the operation of the folded dipole. The presentation is in two parts—folded dipole with equal elements, and folded dipole with unequal conductors.

Introduction

THE folded dipole has become a familiar expedient for increasing the input impedance of a dipole antenna to a value more suitable for matching a transmission line. It is usually made up as shown in Figure 1, the overall length being approximately the same as for an

Fig. 1—Folded dipole, auxiliary element same size as driven element.

Fig. 2 — Folded dipole, two auxiliary elements.

ordinary half wave dipole, and the auxiliary element being of the same size as the driven element. It is well known that this arrangement has four times the impedance of a simple dipole. But if two auxiliary elements are used, for example as shown in Figure 2, the impedance is multiplied by something more like nine. And finally it is generally known in a qualitative sort of way that if the two dipoles in Figure 1 are of different diameters, the impedance multiplier is no longer four, but more or less than four according as the auxiliary element is of greater or less diameter than the driven element. The arrangement

---

of Figure 2 is in fact merely the parallel connection of two thin auxiliary elements to obtain the effect of a single auxiliary element of larger diameter.

There appear to be no formulas readily available in the literature which give the impedance in the general case of elements of arbitrary size, shape, number and arrangement. The following analysis is an attempt to provide such formulas and also to furnish a physical picture of the operation of a folded dipole.

Folded Dipole With Two Equal Elements

First of all the problem can be simplified somewhat by cutting the folded dipole in half by a ground plane as shown in Figure 3. Such an antenna is sometimes called a folded unipole and its operation and impedance characteristics are exactly the same as for the folded dipole except that all impedances are cut in half. The amount that the impedance is multiplied by folding is the same in both cases.
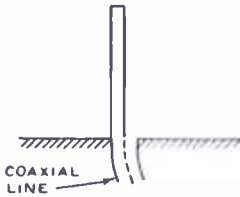
Fig. 3 — Folded dipole, with ground plane (folded unipole).
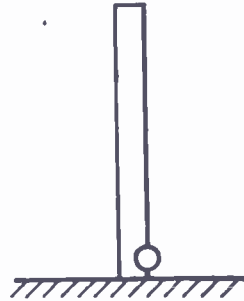
Fig. 4—Folded unipole, with co-axial feed line replaced by small radio-frequency generator.

The coaxial feed line of Figure 3 can be replaced for purposes of analysis by a small radio-frequency generator connected between ground and the lower end of the driven element, as shown in Figure 4. Assuming a known voltage for this generator the problem of finding the input impedance of the antenna reduces to finding the current flowing into the lower end of the right hand element.

To do this an expedient will now be introduced which forms the basis of the present method of analysis.* The single generator of

---

* Subsequent to the completion of the calculations presented in this paper, a book TRANSMISSION LINES, ANTENNAS AND WAVE-GUIDES by King, Munro and Wing has been published which employs essentially the same "trick" for the analysis of the folded dipole composed of similar conductors.

Figure 4 is replaced by three generators connected as shown in Figure 5. Since these generators are purely imaginary they can have zero internal impedance and perfect regulation. (In order to make room for the generators in the diagram the antenna elements have been drawn much too widely separated in comparison to their length. Their spacing in actual practice is usually very small compared with their length.) The generators all operate in the same phase, the polarities being indicated by arrows, and the voltages are each *e*.

It will be seen that the left hand generator and the lower generator are opposing each other with respect to the lower end of element 2 so that this element is grounded as far as any impressed voltage is con-
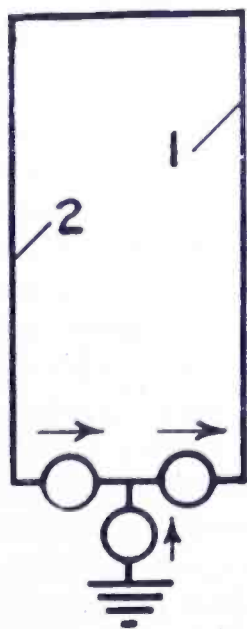
Fig. 5—Folded unipole, with single generator of Figure 4 replaced by three similar generators.

cerned. The lower and right hand generators however impress a voltage 2*e* on the lower end of element 1. Thus Figure 5 is strictly equivalent to Figure 4. The reason for putting in the extra generators is that it is relatively easy to obtain the currents produced by the individual generators, and then by the principle of superposition add these currents to obtain the actual current entering the lower end of element 1. Assume that there is no voltage (for the moment) in the lower generator. There is then only the voltage 2*e* acting between the lower ends of the two elements. Since these elements form a quarter-wave line shorted at the far end, their impedance is very high and only a negligibly small current will flow into element 1. Next assume

there is voltage only in the lower generator. Then, since the lower ends of the elements are shorted together (by the zero internal impedance of the generators) the two elements act as a simple quarter-wave radiator made up of the two elements connected in parallel. If R is the radiation resistance of this radiator the lower generator will supply a total current e/R to this composite antenna. But by symmetry this current divides equally between the two elements so that the current entering element 1 is $\frac{1}{2}e/R$. Thus if all the generators are working at once the voltage impressed on element 1 is $2e$ while the current entering it is $\frac{1}{2}e/R$ plus a negligibly small amount produced by the upper generators acting alone. The input resistance to element 1, being the ratio of voltage impressed to resulting current flow, is therefore approximately $4R$.

If the two elements are close together the value of R will be very little different from that of a single conductor radiator, so that the impedance multiplication due to folding is approximately 4. This result was known in advance but the foregoing proof has been carried through because it prepares the ground for the more difficult case of unequal elements, and also because it brings out the mechanism of the folded antenna in a way that throws light on some other questions. For one thing it can now be seen how such a folded antenna can act as more of a wide band antenna than the simple dipole. Assume that the operating frequency is lowered a little below its resonant value. Then the antenna system is too short and the lower generator acting alone produces a leading current flow into element 1. But the upper generators acting alone are now operating on a line shorter than a quarter wave long and hence produce a lagging current flow into element 1. Furthermore the impedance of the electrically shortened line is no longer extremely high so that the lagging current is no longer negligible. The current entering element 1 is thus composed of one component which becomes smaller and more leading as the frequency is lowered, plus another component which becomes larger and more lagging as the frequency is lowered. The resultant current tends to be more nearly constant and in phase with the driving voltage over a band of frequencies than in the case of the simple dipole. A similar result can be obtained by connecting an antiresonant circuit between the input terminals of a simple dipole. In fact the broad band characteristics of the folded dipole should be the same as those of a hypothetical antenna made up as shown in Figure 6, using four pieces of transmission line each shorted at the far end and each identical with one half of the folded dipole. The input admittance of Figure 6

is simply the sum of the admittances of the horizontal radiating dipole and of the vertical "half-wave frame."

The analysis also gives some idea of the effect of varying the spacing between elements. For example, if the spacing is extremely small the impedance between the lower ends of the elements will be lower and will fall rapidly as the frequency departs from exact resonance. The upper generators acting alone will then produce a considerable push-pull flow of current in the elements. This current adds nothing to the radiation and merely wastes power.

The effect of very wide spacing is more difficult to predict because the validity of the present analysis is evident only where the spacing can be considered very small. Following the present theory and making the plausible assumptions that the radiation resistance of two elements connected in parallel will be less than that of one alone, and that as
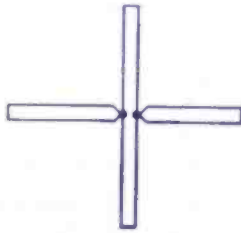
Fig. 6—Hypothetical antenna, with four transmission lines shorted at far end and each identical in length with one-half of the folded dipole.

the spacing is increased the element length will have to be decreased to compensate for the increased length of the shorting bars, the conclusion would be that increase of spacing decreases the driving point resistance. This conclusion has been verified experimentally by Mr. O. M. Woodward* in a series of experiments in which the spacing was increased until the folded dipole became a square loop fed in the center of one side. In these experiments it was found that the perimeter of the antenna for resonance remained nearly constant and approximately one wave length. If the spacing were to be still further increased the antenna would ultimately become a two wire transmission line a half wave long and shorted at the far end, in which configuration the radiation resistance would, of course, be extremely low. It thus appears that for ordinary narrow band operation very wide spacings are perfectly satisfactory if the resulting reduction in resistance is not objectionable. However, to approach as closely as possible to a particular desired broad band characteristic it is perhaps worth while to experiment with the spacing.

---

* Research Department, RCA Laboratories Division, Princeton, N. J.

In concluding the discussion of the case of two equal elements it is interesting to consider the use of two-wire transmission lines, of the type where the wires are imbedded in a flexible dielectric ribbon, as the elements of a folded dipole. The wave length of push-pull currents in such a line is considerably less than in air. With the currents flowing in the same direction in both conductors the wave length is more nearly—usually *very* nearly—equal to its value in air. Hence it would appear impossible to cut the antenna so that one has both push-pull resonance and also at the same time parallel resonance of the radiator. If the length (of the unipole) is made the usual approximate quarter wave so that the lower generator will work into a purely resistive radiation load, then the upper generators will be working into a line more than a quarter-wave long electrically and hence acting as a capacitive reactance. The resultant input impedance is therefore capacitive. On the other hand if the unipole is shortened until push-pull resonance exists, the radiator will be too short and the input impedance is again capacitive.

A way out of this dilemma would be to connect the conductors at the top of the antenna through a condenser instead of shorting them together. The antenna length would be chosen to provide a pure resistance load for the lower generator acting alone, and the condenser chosen to resonate with the excess length of the elements as excited in push pull. In this way the upper generators again work into a high impedance but in this case it is the equivalent of a half-wave line open at the far end. To illustrate, suppose the wave length in 300-ohm "ribbon" is 82 per cent of the wave length in air, and that the resonant length of a dipole composed of this line with conductors connected in parallel is 95 per cent of a half wave. Then for push-pull operation each side of the dipole is electrically about 1.16 quarter-waves long. The excess 0.16 quarter wave will react like a short circuit if it is terminated by a condenser whose reactance is 300 tan (0.16 times 90 degrees), or about 77 ohms. This calls for a condenser of 69 micro-microfarads per meter of the operating wave length. That is, if the antenna is designed for ten-meter operation the capacity required would be 690 micromicrofarads.

Another, and even simpler scheme, is to make the dipole elements of proper length for radiation, and then to short them together at the point that produces quarter-wave resonance for push-pull excitation. In the case discussed above, this would be about 86 per cent of the distance to the ends. In addition, the ends may be connected together, if desired.

Folded Dipole with Unlike Conductors

Following the method previously used, consider the equivalent circuit Figure 7 which differs from Figure 5 in that the generators are no longer all alike. The lower and left hand ones must still be alike in order to put zero voltage on the auxiliary element 2, but the right hand generator voltage must now be so chosen that no current will flow through the lower generator when it is not producing voltage. The determination of this voltage e_1 is one of two essentials to the solution of the problem. The other is to determine how the current produced by the lower generator acting alone divides between the two elements. Neither of these questions was at all difficult in the case of equal elements because of its symmetry.

The electrical engineer, being used to dealing with impedances,
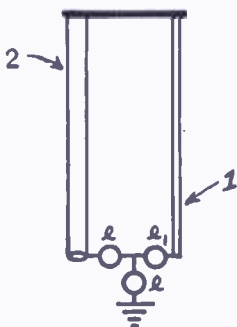
Fig. 7—Folded unipole, with single generator replaced by three dissimilar generators.

would be inclined to attack the problem by postulating that current produced by the lower generator will divide between the elements inversely as their impedances, while the ratio of the upper generator voltages will be the same as the ratio of their associated element impedances. This leads to a solution in terms of impedances but leaves the impedances undefined. Impedance definitions can undoubtedly be written which make the solution come out correctly, but such definitions do not appear obvious.

The physicist on the other hand, being more used to electrostatics, might say that the current will divide directly as the capacities of the elements, while the voltage ratio will be the inverse capacity ratio. This also leads to a solution in terms of undefined quantities, but a definition is perhaps somewhat more readily obtained.

First, the problem is solved in terms of the undefined capacities c_1 and c_2. This gives $e/e_1 = c_1/c_2$; the current entering element 1 is

the total current produced by the lower generator acting alone, multi-
plied by $c_1/(c_1 + c_2)$, neglecting the very small current produced by
the upper generators acting alone as explained in the case of equal
elements. The total current due to the lower generator alone is e/R
where R is the radiation resistance of the two elements connected in
parallel. The driving point impedance of the antenna is $(e + e_1)$
divided by the current entering element 1. From the foregoing it is
readily determined that the driving point impedance is

$$R \left(1 + \frac{c_2}{c_1} \right)^2$$

This appears to check with what is already known about various
cases. For instance if the elements are alike the impedance multiplier

(a)   (ℓ)
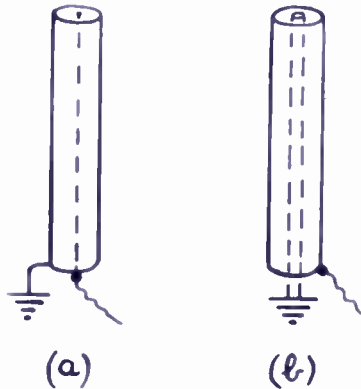
Fig. 8—Folded unipole, one unit completely enclosing the other.
(a) Driven element enclosed. (b) Auxiliary element enclosed.

is 4 while in a structure like Figure 2, if it is assumed that the two
auxiliary wires have twice the capacity of the driven wire, the im-
pedance multiplier is 9. But a question arises in the case of structures
such as shown in Figure 8 where one element completely encloses the
other. It is evident that the impedance of Figure 8-a is extremely
high and it is almost as evident that in Figure 8-b it is substantially
unaffected by the presence of the quarter-wave-long inner element.
If the formula is to be satisfactory it should take care of even these
extreme cases. It appears that the capacities must be defined more
precisely.

In a system composed of any two conductors,

$$E_1 = q_{11} V_1 + q_{12} V_2$$

$$E_2 = q_{12} V_1 + q_{22} V_2$$

where E_1 and E_2 are the charges on the conductors, V_1 and V_2 are their potentials, and the q's are constants determined by the geometry of the conductors. Let the two elements 1 and 2 of Figure 7 be the two conductors. When the lower generator is acting alone the two elements are connected together so that $V_1 = V_2$. Under these circumstances the equations give $E_1/E_2 = (q_{11} + q_{12})/(q_{22} + q_{12})$. This is the ratio of the charges that would be put on the two elements by a direct-current generator and it seems plausible that it should also represent the ratio of currents produced by the alternating-current generator. If so, this ratio is the precise definition of what was previously written as c_1/c_2. However, it is also necessary to determine what the electrostatic equations give for the unknown voltage ratio. If this voltage ratio (of the upper generators) is correct, no current will flow through the lower one. Hence equal and opposite charges must flow into the two elements. Therefore, setting $E_1 = -E_2$ in the electrostatic equations, it is determined that $V_1/V_2 = (q_{22} + q_{12})/(q_{11} + q_{12})$, which is the precise expression for what was previously written as c_2/c_1. Thus the original formula for input impedance is correct with the understanding that the ratio c_2/c_1 in the formula is to be defined as $(q_{22} + q_{12})/(q_{11} + q_{12})$.

The constants q_{11} and q_{22} are known as the coefficients of capacity of the elements 1 and 2 and are always positive while q_{12} is known as the coefficient of induction between them and is always negative. They may be measured or sometimes calculated but for present purposes it is sufficient to consider some of their properties from a physical and qualitative point of view.

From the equations it is evident that $(q_{11} + q_{12})$ is the ratio of charge to potential on element 1 when element 2 is at the same potential. This quantity is therefore of the nature of a capacity but with a special definition. A similar definition applies to $(q_{22} + q_{12})$. When two conductors are raised to the same potential no lines of force pass from one to the other. Hence if both conductors are at the same potential, the ratio $(q_{11} + q_{12})/(q_{22} + q_{12})$ is the ratio of the number of lines leaving conductor 1 (none of which go to conductor 2) to the number of lines leaving conductor 2 (none of which go to conductor 1). In case one conductor encloses the other, lines leaving the inner one have nowhere to go except to the outer one. Since no lines *can* go to the other conductor there can therefore be none leaving the inner one. Thus the ratio appearing in the impedance formula becomes zero if the auxiliary element is enclosed as in Figure 8(b) and becomes infinite if the driven element is enclosed as in Figure 8(a).

A formal solution has been obtained, which, using a particular definition for the ratio appearing in the formula, appears to give correct results in a number of cases where the results are already known. It also appears possible to write the formula equally precisely in terms of a ratio involving self- and mutual-inductance coefficients of the elements, but it is questionable if this would be any easier to evaluate in practice. Thus the exact formula, whether written in terms of capacities or inductances seems to be chiefly of academic interest. However, in case the two elements are spaced quite far apart in comparison with their diameters a practically usable approximate formula can be obtained as shown in the following paragraph.

First the equations are written for a system of three conductors:

$$E_1 = q_{11} V_1 + q_{12} V_2 + q_{13} V_3 \qquad\qquad E_2 = q_{12} V_1 + q_{22} V_2 + q_{23} V_3$$

$$E_3 = q_{13} V_1 + q_{23} V_2 + q_{33} V_3$$

Now, let $V_3 = 0$ and $E_1 = - E_2$ and $E_3 = 0$. As a result $(q_{22} + q_{12})/(q_{11} + q_{12}) = q_{23}/q_{13}$. A third conductor satisfying the above requirements can always be found as there must be an equipotential surface of zero potential between the oppositely charged elements and if this surface be materialized into a thin metal sheet it will not disturb any lines of force and hence can have no charge. It does however introduce the quantities q_{13} and q_{23} in the ratio given above. These quantities are what are commonly called the capacities "between" elements 1 and 2, and the sheet. Hence the problem has been transformed to finding the zero potential surface and the capacities between it and the elements. This is not difficult if the elements are well spaced, for the zero potential surface between two oppositely charged thin cylinders is approximately the infinite plane half way between their centers. The capacity between either element and this plane is twice the capacity between the element and its image in the plane, that is, between two similar elements. A formula is available for this but for the present purposes it is preferable to make use of the relation $ZC = 30$ in which Z is the characteristic impedance in ohms of a two-conductor air-dielectric line and C is the capacity between its conductors in cms per cm of line. This relation gives capacity in terms of characteristic impedance which is a familiar quantity to the radio engineer. To summarize the steps of the foregoing argument,

$$\frac{q_{22} + q_{12}}{q_{11} + q_{12}} = \frac{\text{capacity between element 2 and sheet}}{\text{capacity between element 1 and sheet}} = \frac{Z_1}{Z_2}$$

where Z_1 is the characteristic impedance of a line formed of two conductors each like element 1 and with the same center-to-center spacing as elements 1 and 2 while Z_2 is the characteristic impedance of a line similarly formed of conductors like element 2. Thus, for a folded dipole with well spaced elements

$$\text{Input impedance} = R\left(1 + \frac{Z_1}{Z_2}\right)^2$$

This formula can be readily applied, within its limitations, to numerical calculations. For example, assume element 1 is 0.1 inch in diameter while element 2 is 1.0 inch in diameter and the center-to-center spacing is 6.0 inches. Then Z_1 is approximately 575 ohms, Z_2 is 298 ohms and the multiplier is $\left(1 + \dfrac{575}{298}\right)^2$ or about 8.6. This result

Fig. 9—Single composite dipole, driven and auxiliary elements considered to be connected in parallel.

is interesting because it shows that a very large auxiliary conductor is required to get as large a multiplier as can be obtained by using two auxiliary wires of the same size as the driven element, as shown in Figure 2. For still larger multipliers it appears more practical to use several auxiliary conductors connected to form a cage more or less surrounding the driven element according as a more or less high impedance is desired.

CONCLUSION

A formula has been developed for the input impedance of a folded dipole composed of unequal elements. The formula appears to work correctly in various special cases. The method of derivation provides a physical picture of the operation of such antennas which is probably of more usefulness in practice than the formula.

The formula is applied as follows:

Determine the radiation resistance of the driven and auxiliary elements considered as connected in parallel to form a single composite dipole, as shown in Figure 9. This will not be much different from 70 ohms if the elements are fairly closely spaced, except of course that it

is subject to the usual effects of proximity to ground or other reflecting objects.

Multiply the above resistance by $(1 + C_2/C_1)^2$ where C_2/C_1 is the ratio of the number of lines of force leaving the auxiliary element to the number leaving the driven element when both elements are raised to the same potential. See Figure 10.

(The ratio C_2/C_1 is also the ratio of the capacities between the respective elements and an imaginary metal sheet located in the zero
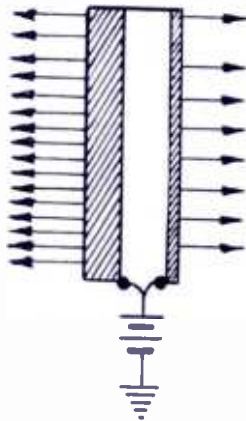
Fig. 10—Folded unipole, with both elements raised to the same potential.

potential surface which would be created by placing equal and opposite charges on the two elements.)

In the case of well spaced conductors the ratio C_2/C_1 may be replaced by Z_1/Z_2 where Z_1 is the characteristic impedance of a line formed of conductors each like element 1 and with the same center-to-center spacing as the actual elements, while Z_2 is the same except that the line is formed of conductors each like element 2.

COAXIAL TANTALUM CYLINDER CATHODE FOR CONTINUOUS-WAVE MAGNETRONS*†

By

R. L. Jepsen

formerly with
Tube Department, RCA Victor Division,
Lancaster, Pa.

Summary—Major factors affecting the design of cathodes for continuous-wave magnetrons are considered. A particular type of structure, the coaxial tantalum cylinder cathode, is analyzed in some detail and its merits and shortcomings discussed. An approximate method is developed for computing optimum geometry and maximum life. Application to a particular magnetron is described and other applications suggested.

INTRODUCTION

THE design of continuous-wave magnetrons is often limited by cathode life, which is chiefly a function of emission density and heat-dissipation requirements. For a particular wavelength of operation and power output, emission density required from the cathode of a continuous-wave magnetron may be adjusted, within limits, by varying certain tube parameters such as anode voltage, number of cavities, and anode height. Sufficient thermal dissipation must be provided to allow a given cathode to operate at proper emitting temperature when subject to electron back-bombardment. Consideration will be limited here to certain design features of a cathode for a given magnetron; i.e., anode geometry and total emission will be considered fixed.

DESIGN CONSIDERATIONS

The major factors affecting cathode design are:

(1) *Emission density:* This may be on the order of several amperes per square centimeter, particularly at short wavelengths. Most receiving tubes operate at current densities less than 0.3 ampere per square centimeter.

(2) *Geometry:* In the present state of the art, magnetron cathodes are cylindrical and concentric with the anode. Hats are em-

---

ployed at the ends of the cathode to minimize leakage currents (Figure 1). The emitting length of the cathode is approximately equal to the anode height, although in some cases it is desirable to shorten the emitting length. The approximate relation of the cathode diameter, d_c, to the anode diameter, d_a, is $d_c \simeq d_a \left(\dfrac{N-4}{N+4} \right)$, where N is the number of magnetron cavities.[1] The tube efficiency is somewhat improved if the cathode diameter is made up to 10 per cent less than the value given by this equation. Although a smaller cathode diameter contributes to higher oscillating efficiency, it also means greater emission density. The choice of the cathode diameter is actually a compromise between oscillating efficiency and emission density.
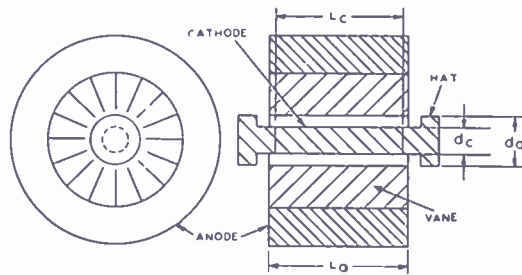
Fig. 1—Arrangement of magnetron anode and cathode.

(3) *Back-bombardment:* Three major effects arise due to the electrons which pick up energy from the oscillating field and return to the cathode. (a) A certain amount of power (back-bombardment power) is dissipated on the cathode surface. The minimum value of such power is about 5 per cent of the total anode input power but the value may rise to 10 or 20 per cent, or even more, depending upon various factors such as loaded Q and standing-wave ratio in the output line. In general, if the heating power supplied to the cathode is not reduced, back-bombardment will cause the cathode temperature to rise. To maintain a constant cathode temperature, heater power must be reduced as back-bombardment power increases. (b) There is evidence that the back-bombarding electrons may actually remove cathode material from oxide-coated cathodes thus effec-

[1] J. C. Slater, "Theory of the Magnetron Oscillator," MIT Radiation Laboratory Report, V-5S, August, 1941.

tively reducing the life of such emitters.[2] (c) Secondary emission may take place thus reducing required primary emission.

(4) *Life:* Cathode failure usually sets the limitation on tube life. Required or desired life may range from a very few hours to many thousands of hours, depending on the application.

(5) *Mechanical stability:* Regardless of application, the cathode should not sag, warp, or become misaligned or off-centered under operating conditions. For certain uses it may be feasible to operate the tube in a particular position which may prevent certain forms of mechanical distortion. Other applications may require operation in any position or the withstanding of vibration or shock.

(6) *Hum:* When unidirectional spirals of wire, such as tungsten or tantalum, are used for the cathode, there sometimes appears to be sufficient interaction between the steady magnetic field of the magnetron and the alternating magnetic field around the cathode (produced by the alternating current flowing through the cathode) to cause mechanical vibration of the cathode at a 60-cycle rate (or whatever the frequency of the cathode heating supply happens to be). Such mechanical vibration of the cathode gives rise to frequency modulation of the magnetron which, for many applications, cannot be tolerated. It may presumably be overcome by making the system sufficiently rigid mechanically, by heating the cathode with direct current, or by making the alternating magnetic field zero through the use of a double-wound spiral or coaxial construction.

(7) *Frequency drift:* Most types of emitters will gradually evaporate metal onto the vane tips of the magnetron anode. This deposit will in general give rise to a downward frequency drift with time. The rate of this drift depends upon the composition of the cathode surface, its temperature, and, perhaps, the amount of back-bombardment. For certain applications, automatic frequency control may be required to hold the magnetron on the right frequency. Tapering the magnetron vane tips may also help.

(8) *Noise:* There is evidence that an objectionable noise may come

---

[2] R. L. Sproull, "Excess Noise in Cavity Magnetrons," *Jour. Appl. Phys.*, Vol. 18, No. 3, pp. 314-320, March, 1947.

from magnetrons employing oxide-coated cathodes.[2] Whether or not this effect occurs with other types of cathodes has not yet been ascertained. For certain applications, this noise would be intolerable.

(9) *Heating power* (P_h): In the interest of economy, it is usually desirable that heater power be small. Back-bombardment power may permit reduction in heater power during operation, but very often the fact that the bombardment exists and fluctuates requires that the cathode must be of inefficient design. For example, suppose that back-bombardment power is normally five watts but that under certain conditions it might rise to twenty watts. If the normal heater power required with no back-bombardment were less than twenty watts, a back-bombardment of this amount would cause the cathode to overheat and possibly burn out. If, however, the design of the cathode were such that heater power requirements were, say, one hundred watts for no bombardment, then a temporary increase of fifteen watts in back-bombardment power would not have such a damaging effect on the cathode. In applications, then, where the tube is exposed to output load changes, power supply fluctuations, or circuit variations, it may be necessary to design a thermally inefficient cathode. On the other hand, if operating conditions are carefully controlled, it is possible in some cases to keep the cathode heated during operation by back-bombardment alone.

Although it is often desirable to use standard voltages such as 2.5, 5.0, or 6.3 volts for heating the cathode, this requirement may make it impractical to provide other design features.

A Tantalum Cylinder Cathode

In the development of a particular magnetron, a cathode design was worked out in which the emitting surface is a tantalum cylinder. The design and construction of this cathode is presented below and its merits and short-comings discussed.

A. *Design and Construction Theory*

There are four readily available metals that might be used as pure metal emitters: Tungsten, tantalum, molybdenum, and columbium. Below are tabulated temperatures and rates of evaportion of these metals for an emission density J_o equal to 3 amperes per square centimeter.

Table 1—Temperature and Rate of Evaporation for Pure Metal Emitters.

Metal	Temperature in °K for $J_c = 3$ amps/cm^2	Rate of Evaporation in gm/cm^2	References
Molybdenum	2580	14×10^{-6}	3, 4
Columbium	2560	0.42×10^{-6}	5
Tantalum	2585	0.043×10^{-6}	3, 6
Tungsten	2780	0.043×10^{-6}	7, 8, 9

The rate of evaporation of tungsten tabulated here on the basis of papers by Reimann[7] and by Bell, Davies and Gossling[8] is about one-half that given by Jones and Langmuir.[9] From the rates of evaporation, it is seen that tungsten and tantalum should give much better life than columbium or molybdenum.

It was decided to construct the cathode as a single-ended coaxial device, with tantalum as the outer conductor and emitting surface, and tungsten as the inner conductor and return path for the heating current (Figure 2). From the standpoint of life, the outdoor conductor could be either tungsten or tantalum. The inner conductor should have as low an evaporation rate as possible since its temperature must always be greater than that of the outer conductor. For these reasons, the combination of tantalum for the outer conductor and tungsten for the inner conductor was chosen.

With diameters defined as in Figure 2, cathode diameters (d_c) fixed by magnetron design considerations are assumed. It now remains to choose the inside diameter of the outer conductor (d_o), and the outside diameter of the inner conductor (d_i). The criterion used here

---

[3] W. G. Dow, FUNDAMENTALS OF ENGINEERING ELECTRONICS (p. 537), John Wiley and Sons, New York, N. Y., 1937.

[4] H. A. Jones, I. Langmuir, G. M. J. Mackay, "The Rates of Evaporation and the Vapor Pressures of Tungsten, Molybdenum, Platinum, Nickel, Iron, Copper and Silver," *Phys. Rev.*, Vol. 30, pp. 201-214, August, 1927.

[5] A. L. Reimann and C. K. Grant, "Some High-Temperature Properties of Niobium," *Philosoph. Mag.*, Vol. 22, pp. 34-48, July, 1936.

[6] D. B. Langmuir and L. Malter, "The Rate of Evaporation of Tantalum," *Phys. Rev.*, Vol. 55, pp. 748-749, April 15, 1939.

[7] A. L. Reimann, "The Evaporation of Atoms, Ions, and Electrons from Tungsten," *Philosoph. Mag.*, Vol. 25, pp. 834-838, June, 1938.

[8] J. Bell, J. W. Davies, B. S. Gossling, "High Power Valves; Construction, Testing and Operation," *Jour. Inst. Elec. Eng.*, Vol. 83, p. 195, 1938.

[9] H. A. Jones and I. Langmuir, "The Characteristics of Tungsten Filaments as Functions of Temperature," *Gen. Elec. Rev.*, Vol. 30, No. 6, pp. 310-319, June, 1927.

is that life shall be maximized. A simplified but highly approximate method for computing life and optimum values for d_o and d_i follows. The design resulting from this computation may be used as an experimental starting point. After the values for d_o and d_i are calculated, a number of test cathodes should be constructed in which variations of d_o and d_i up to about $\pm$ 10 per cent are incorporated. Actual life-tests, possibly accelerated by operation at some higher temperature, should be used to refine the design.

Mechanical limitations require that $\dfrac{d_o - d_i}{2} \geqq K$ in order that short-circuiting will not take place between inner and outer conductor. K will depend on cathode length, precision of machining and assembly, and amount of deformation upon heating. Life requires that $\dfrac{d_o - d_i}{2}$
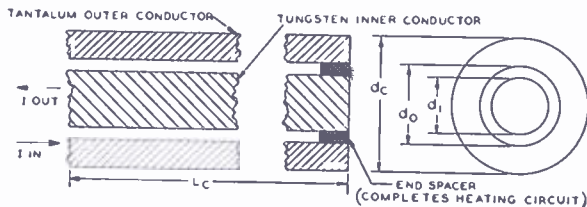
Fig. 2—Cross-sectional view of coaxial tantalum cylinder cathode.

be as small as possible. Hence, the relation $\dfrac{d_o - d_i}{2} = K$ may be used.

Burn-out (end of life) of a straight-wire filament is usually considered to occur when about 10 per cent of the volume of the metal has evaporated. Although there is reason to believe that this assumption is not entirely valid for a coaxial structure, since the outer conductor is heated in part indirectly, the 10 per cent criterion will be used in the following analysis for lack of complete data concerning life as a function of the percentage of indirect heating. However, this paper is concerned with determining the optimum relative dimensions of the coaxial cathode members by the intersections of curves such as those of Figure 3; the abscissa value of such an intersection is independent of the relative loss of volume at burn-out if this is the same for both components of the coaxial cathode.

It is also assumed that the outer conductor evaporates metal from its outside surface only and that the inner conductor loses metal as though it were evaporating into empty space. Evaporation surface areas are considered constant. Actually, tungsten from the inner conductor condenses on the inside of the tantalum cylinder. This has the

effect of increasing the life of the outer conductor and decreasing the life of the inner conductor. To compensate for this effect, d_o and d_i should be increased slightly.

In addition, it is assumed that the outer conductor is operated at some designated temperature which is adequate for supplying the required electron emission. Temperature of the inner conductor may then be determined.

In order to ascertain $\dfrac{d_o}{d_i}$ for maximum life, the following procedure is used. A curve of life versus $\dfrac{d_o}{d_c}$ for the tantalum outer conductor is obtained using tables of the intrinsic properties of tantalum[6] and the equation

$$\text{Life}_{Ta} \text{ (in hours)} \cong (1.153 \times 10^{-4}) \frac{d_c \text{ (in cm.)}}{M_{Ta}\left(\text{in }\dfrac{gm}{cm^2}\right)} \left[1 - \left(\frac{d_o}{d_c}\right)^2\right]. \tag{1}$$

d_c is considered constant since, even in the case of a solid rod which burns out after 10 per cent evaporation, final d_c is 0.95 of initial d_c. A similar curve of life versus $\dfrac{d_o}{d_c}$ for the tungsten inner conductor is next obtained using tables of properties of tungsten[9] and the equation

$$\text{Life}_W \text{ (in hours)} \cong (1.344 \times 10^{-4}) \frac{d_c \text{ (in cm.)}}{M_W\left(\text{in }\dfrac{gm}{cm^2}\right)} \left[\frac{d_o}{d_c} - \frac{2K}{d_c}\right], \tag{2}$$

and taking into account the temperature difference between the inner and outer conductors by means of the approximate equation

$$T_W = T_{Ta}\left[1 + \frac{\varepsilon_{Ta}}{\varepsilon_W}\frac{d_c}{d_i}\frac{(d_c^2 - d_o^2)\,\rho_W}{[(d_c^2 - d_o^2)\,\rho_W + d_i^2\rho_{Ta}]}\right]^{\frac{1}{4}}. \tag{3}$$

In these equations: $d_o = $ cathode diameter; $d_o = $ inside diameter of outer conductor; $d_i = $ outside diameter of inner conductor; $M_{Ta} = $ rate of evaporation of tantalum; $M_W = $ rate of evaporation of tungsten; $d_i = d_o - 2K$; $T_W = $ temperature of tungsten in °K; $T_{Ta} = $ temperature

of tantalum in °K; ϵ_W = thermal emissivity of tungsten; ϵ_{Ta} = thermal emissivity of tantalum; ρ_W = resistivity of tungsten; and ρ_{Ta} = resistivity of tantalum.

From the intersection of the two curves of life versus $\dfrac{d_o}{d_c}$ (see Figure 3), maximum life and optimum $\dfrac{d_o}{d_c}$ may be predicted. As stated before, because of the approximations made in these calculations, it may be desirable to refine the design by constructing a number of test cathodes incorporating variations in $\dfrac{d_o}{d_c}$ and running actual life tests.
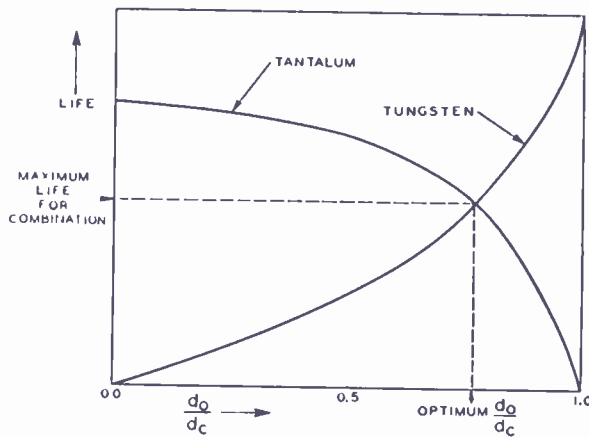
Fig. 3—Life of tantalum outer conductor and tungsten inner conductor versus ratio of inside diameter of outer conductor to cathode diameter, $\dfrac{d_o}{d_c}$.

Accelerated life tests (by operation at a higher temperature) may be of use, particularly in locating flaws in a particular design, but there is still some question regarding their complete validity.

Diode life tests may give results different from oscillating magnetron life tests for several reasons: (a) It is not yet known with certainty what the temperature-limited emission should be for a given anode current (this may include secondary-emission effects). (b) The rate of evaporation of tantalum from the surface may be affected by back-bombardment. (c) If back-bombardment supplies an appreciable fraction of the total heating power, heating current may be reduced; this should enhance life.

In designing an actual cathode structure, it must be remembered that heat conduction takes place at both ends of the cathode. To minimize this heat loss and to obtain uniform temperature distribution

across the emitting surface of the cathode, it may be desirable to machine thermal barriers into the inner and outer conductors.

B. *Merits and Shortcomings*

Under DESIGN CONSIDERATIONS, nine major factors affecting cathode design were discussed. A brief survey will now be made to see wherein the coaxial tantalum cylinder cathode fulfills and departs from the desired requirements.

(1) *Emission density:* Virtually any emission density may be obtained, but life decreases rapidly with increasing emission.

(2) *Geometry* presents no particular barrier or difficulty.

(3) *Back-bombardment:* There are indications that tantalum stands up under back-bombardment much better than oxide coatings. The high operating temperature as compared with that of oxide cathodes, however, simplifies dissipation of back-bombardment power.

(4) *Life:* Presumably, life may be calculated approximately from the geometry and the intrinsic properties of tantalum and tungsten. Once the actual lives of a few cathodes have been established under operating conditions, there should be little variation in the lives of subsequent cathodes.

(5) *Mechanical stability* should be much greater than for a spiral or loop type of filamentary cathode. If the tantalum wall is too thin or the length too great, sagging or distortion may occur.

(6) *Hum* is inherently eliminated by the coaxial design.

(7) *Frequency drift* will occur due to the comparatively rapid deposition of evaporated tantalum on the vane tips. Tapering the ends of the vanes should lessen this effect.

(8) *Noise:* The objectionable type of noise noted in magnetrons employing oxide cathodes[2] should be completely absent in the case of tantalum.

(9) *Heating power* will usually be somewhat in excess of that desired for general application. Current will be high and voltage low. An automatic power or current control should help to maximize life.

APPLICATION TO A CONTINUOUS-WAVE MAGNETRON

The coaxial tantalum cylinder cathode evolved in connection with a project for the development of a 3-centimeter tunable continuous-wave magnetron designed to deliver 200 watts of power at 2000 volts. This tube has a double-strapped 18-vane anode, 0.200 inch high, with an interaction-space diameter of 0.120 inch. The emission density desired
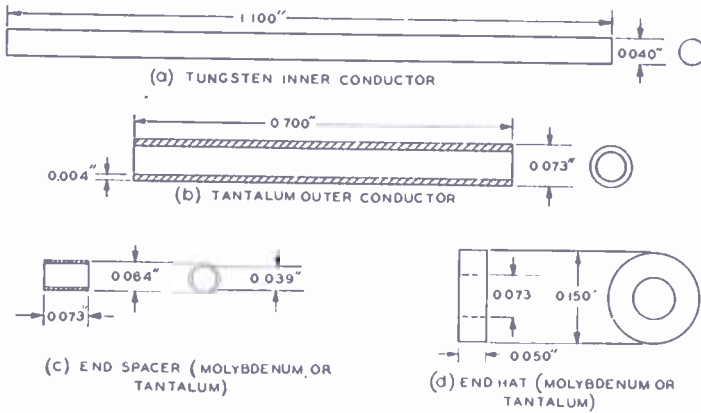
Fig. 4—Cathode details.

from the cathode was at least 1 ampere per square centimeter, a value which, it was believed, could not be obtained from oxide-coated cathodes with adequate life.

The details and assembly of the cathode parts are shown in Figures 4 and 5. Some important points in the fabrication and assembly processes are:

(1) The molybdenum inner and outer conductors are glassed together (not shown) with the hole for the tungsten inner conductor concentric with the hole for the tantalum outer conductor.

(2) A snug fit is obtained between tungsten inner conductor and end spacer as follows: (a) start with a fairly long piece of tungsten; (b) electropolish a taper on one end; (c) force the end spacer on as far as it will go; (d) grind off end of tungsten flush with spacer; (e) grind other end of tungsten to final length.

(3) The tantalum sleeve is formed from a rectangular sheet 0.004 inch thick.

(4) Parts are pushed together and held by friction. This requires careful machining. Slight deformations may be made at the
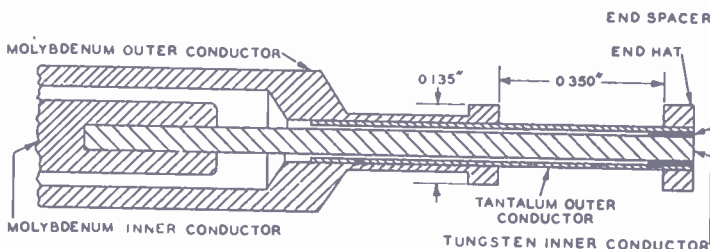
Fig. 5—Cathode assembly.

ends of the tantalum outer conductor to increase holding friction to end hat and molybdenum outer conductor.

(5) When current is passed through the assembly in vacuum, regions of high electrical resistance develop local hot spots and a sintering action takes place at these points. After a few hours of operation, most of the parts are held as securely as though they had been welded.

Time did not permit the cathode design actually used to be optimized and no effort was made to correct for non-uniform temperature distribution. Consequently, although an emission density of only about 1 ampere per square centimeter was drawn by the magnetron, a temperature of about 2600°K existed over a portion of the tantalum. Estimated life was on the order of 100 to 200 hours. Measured life of one developmental magnetron tested under oscillating conditions was 91 hours. Because of a deposition of tantalum on the vane tips, a frequency shift of 1.6 per cent took place in this tube during the life test. The heating current required was 50 amperes at 3 volts for the tube not oscillating. During operation, this could be backed off to about 35 or 40 amperes at 2 volts.

Conclusions

The coaxial tantalum cylinder cathode is not, it is hoped, the ultimate in magnetron cathodes. It does not fulfill all of the desired requirements. Its chief shortcomings are high heating power, high heating current, frequency shift due to deposition of tantalum on vane tips, and limited life. Its significant merits appear to be absence of hum and noise, consistent life, ability to supply emission of several amperes per square centimeter, and ability to withstand a large part of the detrimental effects of back-bombardment.

For some practical applications, the above-mentioned shortcomings may make it desirable to investigate other types of emitters. For many experimental purposes, however, where life, heating power, and frequency shift are not, at the moment, prime considerations, the reliability and reproducibility of tantalum cylinder cathodes may contribute to the solution of particular problems.

RADAR FOR MERCHANT MARINE SERVICE*

By

Frank E. Spaulding, Jr.

Engineering Department, Radiomarine Corporation of America,
New York, N. Y.

Summary—This paper discusses the technical features of a new 3-centimeter merchant marine radar equipment. Factors relating to the basic design are treated and operation of the various circuits is explained by reference to functional block diagrams. The physical form of the apparatus is shown and plan-position-indicator (PPI) photographs are included to illustrate the navigational data furnished by this instrument. Specifications defining the performance characteristics are also included.

Introduction

SINCE the end of the war, a great amount of effort has been devoted to the design and development of radar equipment which would be suitable for Merchant Marine service. An earlier paper,[1] treated the basic factors involved in such radar system design. The present article describes the technical features of radar equipment designed for navigational and anti-collision applications on passenger and cargo vessels, both on the high seas and on inland waterways such as the Great Lakes and Mississippi River.

Extensive field tests were carried out in the summer and fall of 1946 on the Great Lakes. The knowledge gained through these trials has been applied to the radar which is described herein.

This equipment is a modern type of search radar designed specifically for Merchant Marine use. Operating at 3.2 centimeters (9375 megacycles), it possesses the sharp definition and clarity of picture obtainable through use of the higher frequency band without introducing unreasonably large antenna structures. In addition, by presenting its information on a 12-inch cathode-ray tube, it becomes possible for ship personnel to observe the plan-position-indicator (PPI) presentations for long periods of time without the eye-strain occasioned by viewing smaller tubes.

Design Considerations

In establishing the basic design, serious consideration was given

---

* Decimal Classification: R537 × R510.
[1] I. F. Byrnes, "Merchant Marine Radar", *RCA REVIEW*, Vol. VII, No. 1, pp. 54-66, March, 1946.

to several important factors affecting the usefulness and reliability of a radar. These included choice of frequency; amount of transmitter power; need for short minimum range; simplified operating controls; fewest possible moving parts; and the minimum number of tubes.

Choice of the proper frequency was of paramount importance. Both 3- and 10-centimeter radars had been in use during the war and information and techniques on both frequencies were available. However, the antenna beam width is directly proportional to the wave length for a given size of reflector; shorter wave lengths will, therefore, give better bearing resolution and sharper images. Furthermore, since at 3.2 centimeters an antenna which gives a 2-degree (or less) beam width already approaches practical limits in size for commercial use, it is apparent that the shorter wave length should be used. The antenna design of this radar provides a 1.6-degree horizontal beam.

It was felt that the effects of sea return and heavy rain on 3-centimeter presentation had been overestimated and that the need for good bearing resolution had been correspondingly underestimated. While sea return is somewhat less on 10 centimeters due to the higher grazing angle of the first lobe over the surface of the sea, more important is the fact that buoys and other low targets are apt to be missed for the same reason.

This has been borne out by extensive tests on the Great Lakes and Mississippi River. On the Lakes, where the trials included both 3- and 10-centimeter radars, the conclusion was reached that only the 3-centimeter designs could give the necessary performance. On the rivers, where the sharpest resolution is demanded at all times, the use of the higher frequency was a foregone conclusion. It is evident that radar for ocean-going vessels must likewise be capable of displaying the sharp outlines obtainable on 3 centimeters if it is to be of value in pilot waters.

While 15 kilowatts was recommended as a suitable minimum peak power requirement, it was felt that ample reserve should be provided to meet all conditions of weather and propagation. Accordingly, a value of 30 kilowatts was chosen.

Short minimum range and good range resolution were two major factors in the design to meet the needs of difficult piloting operations in narrow channels and harbors. Accordingly, a pulse length of 1/4 microsecond was selected for use on the 1.5- and 5-mile range scales. Such a pulse has a length in space of 82 yards. Since the beam has to make a round trip for target detection, the theoretical minimum range would be 41 yards. However, to allow for receiver recovery

time and spot size on the PPI tube, a value of 80 yards has been established for these factors.

It may be shown that when the range scale in use is greater than about 5 miles, the minimum spot size of the cathode-ray tube becomes the limiting factor in determining image definition, rather than the ¼-microsecond transmitted pulse length. This makes it possible to use a longer pulse on the fifteen- and fifty-mile range scales without sacrificing sharpness of the scope presentation. Accordingly, a one-microsecond pulse is used on these ranges, thus enhancing the long range performance.

INDICATOR UNIT   TRANSMITTER-RECEIVER UNIT
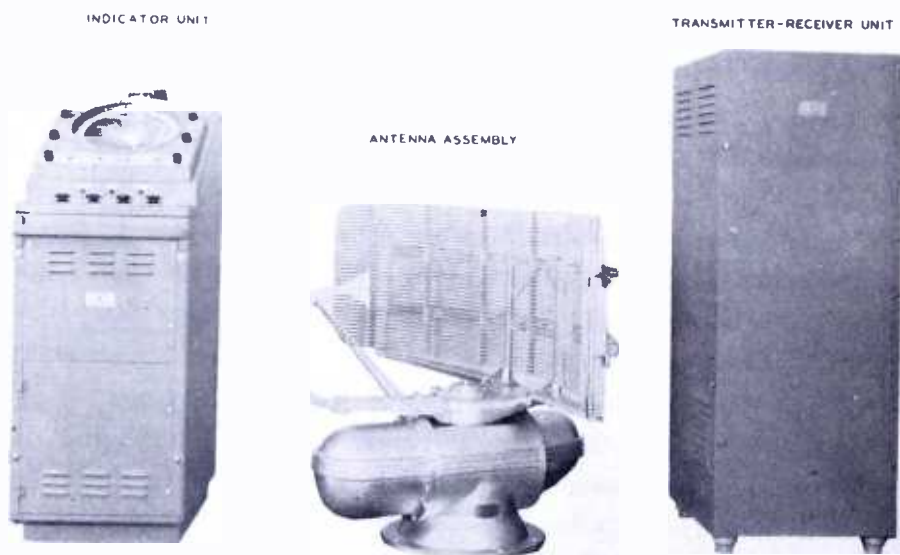
ANTENNA ASSEMBLY

Fig. 1—Indicator, antenna assembly, and transmitter-receiver.

By using a 3000-cycle repetition rate with the ¼-microsecond pulse, and a 750-cycle rate with the one-microsecond pulse, the duty cycle remains at 0.00075 and the average transmitted power is kept constant at about 23 watts.

With these repetition rates the number of hits per beam width are 133 and 33 respectively. This insures that the echoes will build up to full brilliance on the scope even though the target may be small in size and may present a poor aspect to the radar beam.

Particular stress is placed on keeping the number of operating controls at a minimum. This is felt to be particularly important since the equipment is operated by the ship's navigating personnel.

It is also desirable to keep the number of moving parts at a minimum, both from the standpoint of reliability as well as quiet opera-

tion. Silence is essential in a pilot house when listening for fog signals. With this in mind, a stationary deflection-coil system for the PPI was chosen instead of the usual motor-driven rotating coil mechanism.

The equipment consists of three major units, namely, the indicator, the transmitter-receiver and the antenna assembly.
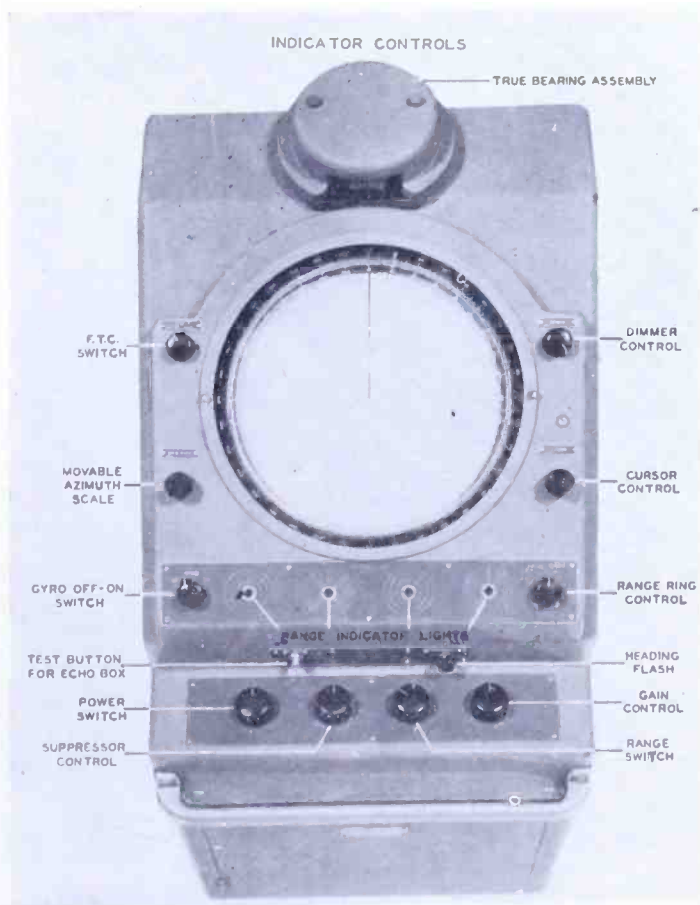
Fig. 2—Closeup of indicator unit, control panel and 12-inch PPI.

INDICATOR

The indicator unit has been designed primarily for installation in the pilot house where it may be viewed and controlled by the navigating officers. It is built into a binnacle-type housing which contains the main operating controls and the 12-inch cathode-ray PPI scope. Its construction is illustrated in Figure 1 which shows the three major units of this equipment. This unit also houses a synchronizer chassis unit which generates all of the complex waveforms essential to operation of the radar, such as sweep, unblanking, trigger, range marks and sensitivity time control. The binnacle also provides room

for the true-bearing assembly which, when connected to the ship's master gyro introduces north-stabilization of the PPI pattern and at the same time constitutes an extra ship's gyro-repeater station. The remaining space is devoted to high- and low-voltage power supplies associated with the synchronizer and scope. Operating controls for this equipment may be seen in Figure 2. This is a view of the top of the binnacle as it appears to the navigator. Most frequently used controls are: power, suppressor, range and gain. These four may be seen on the horizontal shelf at the front. Secondary controls are
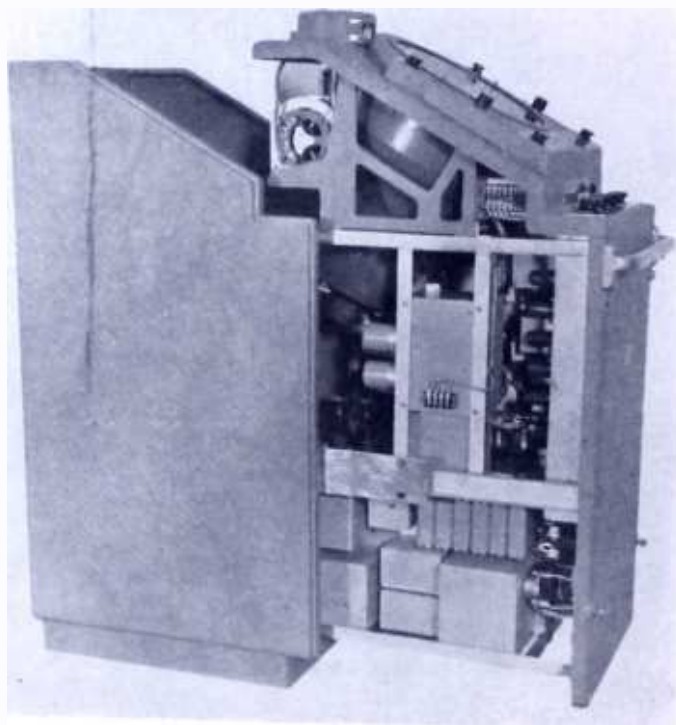
Fig. 3—View of indicator unit open for servicing.

symmetrically arranged on the sloping panel and are also identified in Figure 2. Range indicator lamps show which range scale is in use and remind the user as to the distance between range rings.

Behind a hinged lower door is an auxiliary test panel containing a built-in test meter, two-hour meter for observing "stand-by" and "operate" time of the radar, antenna motor-circuit breaker, 115-volt a-c convenience outlet and several fuses with individual blown-fuse indicator lamps. Several controls, normally set at the time of installation, also occupy this space. These are focus, intensity, video gain and manual tuning. An automatic-frequency-control off-on switch is also present.

Certain mechanical features of the binnacle are of interest. The entire indicator mechanism rolls out of the housing for servicing. In this manner, all of the interior portions may be easily reached. Figure 3 shows this unit open for servicing. The radar may be operated in this fully withdrawn position. The sloping operating panel housing
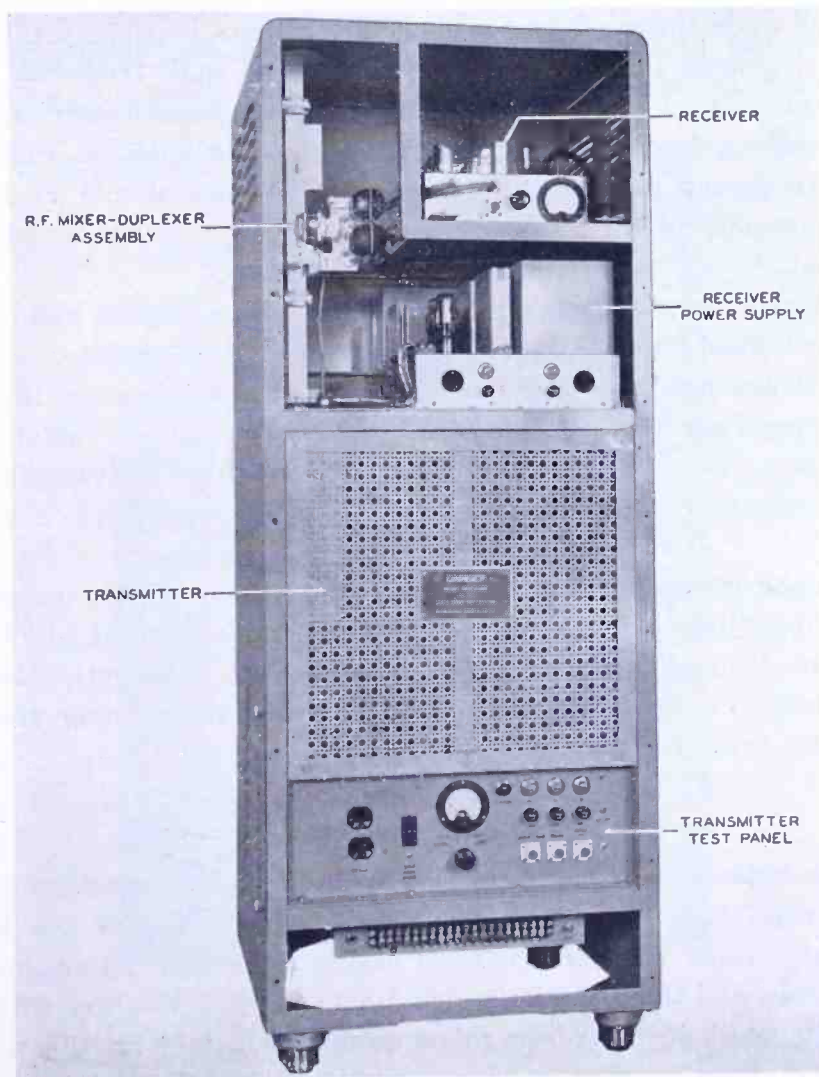
Fig. 4—Interior view of transmitter-receiver unit.

the PPI tube is hinged and may be swung open and latched so as to give access to the azimuth scales and to the 12-inch tube itself. The true-bearing assembly cover is also hinged. This unit may be quickly reset whenever the ship's gyro has been shut down, as frequently occurs when the vessel is in port. The binnacle housing itself is of cast aluminum construction.

TRANSMITTER-RECEIVER UNIT

The transmitter-receiver unit may be located in the pilot house, chart room or in any other location reasonably close to the antenna. As shown in Figure 4, the lower portion, behind the protective screen, houses the pulse modulator components, the magnetron and associated high-voltage power supplies. The receiver is located at the top of the cabinet while the receiver power supply mounts between the two. At the left side of the receiver may be seen the radio-frequency mixer-duplexer unit. Behind this is mounted the 3.2-centimeter echo box. The receiver, its power supply and the echo-box units, as well as the radio-frequency assembly, may be quickly removed and replaced if necessary during servicing operations. The wave-guide output from this unit to the antenna may be seen at the top.

Access to the various units within this cabinet may be had by opening the hinged front door. This also exposes the transmitter test panel in the lower portion without permitting personnel to come in contact with dangerous high voltages. The test analyzer allows instantaneous checking of essential voltages and currents within the transmitter. It also contains a high-voltage circuit breaker, convenience outlet and fuses.

On the lower left side is a small hinged door giving access to a replaceable filter cartridge associated with the blower unit which circulates air through the transmitter-receiver unit. The entire assembly is installed on shock mounts, and in addition, the receiver chassis is similarly protected from vibration.

ANTENNA DESIGN

The antenna assembly is installed on top of a tower or pedestal sufficiently elevated to allow 360-degree observation of the horizon without serious interference from obstructions such as smokestacks, king posts, and the like. An 8-inch diameter pipe structure with work platform and ladder has been found quite satisfactory for this purpose. Figure 5 shows a typical antenna installation utilizing a tower 35 feet high. The antenna is also shown in Figure 1.

The 18 x 62-inch revolving grid reflector, shaped like a parabolic cylinder, establishes a horizontal beam pattern 1.6 degrees wide at the half-power points. The vertical pattern is 17 degrees wide to allow for rolling and pitching of the ship in rough weather.

Housed within the large end bell is the antenna-drive motor while the smaller end bell covers a synchro generator, heading flasher switch and terminal board. A phone jack and heading flasher adjustment are

located behind a water-tight removable cap on the side of the smaller end bell. This allows installation and inspection personnel to plug in a standard telephone handset and converse with observers at binnacle or transmitter units while making necessary adjustments. A motor on-off switch is also present so that persons on the antenna platform may turn off the drive motor at will for reasons of safety.

Reduction gearing to rotate the reflector and horn feed at approximately 10 revolutions per minute is contained within the oil-filled enclosure of the main casting. A rotating joint, also built into the
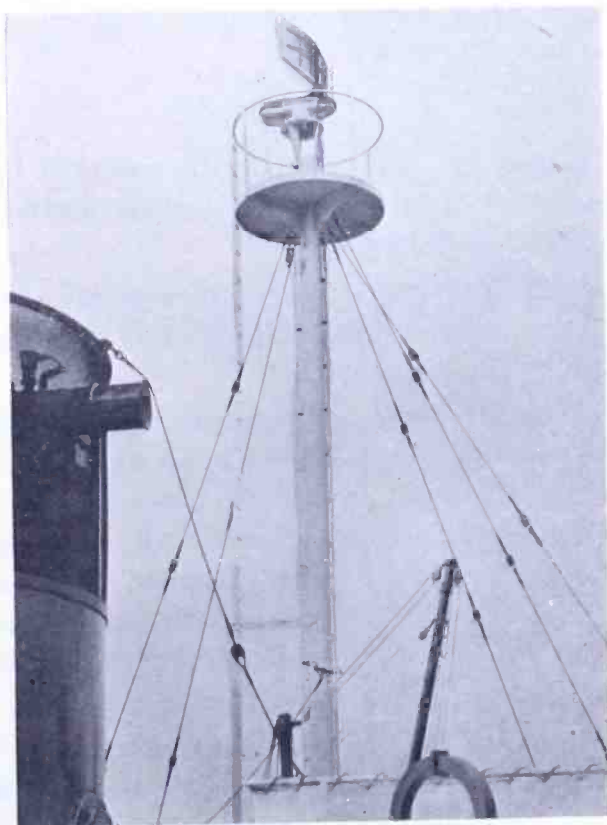
Fig. 5—Typical antenna installation.

aluminum casting, transfers the radio-frequency energy from the stationary wave-guide input to the revolving horn feed which "illuminates" the reflector.

A standard 115-volt watertight receptacle is included on the tower for servicing operations. Inter-connections between the antenna and other portions of the radar consist of the ⅝ x 1¼-inch waveguide, one coaxial cable, one 3-conductor and one 8-conductor armored shipboard cable. The wave guide is silver plated inside and out to insure low losses (0.026 decibel/foot). Connections between binnacle and

transmitter units consist of three coaxial cables and two 8-conductor power and control cables.

POWER SUPPLY

The radar is designed basically for operation on 115 volts, 60 cycle, single-phase power with a current drain of 12 amperes at about 85 per cent power factor. When used in the "standby" condition (heater and bias voltages only are present) the load is about 6 amperes. When the ship's power source is 115 or 230 volts d-c, a motor generator is used to furnish the necessary a-c power.

CIRCUITS

The basic system of operation may be observed by studying the block diagrams. The various circuit functions indicated on the diagrams are discussed as follows:

1)—Generation of sweep, trigger, unblanking and range-marker waveforms in the synchronizer chassis (this establishes the basic timing sequence of the radar);

2)—Passage of the sweep sawtooth waveform through the antenna synchronizer to modulate the sweep with the rotational azimuth information, return of the sweep waveform through the "live" synchro differential generator to take into account the ship's gyro data (for *True* presentation), or through the "Dummy" differential generator (for relative presentation), and impression of the sweep voltages, thus modified, on the stationary three-phase deflection coil to appear finally as the revolving sweep line on the cathode-ray tube;

3)—Transfer of the trigger to the transmitter and its subsequent amplification to a 12-kilovolt pulse applied to the magnetron;

4)—3.2-centimeter oscillation of the magnetron for the duration of the pulse, conduction of the microwave energy by waveguide to the antenna and its subsequent projection in a narrow revolving beam;

5)—The gathering of the echoes by the antenna and their transfer to the receiver for amplification, detection and finally their application to the cathode-ray tube grid to produce the bright and dark areas of the picture;

6)—Application of the unblanking pulse so that only the outward moving portion of the sweep will be brightened; and

7)—Introduction of timing pulses as range rings to permit the measurement of distance on the PPI scope.

The Synchronizer

An analysis of the synchronizer block diagram, Figure 6, in greater detail is given in the following paragraphs.

The basic pulse repetition rate is established by a free-running master multivibrator. This square wave is used to excite a sawtooth sweep generator. Its output, when amplified and applied to a pair of 807 drivers is finally transformer-coupled to the coaxial line feeding the single-phase rotor of the antenna synchro-generator. The three-
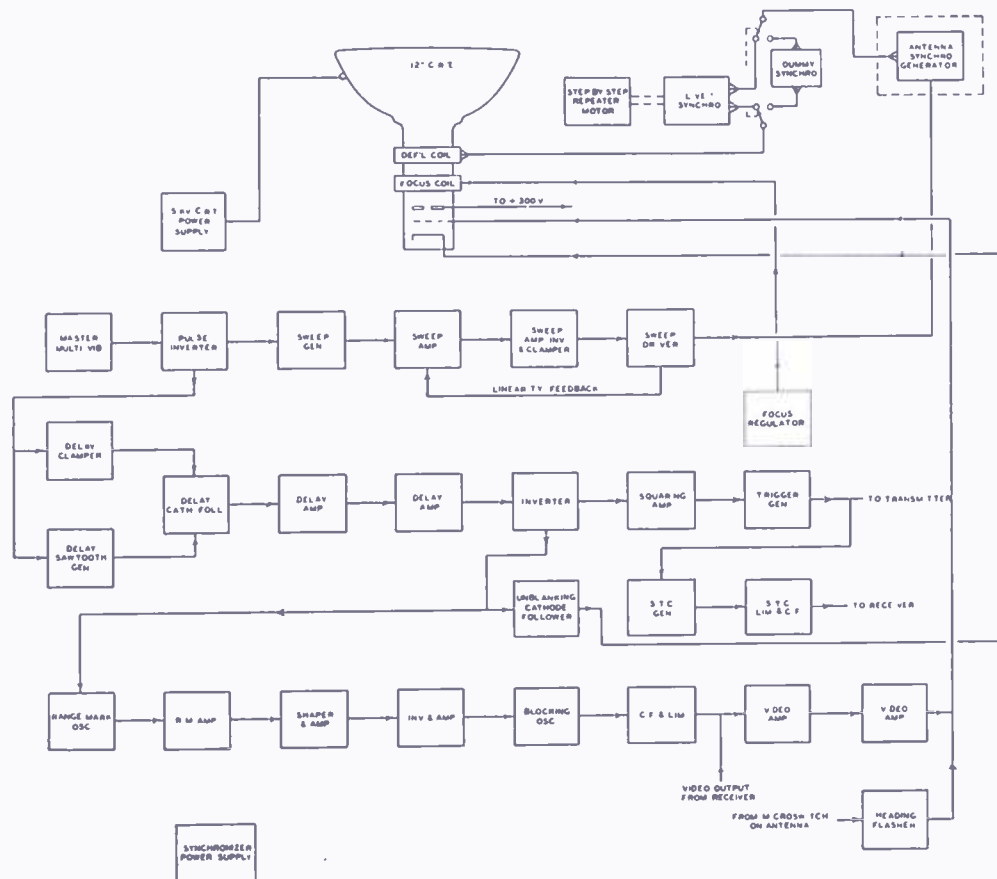
Fig. 6—Block diagram of indicator unit.

phase output of this generator ultimately reaches the deflection coil on the cathode-ray tube.

Referring to the timing sequence diagram, Figure 7, it will be seen that with this deflection system the cathode-ray tube beam inherently integrates the entire waveform. Thus, when line "A" is at such a height above "B" so that area I equals area II, then the cathode-ray-tube beam will pass through the center of the PPI picture at "A".

The function of the delay sweep generator now becomes apparent, since by delaying the firing of trigger, range markers and unblanking

pulses until the point "A" is reached, the sweep line will *appear* to start at the center of the tube. Echoes will then show up on the sweep between "X" (the center) and "Y" (the circumference) of the tube.

The delay circuit consists of an auxiliary sawtooth generator which feeds a triode having an adjustable bias. Hence, the exact moment at which it starts to conduct may be controlled by its bias. After suitable squaring and amplifying, the unblanking pulse is obtained. Differentiation of the leading edge to fire a gas tube provides the sharp trigger pulse. Finally, the unblanking pulse excites the range mark generating circuits to produce the extremely sharp pulses required for clear range rings. The unblanking wave is applied to the cathode while range marks are combined with video from the receiver to reach the grid.
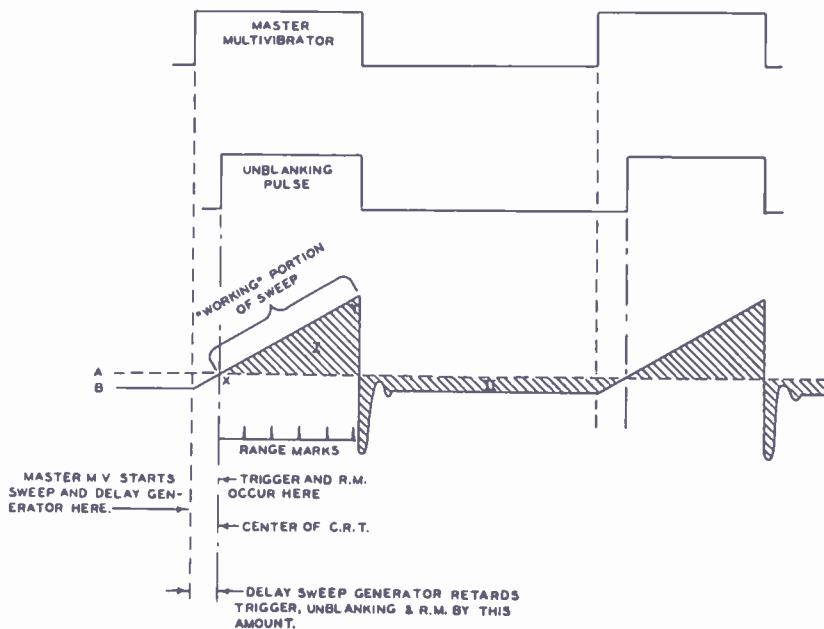
Fig. 7—Timing sequence diagram.

THE TRANSMITTER

With reference to the transmitter block diagram, Figure 8, the low-level trigger pulse arrives from the synchronizer. A "hard tube" pulser circuit is used containing a type 6SN7 tube as an isolation stage and low-level blocking oscillator, and then an 829-B tube as a high-level blocking oscillator. The pulse from the latter drives the 5D21 class-C amplifier or switch tube. A 12-kilovolt pulse appears across the plate-load resistor of this tube and thence is coupled to the magnetron cathode through a capacitor. The high power for this pulse is furnished by the 15-kilovolt power supply which incorporates two type 3B24 rectifier tubes in a voltage doubling circuit arrangement. Ade-

quate protective devices for overload are incorporated, and layout of high-voltage components is in accordance with good transmitter design practice.

The length of the pulse is established by the delay network in the 829-B grid circuit. The trigger pulse received from the synchronizer is about 40 volts in amplitude and approximately 1 microsecond long. This fires the 6SN7 low-level blocking oscillator to produce a sharper positive pulse of about 150 volts amplitude. It, in turn, is now applied to the 829-B and to the delay line simultaneously. The positive leading edge of this pulse fires the 829-B blocking oscillator which was previously quiescent. A pulse travels along the artificial delay line until it reaches the open end of the line and is then reflected back. This reflected pulse hastens the cutoff of the 829-B which then remains inoperative until the next positive pulse arrives. In this manner, the delay line determines the pulse length of the transmitted signal.
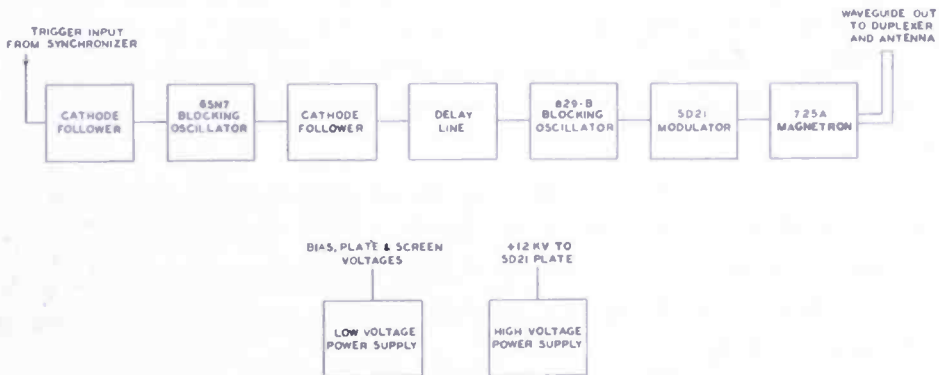
Fig. 8—Transmitter block diagram.

The delay line has two sections. On the two shorter ranges (0-1½ and 0-5 miles) only the first portion is connected and a 0.25-microsecond pulse results. For the two longer ranges, a relay adds on another section, giving a 1.0-microsecond pulse.

Experience has shown the hard tube modulator to be equal to or better than the hydrogen thyratron type for the relatively low power levels such as are used; in addition, it has greater flexibility for changing pulse lengths.

RADIO-FREQUENCY MIXER-DUPLEXER

The magnetron mounts at the bottom of, and feeds power into, the duplexer waveguide, while the outgoing transmitter power is passed on the antenna waveguide protruding through the top of the transmitter-receiver cabinet.

There are two horizontal branch chambers leading into the mixer

portion of the assembly. The lower one has an aperture which passes a small amount of magnetron power to the automatic-frequency-control (AFC) crystal. The upper horizontal member contains the transmit-receive (TR) tube. This is the gas switching tube which short circuits the mixer input during the time the transmitted pulse is present. When the received echoes are present this tube allows them to pass into the mixing chamber and signal crystal at the right.

The 1B35 anti-TR tube may be seen in the duplexer portion. This tube prevents the weak echo power from being fed back into the magnetron and wasted.

On the mixer portion at the right are the signal and AFC crystals and two shielded tube sockets. The lower one contains the 723 A/B klystron oscillator which feeds its energy into both signal and AFC crystals. The upper socket is reserved for possible future beacon applications. Within this mixer assembly the signal, local oscillator and magnetron voltages combine in the 1N23B crystals to produce the intermediate-frequency currents. The 30-megacycle signals from signal and AFC crystals pass to the receiver chassis through shielded coaxial cables.

At the upper left is a 20-decibel directional coupler which is provided for system testing purposes and to which the echo box may be connected. The echo box, when installed, furnishes an artificial echo, thus providing a check on the over-all system performance when no targets are in sight.

THE RECEIVER

Referring to Figure 9, the receiver block diagram, it will be seen that this chassis receives the intermediate-frequency inputs from signal and AFC crystals. The weak signals are amplified through eight stages of 30-megacycle intermediate-frequency amplification and rectified. The resulting video pulses are further amplified, limited, and then passed through a coaxial cable to the indicator. After final amplification they are fed to the cathode-ray grid.

The AFC signal, after amplification, enters a discriminator network and d-c amplifier. By means of two sawtooth generators it controls the klystron reflector voltage in such a manner as to lock in the local oscillator to a frequency exactly 30 megacycles higher than the magnetron (and hence signal) frequency.

The signal intermediate-frequency amplifier contains a low noise triode input stage, followed by three pairs of stagger-tuned stages

using 6AK5 pentodes. The resulting gain is approximately 120 decibels with a band width of 6 megacycles. The over-all noise factor for mixer and receiver is less than 15 decibels above $KT\triangle F$ (the theoretical value).

A fast time constant circuit (FTC) in the receiver is operated from the binnacle control panel. This assists in breaking up the solidarity of some types of interference such as sea return and heavy rain or snow.

Sensitivity time control (STC) is very effective in minimizing response due to sea return. With this circuit arrangement an exponential waveform of adjustable amplitude and duration is produced. This is generated in the synchronizer and is applied to the receiver gain control lead. Its effect is to lower the gain of the receiver for targets close by and to increase the sensitivity to maximum for more distant objects.
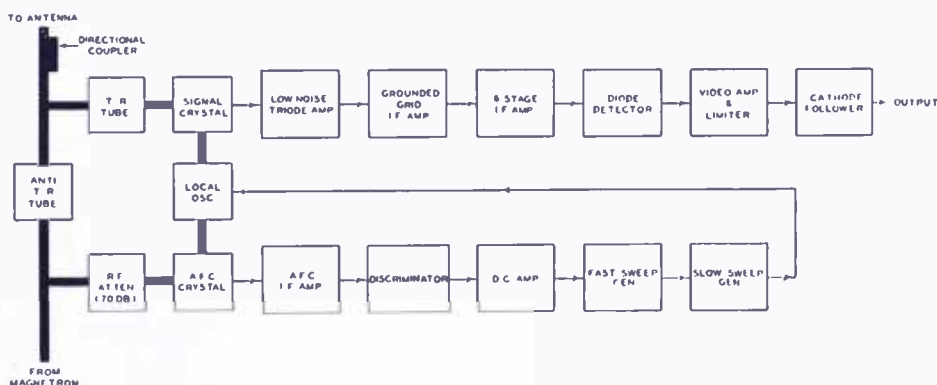
Fig. 9—Receiver block diagram.

By suitable adjustment of the continuously variable suppressor control it is possible to thin out the solid pattern of sea return so that stronger ship targets, otherwise obscured, may be observed.

The receiver contains a built-in test meter to provide quick checks on all essential voltages and currents. It is also possible to shift from AFC to manual tuning. Power to operate the receiver is supplied by the chassis immediately below the receiver.

COMPONENTS

In this equipment, particular care has been taken in the choice of components to allow ample safety factors for long trouble-free operation. Transformers and reactors are of the hermetically sealed type. Filter capacitors are oil filled and all components are selected in accordance with good design practice to meet the requirements of marine service.

Performance Features

The following tabulation lists the various performance character-
istics of this radar equipment:

Frequency: 9320 — 9430 megacycles.
                          Magnetron center frequency = 9375 mega-
                          cycles (3.20 centimeters).

Transmitter Peak Power Output: 30 kilowatts from Type 725-A tube.

Range Scales: 0-1½; 0-5; 0-15; 0-50 miles, with calibration
                          in nautical or statute miles.

Range Rings: 1½ mile range - - - 3 rings—½ mile apart.
                            5 mile range - - - 5 rings— 1 mile apart.
                           15 mile range - - - 3 rings— 5 miles apart.
                           50 mile range - - - 5 rings—10 miles apart.

Pulse Length: ¼ microsecond on 1½ and 5 mile ranges.
                          1 microsecond on 15 and 50 mile ranges.

Pulse Repetition Rate: 3000 cycles per second on 1½ and 5 mile range.
                          750 cycles per second on 15 and 50 mile range.

Duty Cycle: 0.00075 on all ranges.

Heading Flash: This electronic marker shows ships heading
                          (brightness of flash adjustable).

Range Markers: ± 2 per cent or 100 yards (whichever is
                          greater).

Range Resolution: Capable of showing two visible objects as two
                          distinct images if they are separated by 80
                          yards in range with the radar operating on
                          the shortest range scale.

Bearing Resolution: Approximately 3 degrees or less.

Bearing Accuracy: Less than 2 degrees error between antenna and
                          indicator.

Display: PPI display on 12-inch cathode-ray tube.

Azimuth Scales: Fixed illuminated scale—11½ inches in diam-
                          eter—1 degree marks.
                          Movable illuminated scale 10½ inches in diam-
                          eter—1 degree marks.

Bearing Cursor: Adjustable cursor line for measuring bearing
                          of targets.

Description of PPI Pictures

Figure 10 is an unretouched PPI photograph taken as a ship using
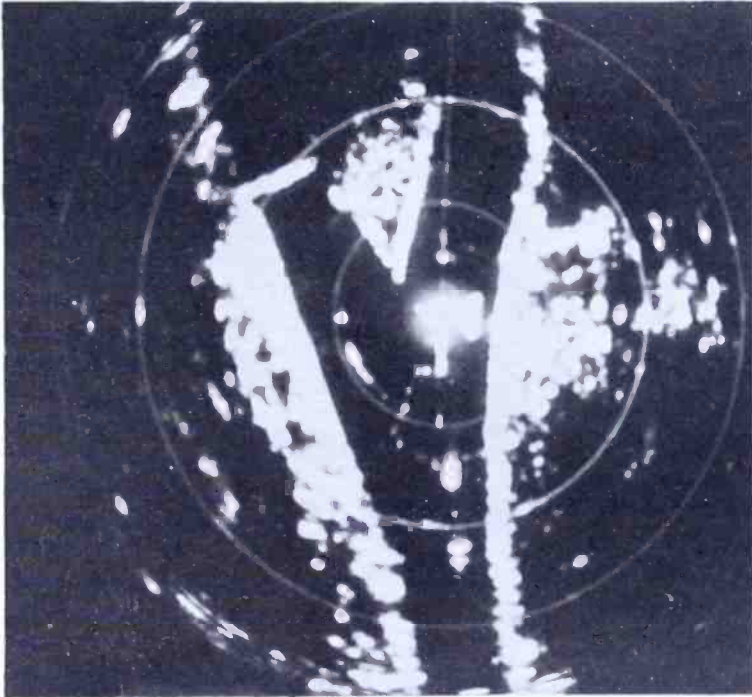
Fig. 10—PPI photograph showing ship approaching Belle Isle at Detroit. (1½ mile range; range rings are ½ mile apart.) Compare this picture with Figure 11 which shows a map of this area.

Fig. 11—Map of area shown in Figure 10.

this radar approached Belle Isle at Detroit, Michigan. The ship is at the center of the picture and is traveling in the direction shown by the heading flash. The rear of the ship may be seen clearly as well as another large ship being passed on the starboard side. Two smaller vessels are visible astern (toward the bottom of the picture) at about ¾ mile and 1¼ miles respectively. Range circles on this 1½-mile scale photo are ½ mile apart.

Figure 11 shows a map of this area. It can be noted how the clear sharp outlines of the river banks and the tip of Belle Isle in the PPI picture check with their position on the map.
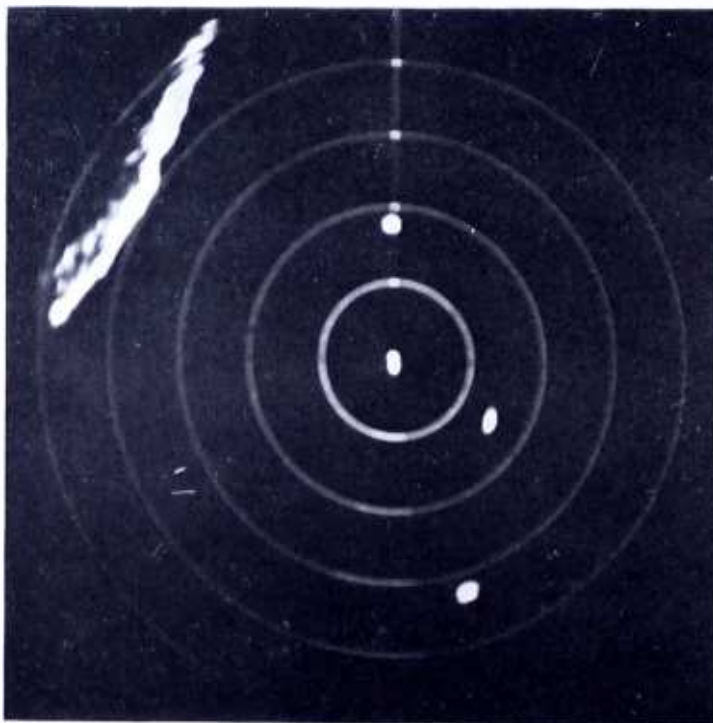
Fig. 12—Five mile PPI photograph showing ships and coastline. (Range rings are one mile apart; heading flash line shows ship's direction.)

Figure 12 shows operation on the 5-mile range position. In this PPI photograph, the range rings are one mile apart. A ship appears 1.8 miles dead ahead and two others at 1.5 and 3.3 miles on the starboard side astern. The coast line stands out clearly at 4 miles off the port bow.

Figure 13 shows the presentation on the 15-mile range scale. This was taken in Whitefish Bay on Lake Superior. Range circles are five miles apart. The ship is downbound, having passed Whitefish point which is about five miles astern, with shoreline extending away to the right to 15 miles. About seven miles ahead, at the left of the heading
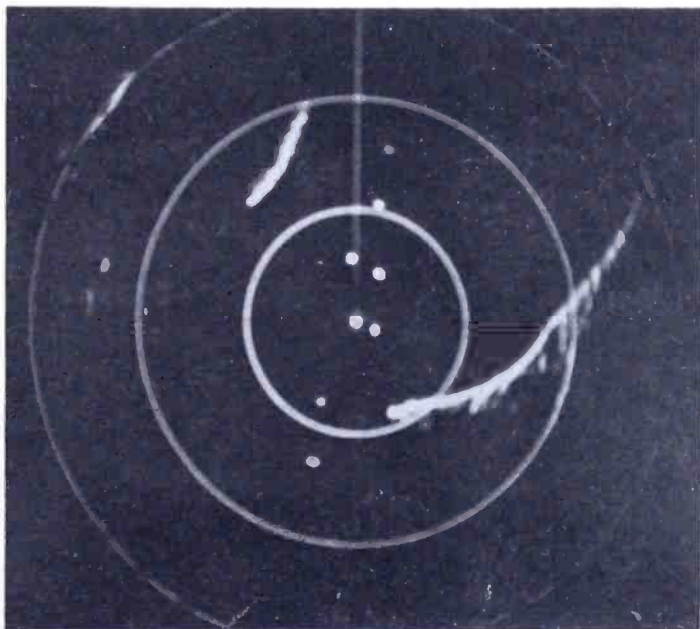
Fig. 13—Fifteen mile PPI picture showing coastline at right, island at left near top, and other ships. (Rings are five miles apart.)

flash, may be seen the shoreline of Isle Parisienne. Other ships may be seen up to seven or eight miles both ahead and astern.

In Figure 14 the radar is operating on its 50-mile range scale. Circles are 10 miles apart. Ship is on Lake Erie, westward bound,
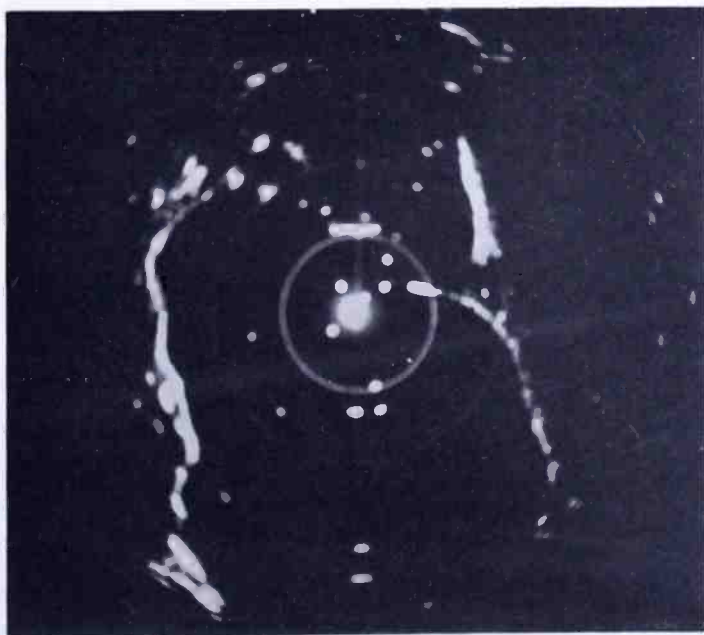
Fig. 14—Fifty mile PPI photograph taken on Lake Erie. (Rings are ten miles apart; ship is going westward with American shoreline at left and Canadian shore at right.)

approaching Pelee Passage. It will bear to starboard to pass between Pelee Point, seven miles to starboard and Pelee Island, which is dead ahead at 10 miles. The southern shore of Lake Erie is at the left, 30 miles away, while the Canadian shoreline is at the right.

ACKNOWLEDGMENTS

MINIATURE TUBES IN WAR AND PEACE*

By

N. H. GREEN

Tube Department, RCA Victor Division.
Harrison, N. J.

Summary—In 1939, a new line of miniature tubes was made available for use in small personal-type receivers. Since that time, the use of miniatures has been extended into electronic equipment of almost every type. This paper describes the design features which account for the versatility and lower cost of the miniature tube and cites several varied applications of miniatures in both military and commercial equipment. A table showing typical present-day applications for miniature tubes is included.

INTRODUCTION

EACH basic receiving tube enclosure has features which make it particularly suitable for specific fields of application. The miniature tube enclosure incorporates most of the desirable features of the other enclosures. It was first introduced by this company in a line of battery-type tubes in 1939 and has since shown a versatility unmatched by any other of the basic enclosures. The miniature tube design was achieved principally through the elimination of non-essential parts. The high standards of performance, low cost, versatility, and small size of tubes incorporating this design are attributable to a large degree to the simplicity of the construction.

In World War II, miniature tubes were first used in war applications to provide more compact equipment and to make available high-frequency tubes which could be mass-produced. Before the end of the war, however, over 50 million of these tubes had been used in nearly every field of electronic application.

Engineering developments and mass-production techniques are now directed intensively toward many peacetime products. The application of miniature tubes to wartime equipment provided a good proving ground to test their performance and dependability, and the promise held for their widespread commercial use is now being fulfilled.

The purpose of this paper is to describe the miniature tube development and the history of its rapid extension to military and commercial use.

---

* Decimal Classification: R330.

Development of the Miniature Tube

The development of a battery-operated, personal-type receiver having the general size of the average camera and capable of being produced at reasonable cost was begun in 1938. Smaller tubes of high efficiency and low cost were among the first requirements. To provide such tubes, the development of a small tube enclosure was started.

As a result of this work, four filamentary-type tubes in the new miniature envelope were made available in 1939 for use in a personal-type radio receiver (see Figure 1). These tubes were the 1T4 radio-frequency pentode, 1R5 converter, 1S5 diode-pentode, and 1S4 output
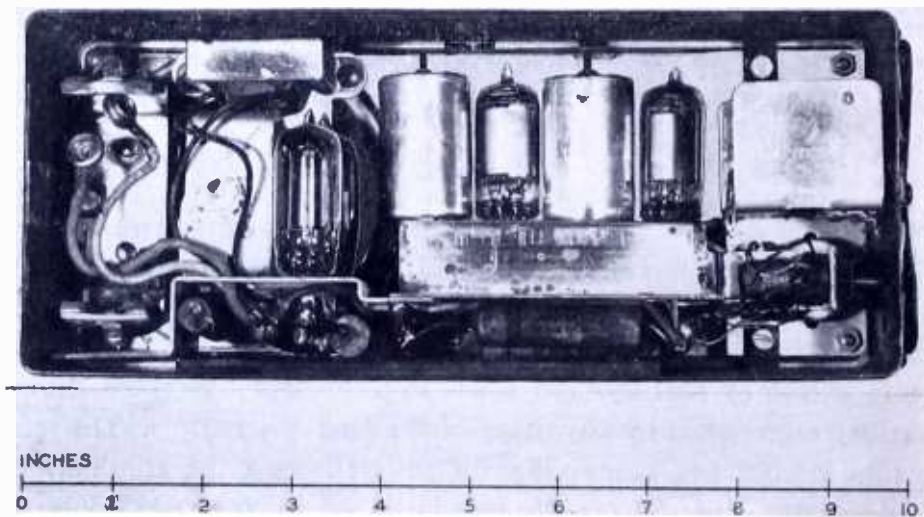
Fig. 1—An early model personal receiver.

pentode. All of the tubes used a 1.4-volt filament with low current drain suitable for small dry-battery operation. The receiver space required for the four tubes was only about one-fifth of the space required for the equivalent tube complement in glass tubular (GT) bulbs.

Although several types of small tubes had previously been available, the new miniature tubes had one very important advantage. The reduction in size was accomplished almost entirely by the elimination or redesign of auxiliary parts, while components of the electrode assembly, or mount cage, were comparable in size to those of the larger receiving tubes. Consequently, the manufacturing techniques for parts and assembly of the mount cage, where the bulk of the labor for tube making is required, were essentially unchanged and high-speed methods developed for standard types were directly applicable to the miniatures.[1]

---

[1] N. R. Smith and A. H. Schooley, "Development and Production of the New Miniature Battery Tubes," *RCA REVIEW*, Vol. IV, No. 4, pp. 496-502, April, 1940.

This feature played an important part in the speed with which mass-production of miniature tubes was achieved in World War II.

The reduction in tube size was effected principally by two design features. First, the conventional base was eliminated on the miniature tube by extending the lead wires from the electrodes through the glass seal to serve as base connections. The temper of the external lead wires was carefully adjusted to provide sufficient stiffness for easy insertion into a socket, yet the leads were kept flexible enough so that severe strains were not placed on the glass seal through misalignment of the pins and socket lugs. Secondly, the conventional press-seal stem used in the larger tubes was replaced by a flat button stem with the
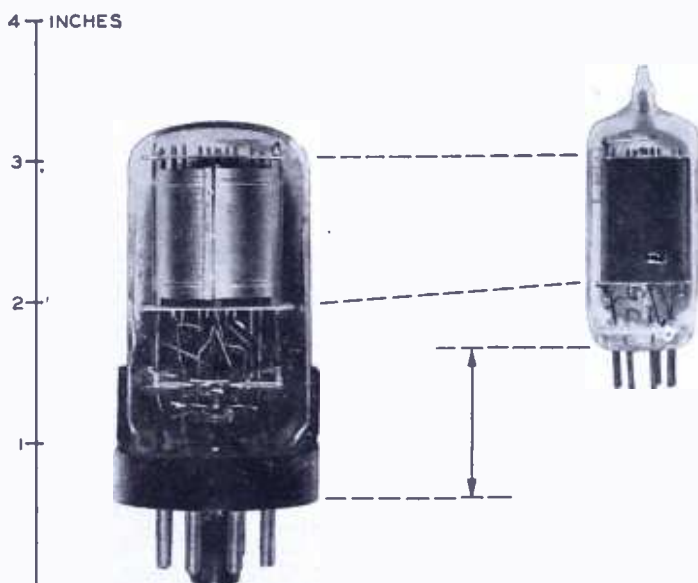
Fig. 2—Comparative dimensions of miniature type 12BE6 and glass type 12SA7-GT.

seven lead wires positioned in a circle and sealed in the same plane as the glass seal between the bulb and stem. This arrangement provided shorter connections to the electrodes, improved the high-frequency performance and the heat conduction through the lead wires, and reduced both the length and diameter requirements of the enclosure. The separation between lead wires in the seal was increased by the circular lead arrangement which reduced the possibility of electrical leakage and minimized the capacitance between lead wires. A wider spacing between pins one and seven gave a positive index for insertion of the tubes in sockets.

Compared to the equivalent GT tubes, the miniatures provided a reduction in diameter from 1 5/16 inches to ¾ inch maximum and a

reduction in overall length from 3 5/16 to 2⅛ inches maximum (see Figure 2). The fact that the miniatures do not have a conventional base removed a source of dielectric losses and a costly operation in manufacture. At standard broadcast frequencies, the two types were comparable in performance but the miniatures gave promise of superior performance at higher frequencies.

MINATURE TUBES IN WAR

With the advent of war, the trend toward more compact, lighter-weight equipment was greatly accelerated. Portable transceivers of smaller size were needed for the infantry. Compact, lightweight units were required for aircraft communication receivers and radar equipment. Balloon transmitters for weather forecasting, detection and trigger equipment for water mines, emergency transmitters for life rafts, and radio controls for guided missiles were but a few of the many applications requiring smaller tubes.

A further war need was for tubes which would operate satisfactorily at higher frequencies. Few GT types are efficient above 100 megacycles, but the military requirements demanded that equipment be made to operate at a frequency of several hundred megacycles.

Anticipating these requirements, work was started in 1940 to develop heater-cathode tubes as well as additional filamentary types in miniature enclosures. Other types of small tubes which were then available required slow, precise assembly by highly skilled operators and could not possibly meet the expected demands.

The most urgent needs in heater-cathode types were for a radio-frequency amplifier, a local oscillator, and a mixer for the conversion of the high carrier frequencies to an intermediate frequency which could be handled by conventional tubes. An early solution to this problem was found by transferring to the miniature enclosure the mount cages of the acorn types 954, 955, and 956, which had already been proven for high-frequency operation. The new miniature heater-cathode types were introduced in 1941 as the 9001, 9002, and 9003 to provide a complement consisting of a mixer, local oscillator, and radio-frequency amplifier. In laboratory tests on the miniature equivalents of the acorn types, some sacrifice in top frequency was observed, but the results were better than predicted. It was evident that small tubes suitable for high-speed manufacture could be made for operation at frequencies of several hundred megacycles.

Using types 9002 and 9003, an Army communications receiver (SCR-522-A) was designed and placed in production for aircraft

service. Operating on a frequency band of 100 to 156 megacycles, this transmitter-receiver unit had a working range of 180 miles at an altitude of 20,000 feet. It was used extensively for aircraft and vehicular communications throughout the war.

As the use of high-frequency miniatures was rapidly extended to other equipments, the advantages of their small size became more evident and the development of other miniatures was undertaken for use at frequencies which could be handled by conventional types if space were not a consideration. Additional features, not anticipated originally, became evident with expanding field use. Under climatic conditions of high humidity, the basing cement on conventional types deteriorated, moisture was absorbed by the base, and high electrical leakage resulted. Also, salt water spray during shipboard operation took its toll in corroding external metal parts of conventional tubes. The baseless miniature tube, however, did not absorb moisture, and the nickel external pins and glass enclosure, which were the only surfaces exposed, were practically impervious to corrosion. A further advantage disclosed by field use was that while the miniatures on casual inspection appeared less sturdy than the larger tubes, the lower mass of the miniatures actually gave better shock-resistant qualities to withstand the impact of gun-fire, the high acceleration of units enclosed in missiles, and the rough usage encountered in mobile service.

One question unanswered at the start of the war was whether heater-cathode types with appreciable wattage input could be made to operate with satisfactory life in the smaller miniature enclosure. Since the size of the electrodes was not reduced appreciably and the short lead connections provided good heat conduction to the socket, the possibilities for higher dissipations appeared favorable except for limitation of increased bulb temperatures, resulting from the greatly reduced radiating area of the miniature enclosure. If higher dissipations could be tolerated, miniature types having better transconductance and higher peak currents could be designed.

In answer to this, the 6C4 oscillator, introduced in 1942, was found to be capable, in Class C oscillator service, of dissipating five watts in the plate with approximately one watt cathode input. At 150 megacycles, the average power output obtainable was 2.5 watts. As a result, this miniature triode found wide use in both local-oscillator service and pulse-modulator applications where higher dissipations were required. One model of aircraft interrogation equipment (AN/AP-2), for example, used nineteen miniature 6C4 tubes out of a total complement of forty-four tubes, of which all but three were miniatures.

With the knowledge that higher wattages were practical in minia-

ture tubes, work was concentrated on the design of a mixer tube and an intermediate-frequency amplifier to complete a high-frequency miniature complement having transconductances of the same values as the comparable larger receiving types. These types were made available during the latter half of 1942 as the 6J6, a twin triode mixer-oscillator with a transconductance of 5300 micromhos at 8.5 milliamperes for each triode section, and the 6AG5, a radio-frequency pentode with a transconductance of 5000 micromhos at a cathode current of 9 milliamperes. The 6J6 was used in pulse-oscillator service at frequencies as high as 450 megacycles and the 6AG5, although used principally in 30-megacycle intermediate-frequency amplifiers, was employed in some applications at frequencies as high as 200 megacycles.

It was soon found that many equipment designers were using the 6J6 connected as a diode for a second detector to conserve space and gain higher perveance than could be obtained with standard types specifically intended for detector use. To provide for this service, the high-perveance, miniature twin diode 6AL5, was introduced in 1944. This tube has a voltage drop in each section comparable to a diode-connected 6J6. For narrow band applications requiring less perveance, the twin-diode high-mu triode 6AQ6 was introduced during the same year.

The introduction of these tubes gave receiver designers a complete miniature complement of heater-cathode types through the second-detector stage for equipment operating up to 400 megacycles. In 1943, the 6AK6 output pentode was introduced to complete the receiver complement.

The rapid development of heater-cathode type miniatures was paralleled by a similar program to provide filament-type miniatures for dry-battery, portable communications equipment for the infantry. The original miniatures introduced for the personal receiver formed the nucleus for a receiver complement, but there were no existing types suitable for a transmitter. In the early part of 1942, the 3A5 twin triode, giving 2-watts output at 40 megacycles with a filament input of only 0.3 watt, was introduced. A radio-frequency power pentode type 3A4 was also made available for class C transmitting service. The 1L4 sharp-cutoff pentode and the 1A3 diode for frequency-modulation detection use completed a working complement of filamentary miniatures for portable transceiver applications.

With these new types and the personal-receiver tubes developed before the war, a "walkie-talkie" frequency-modulation transceiver, SCR-300-A (Figure 3), was developed and became the first radio field telephone which was truly portable. With the necessity for telephone

lines eliminated, the "walkie-talkie" made possible the maintenance of communications between fast-moving combat units and proved to be one of the most important tactical weapons of the war. The "walkie-talkie" contained eighteen miniature tubes in a unit 5 by 11 by 17 inches with total weight, including batteries, of thirty-eight pounds. Operating at a signal frequency of 40 to 48 megacycles, the quick-heating miniatures gave instant switch-on service and a working radius of three miles.

The first large-scale test of the filament-type miniature tubes was provided by the SCR-300-A in the invasion of Sicily. The records of tubes replaced in equipment used by combat divisions during this

Fig. 3—Walkie-talkie transceiver (SCR-300-A).
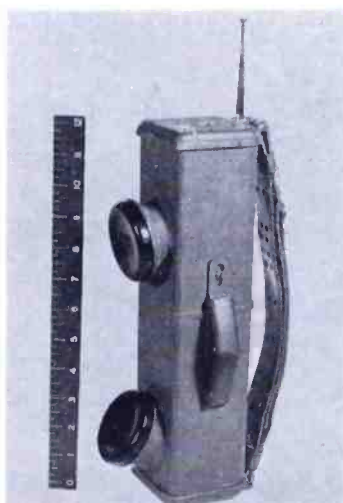
Fig. 4—The handy talkie (SCR-536).

campaign showed that despite the rough usage of battle service the tube replacements for all reasons were less than three per cent of the total number in service. The results firmly established the ruggedness and dependability of the miniature tubes.

A still smaller transceiver of lighter weight, the "handy-talkie" SCR-536 (see Figure 4), was employed in the Pacific during the latter months of the war. Using a total complement of five miniatures and weighing less than six pounds, this unit was only 4 by 6 by 16 inches in size and could be held conveniently in one hand during operation.

The applications of miniature tubes to war equipment were so many and so varied that only a few can be cited. The best indication of their contribution to the war effort can probably be given by production figures. Although this compay was the only manufacturer of miniature

tubes in 1939, the end of the war found all of the seven principal suppliers of receiving tubes producing miniatures in large quantities. Figures available from the War Production Board records from September 1943 to July 1945 show that over the twenty-three month period a total of more than 50 million miniature tubes were produced by the industry for military use (see Figure 5). The monthly production rate for all companies increased from a total of 800,000 tubes in September 1943 to over 3,500,000 tubes in May 1945.

MINIATURE TUBES IN PEACE

The promise of widespread commercial use of miniatures was evident at the end of the war. The shift in frequency allocations to establish frequency modulation in the band of 88 to 108 megacycles,
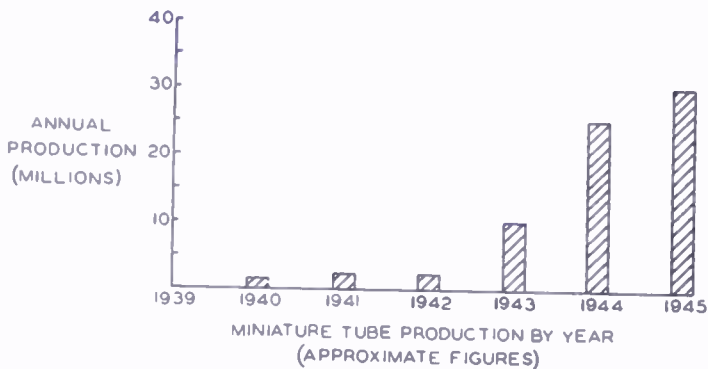
Fig. 5—Miniature tube production by year.

the higher-frequency requirements for television, and a general trend toward more compact ac/dc and battery-portable receivers all indicated that miniature tubes would eventually carry the bulk of the peacetime production load for the new designs of broadcast receivers.

In September 1945, a complete miniature complement of tubes for ac/dc receivers were made available. These tubes include the 12BA6 radio-frequency pentode, 12BE6 converter, 12AT6 twin-diode-triode, 50B5 output pentode, and the 35W4 rectifier (see Figure 6). This complement is comparable in performance and cost to the tube complements used for pre-war ac/dc receivers. Their use has made possible the more compact receivers now available. Coincident with the ac/dc line, the 6.3 volt equivalents 6BA6, 6BE6, and 6AT6 were introduced, together with a sharp-cutoff radio-frequency pentode, the 6AU6.

In order to provide for operation at both amplitude- and frequency-modulation frequencies, the miniature radio-frequency amplifier and the converter were designed to have higher gain and improved high-

frequency characteristics as compared with the pre-war equivalent larger types intended for the lower frequencies only. As a result, the combination amplitude- and frequency-modulation receivers now in production are using the same miniature tubes for both bands. In addition to the savings in receiver cost, a lower unit cost for tubes is made possible by the resulting concentration on fewer tube types.

In December 1945, the new miniature rectifier 117Z3 provided, with existing filamentary types, a complete miniature complement for portable ac/dc-battery receivers. A miniature line for automobile receivers was also provided for with the availability of the 6X4 rectifier, the 6BF6 twin-diode medium-mu triode, and the 6AQ5 beam power amplifier. High-frequency types 12AW6 radio-frequency pentode and the
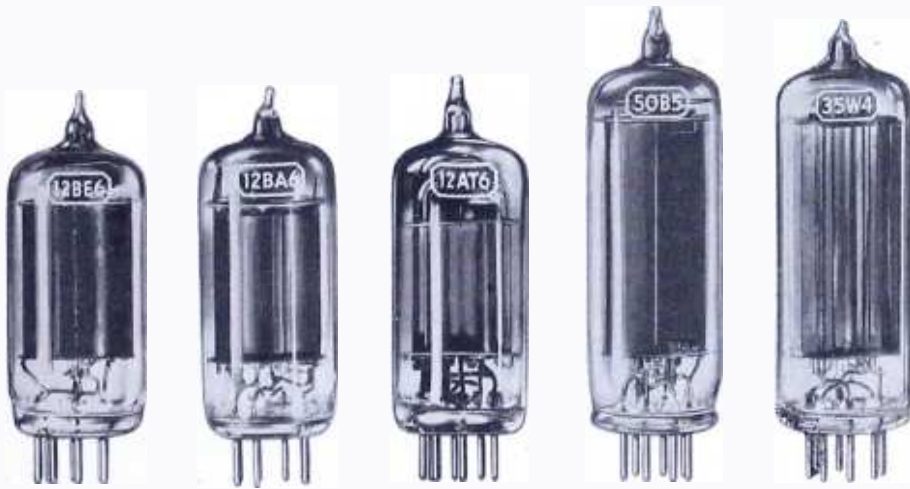
Fig. 6—AC/DC miniature tube kit.

12AL5 twin-diode detector are recent additions designed for use in ac/dc receivers for frequency-modulation reception.

In the television field the space saving and performance afforded by miniatures are particularly desirable because of the large number of tubes required for each receiver and the high frequencies of operation. The current 10-inch table-model television receiver of this company uses 15 miniatures out of a total complement of 30 tubes.

In addition to their use in the field of broadcast entertainment, miniatures are rapidly being extended into industrial applications. The 2D21 thyratron, OA2 voltage regulator, and 1654 high-voltage rectifier are employed in many industrial applications where their small size and ruggedness are of advantage. Recently, a nine-pin miniature twin-triode, 12AU7, was made available in a slightly larger envelope for industrial applications as well as for home-receiver use. Although

intended primarily to provide the additional pin connections required
for multi-unit tubes, the nine-pin miniature envelope also opens up
possibilities for higher-wattage types to supplement the seven-pin
miniature line, since bulb temperatures are the present limiting factor
in the extension of seven-pin types.

CONCLUSION

The four miniature tubes first introduced in 1939 were designed
to fill the need for tubes which could be produced in quantities and at
reasonable cost for a compact personal-type receiver. In the interven-
ing years, however, the practical experience with miniatures has shown
them to be adaptable for general receiving tube use with an exceptional
range of capabilities. The versatility of miniatures holds promise for
higher performance and lower costs in electronic equipment of the
future.

ı

Typical Applications for Miniature Tubes
(See Table on opposite page)

Table 1—Applications for Miniature Tubes

Application	ac/dc Receivers (AM)	ac/dc Receivers (AM-FM)	ac Receivers (AM-FM)	Automobile Receivers	Television Receivers	"Personal" & Three-way Portable Receivers	VHF, Industrial & Low-Power Transceivers
RF Amplifier	12BA6	12BA6, 12AW6	6AG5, 6BA6	6BA6	6J6, 6AG5	1U4, 1T4	6J4, 9003
Converter or Mixer	12BE6	12BE6	6BE6, 6AU6	6BE6	6J6	1R5	6J6, 9001
Oscillator			6C4, **6BE6				9002, 3A5
Sound IF Amplifier	12BA6	12BA6	6BA6	6BA6	6BA6	1U4, 1T4	9003
Picture IF Amplifier					6AG5		
Limiter or Driver		12AU6	6AU6		6AU6		1L4
Detector & AF Amplifier	12AT6	6AQ6, 12AL5, 12AT6	6AL5,* 6AT6	6AT6, 6BF6	6AL5,* 6AT6	1S5, 1U5	1A3*
Power Output	35B5, 50B5	35B5, 50B5	6AQ5	6AQ5	6AQ5	3V4, 3S4, 1S4	3A4
Rectifier	35W4	35W4			6X4	11Z3	
Video Amplifier					6AU6		
DC Restorer					6AL5		
Phase Inverter			6AT6				
Thyratron							2D21
Voltage Regulator							OA2
High-Voltage Rectifier							1654

** Triode Connected

* Has diode(s) only

RADIATION ANGLE VARIATIONS FROM IONOSPHERE MEASUREMENTS*†

By

H. E. Hallborg and S. Goldman

Research Department, RCA Laboratories Division
New York, N. Y.

Summary—The heights of the F and F_2 layers at Washington, D. C. and San Francisco, California, and their variability ranges are studied for the year 1945. These data are applied to determine the optimum radiation angle ranges for various hop modes on the New York-San Francisco Circuit. Wide diurnal and seasonal variations are indicated. Practical applications to effective antenna design are discussed.

Introduction

MINIMUM virtual height measurements, supplied by the Central Radio Propagation Laboratory (CRPL) for the year 1945, are applied to the New York-San Francisco Circuit for determination of radiation angle ranges for that year. Median and hourly height limits are determined throughout the year. Two modes of propagation are considered, and their corresponding ranges of optimum angles of radiation computed. The diurnal and seasonal optimum radiation angle ranges are then fitted to vertical radiation patterns of typical horizontal rhombic antennas on the New York-San Francisco Circuit for analysis of their diurnal and seasonal performances with respect to radiation intensity at the lowest mode of prapagation, and the order of multipath interference from the next higher mode.

Ionosphere Height Ranges in 1945

Prior frequency analysis of the New York - San Francisco Circuit had indicated control by the F and F_2 layers. The analysis is therefore mainly concerned with these layers. Ionosphere conditions at the New York end of the circuit are typified by conditions at Washington, D. C., 39.0° N, 77.5° W. San Francisco, California, 37.4° N, 122.2° W, ionosphere conditions are utilized for the western end of the circuit.

Hourly heights of the F and F_2 layers were directly available from the CRPL form sheets. The hourly range was deduced for quiet con-

---

* Decimal Classification: R113.
† Presented at the International Scientific Radio Union (U.R.S.I.) Conference in Washington, D. C., on May 6, 1947.

ditions, existing for at least 67 per cent of each month. This was done by selection, as limits, of the 6th highest height reading and the 6th lowest for each hour. This procedure eliminates abnormalities due to ionosphere storminess and unusual ionization conditions. It produces results typical of normal circuit conditions.

The normal ranges of F and F_2 layer heights during 1945 measured as indicated above were as follows:

Washington, D. C.	*San Francisco, California*
F range 147 to 180 miles	F range 140 to 190 miles
F_2 range 140 to 245 miles	F_2 range 140 to 237 miles

The month-by-month height variations in terms of median and normal maximum-minimum range limits are shown in Figure 1. The heights are given in miles for better application to formulas and graphs for conversion to radiation angle equivalents.

A wide seasonal variation of daytime heights is indicated in Figure 1. The night heights, on the other hand, are low and show no definite seasonal variations.

GEOGRAPHY OF THE NEW YORK - SAN FRANCISCO CIRCUIT

The airline distance between New York and San Francisco is 2,568 miles. The Rocky Mountains, at an elevation above sea level of about two miles and located 700 miles from the west coast, are fortunately located so as to form no hazard to ground reflection at the most suitable modes of propagation, namely, two and three hops.

The skip distance for the lowest practical mode of propagation, two hops, is 1284 miles per hop. At three hops the individual hop distance is 856 miles.

When the observed hourly F and F_2 layer height ranges are converted to their equivalent optimum radiation angle ranges at two and three hops they provide a graphic outline of the diurnal and seasonal beam angle ranges required.

DIURNAL AND SEASONAL RANGES OF OPTIMUM BEAM ANGLES

Inspection of Figure 1 indicates that the daytime beam angles might be expected to undergo a seasonal cycle, being low in the winter and high in summer. It will suffice for the purpose of this paper to take three months, December, March and July as typical of winter, equinoctial and summer conditions, and to follow the diurnal variations of angles during these months.
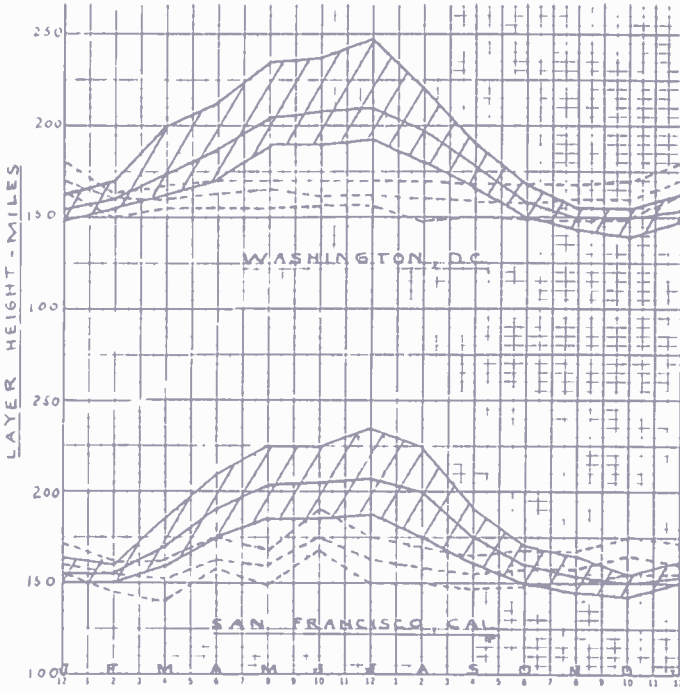
Fig. 1—Mean heights and variability spread of F and F_2 layers from analysis of ionosphere recordings for the year 1945. (Solid lines—average day; dotted lines—average night.)

Winter Conditions

Optimum hourly beam angle ranges for two and three hops, during December 1945, on the circuit of reference, are shown in Figure 2.

Fig. 2—New York to San Francisco circuit optimum vertical beam angles, for two and three hops, from ionosphere height measurements. (December, 1945.)

The daytime beam angle range for two hops is seen to be from 6.8 to 10.6 degrees while for three hops the range becomes 12.6 to 18.6 degrees. Between these modes there exists a very appreciable "guard angle". Inspection of the figure at once suggests that if the antenna beam is constructed to include only the two-hop mode, and to exclude completely the three-hop mode, a great reduction of multipath interference will result.

A word of explanation pertaining to the cross sectional areas representing each hop mode in the figures will be helpful. The area marked "zero spread" is based upon median heights at the first and last ionosphere reflection points. A beam spread occurs only when these reflection points are at different heights. The areas marked

Fig. 3—New York to San Francisco circuit optimum vertical beam angles, for two and three hops, from ionosphere height measurements. (March, 1945.)

"height variability spread" includes the hourly height ranges above and below median value. This procedure is based upon equal hop distances.

Equinoctial Conditions

Optimum beam angle ranges on the circuit of reference during equinoctial conditions are illustrated by Figure 3. A pronounced increase in elevation of daytime angles above winter conditions is evident in this figure. This rise corresponds to the increase in F_2 layer heights from Figure 1. Night angle ranges, however, are quite similar to those of December. A very appreciable "guard angle" exists between the two-hop and three-hop modes in March as well as December.

Summer Conditions

Mid-summer beam angle ranges are illustrated by the month of July in Figure 4. The two-hop beam spread has now increased to include a range from 8 to 20 degrees. The maximum angle occurs at 1300 Eastern Standard Time which is approximately noon at the mid-point of the circuit. The "guard angle" has disappeared during some hours near sunrise and sunset at the midpoint of the circuit. Night conditions, on the other hand, are about the same as during equinoctial and winter conditions.

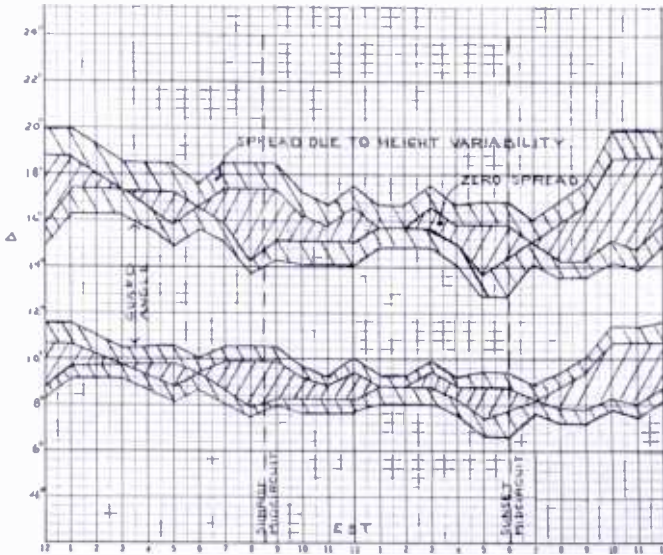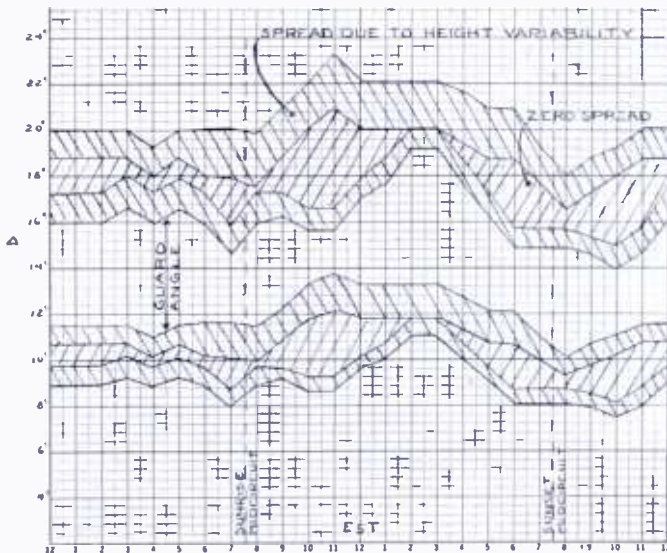The wide range of daytime angles required indicates that no fixed
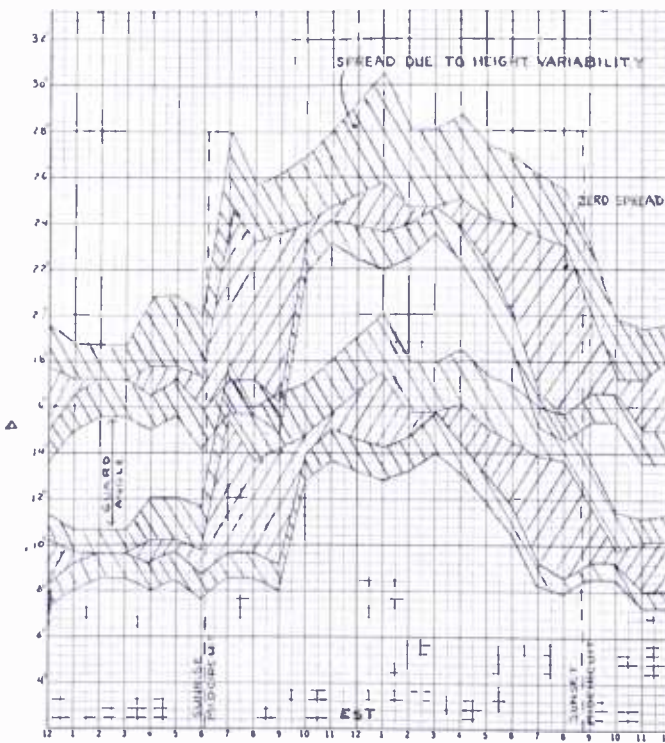
Fig. 4—New York to San Francisco circuit optimum vertical beam angles, for two and three hops, from ionosphere height measurements. (July, 1945.)

beam type of antenna could be expected to be effective·equally at all seasons.

MEASURED ARRIVAL ANGLES AND COMPUTED ·RADIATION ANGLES COMPARED

Just prior to the entry of this country into World War II a series of arrival angle measurements between Bolinas, California and River-head, New York were made by the Riverhead laboratory staff. The

tests extended over a period from September 21, 1941 to December 7, 1941, with Bolinas transmitting on 15.46 megacycles. The daily test period was from 9:00 a.m. to 8:00 p.m. It therefore included the daylight hours and the early night hours. A summary by hours of the observed arrival angle groupings is shown in Figure 5. Superimposed upon the observed angle groups are the computed optimum radiation angle ranges for two and three-hop modes for the corresponding months in 1945. Considering the differences in time between the measured and computed angle ranges the agreement is quite impressive.

The following typical characteristics appear in both observed and computed ranges:
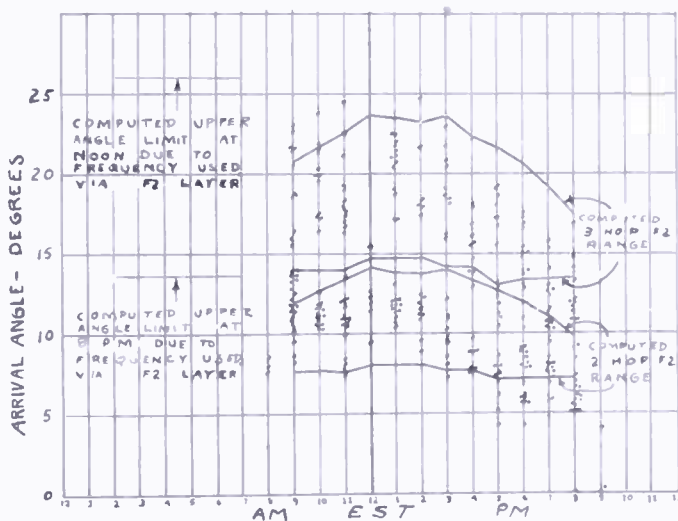
Fig. 5—Vertical arrival angle (KKR-15460 kilocycles) at Riverhead 9/21/41 to 12/7/41 compared to computed optimum angle range 2 and 3 hops via F_2 layer, September-November, 1945. (Only pulses of maximum amplitude and those of greater than 50 per cent of that value are recorded.)

1. Two main groups of angles, an upper and a lower group, corresponding to the two- and three-hop modes, are clearly discernible.

2. Highest values occur at midday on the circuit, 1:00 p.m. Eastern Standard Time, and the lowest values at night.

Observed angles on the order of 5 degrees may be accounted for by disturbed ionosphere conditions, included in the five low hourly readings which were discarded by the analysis method, or to generally lower ionosphere heights prevailing in 1941. Angles considerably higher than the normal day limits are excluded by ionosphere penetra-

tion. Computed upper limits of this penetration for both hop modes are shown at the lower left of the figure.

ANTENNA COMPARISON METHODS

Ordinary methods of comparing high-frequency antenna performances by means of signal recorders provide no means for discrimination between hop modes. The signal is usually an integration of several modes, unless specific precautions have been taken at both ends of the circuit to control the antenna patterns. When the receiving antenna is of the dipole type it normally covers a wide range of arrival angles. The signal picked up will then be the vector sum of all modes within its vertical pattern range.

High-speed high-frequency circuits require selected propagation modes. The circuit may be analyzed for such modes by the procedure outlined in the following sections.

HIGH-FREQUENCY DAY RHOMBIC PERFORMANCE COMPUTED

When the vertical radiation pattern of a day rhombic antenna is matched to the required hour-by-hour optimum beam angle ranges, determined from ionosphere height data, it is possible to compute the performance to be expected from the antenna for each month of the year. A horizontal reference rhombic having a leg length of 6.16 wavelengths, a half-side angle of 72.5 degrees, and respective heights above ground of 1.07 and 1.78 wavelengths will be applied for this purpose. It will suffice to state that the main lobe of the vertical pattern peaks at 8.5 degrees when the height is 1.78 wavelengths, and at 12.5 degrees when the height is 1.07 wavelengths. The comparison will be with respect to height only, but it will be understood that the 1.78 wavelength height corresponds to low angle radiation and 1.07 wavelength height to high radiation angles, and a considerably wider beam.

Radiation intensity equivalents for the hourly optimum beam angles, corresponding to two- and three-hop modes, are taken from the vertical radiation pattern of the rhombic. Radiation intensities in all cases are compared at the two-hop mode. The height that shows greater intensity at the two-hop mode is that giving better performance, but the selection must further be referred to comparative freedom from multipath interference due to the third mode.

The multipath comparison is made in terms of radiation intensities at the three-hop mode, referred to the two-hop mode, in decibels. A — 4 decibel reference level may be applied as the limit within which interference from the three-hop mode would cause serious distortion

to teletype transmission with frequency-shift keying when the shift is 100 cycles.

Figure 6 summarizes the results of analysis of the performances of the reference rhombics for daylight conditions on the New York-San Francisco Circuit during the year 1945.

The low angle, 1.78 wavelength high rhombic, is seen to give better performance from September through March. The high angle, 1.07 wavelength high rhombic is the better performer from April through August. The high rhombic is limited by radiation intensity in summer, the low rhombic by multipath interference in winter.
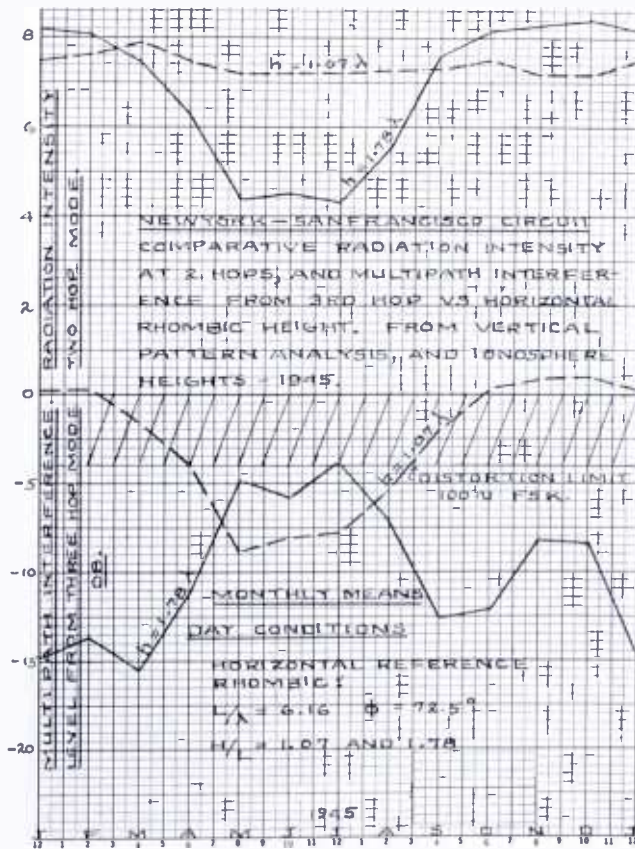
Note: H/L in above figure should read H/λ.

Fig. 6—New York-San Francisco circuit, comparative radiation intensity at 2 hops, and multipath interference from 3rd hop vs. horizontal rhombic height; day conditions. (From vertical pattern analysis and ionosphere heights—1945.)

HIGH-FREQUENCY NIGHT RHOMBIC PERFORMANCE COMPUTED

When the vertical radiation patterns of the 1.07 and 1.78 wavelength high rhombics are analyzed by the process outlined above, for

night conditions over the New York-San Francisco Circuit in 1945, the performance results are as shown in Figure 7.

This figure indicates that the limitation here is definitely distortion due to multipath interference from the three-hop mode. Both rhombic heights deliver a good signal at two hops throughout the year. The 1.07 wavelength high rhombic, however, delivers a signal via the third hop that is within the $- 4$ decibel distortion limit throughout the year. Such an antenna would limit the circuit to slow-speed service types, and render an inferior quality of service.
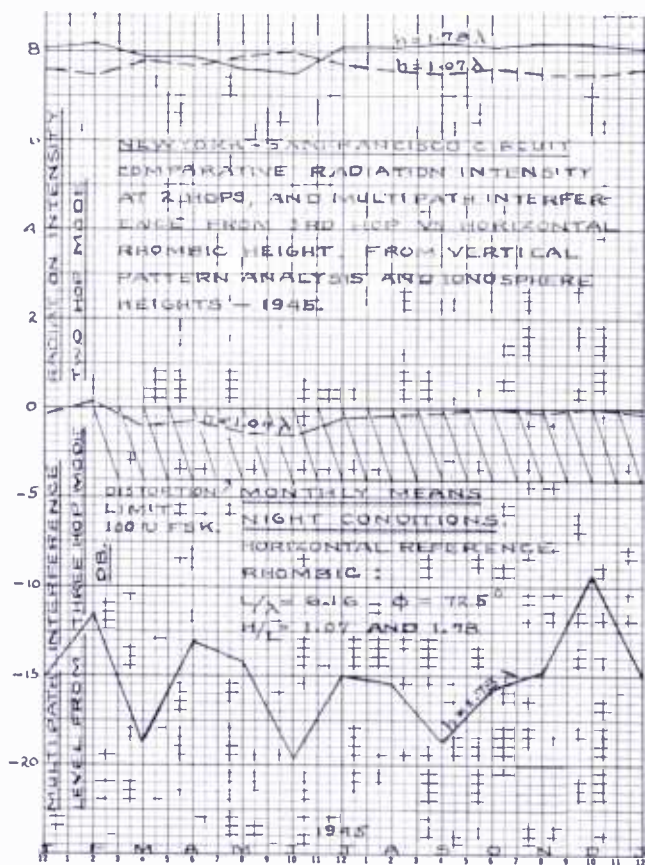
Note: *H/L in above figure should read H/λ.*

Fig. 7—New York-San Francisco circuit, comparative radiation intensity at 2 hops, and multipath interference from 3rd hop vs. horizontal rhombic height; night conditions. (From vertical pattern analysis and ionosphere heights—1945.)

It is important to note that whereas the electrical dimensions of the day and night rhombics considered above are the same, their physical dimensions will differ greatly. This is due to the lower frequency that must be used at night.

This natural limitation of frequency usage further reacts to offset

the well-known frequency flexibility of the rhombic, as far as impedance matching conditions are concerned. A two-to-one frequency range between day and night, applied to a given rhombic will cause its nighttime electrical length and height to be halved. This electrical condition will result in a higher and wider vertical pattern at night with results as indicated in Figure 7. Viewed from the dual viewpoints of operation and economy this is an unfortunate characteristic of the ionosphere.

CONCLUSIONS

1. F_2 layer heights at Washington, D. C. and San Francisco, California in 1945 ranged from 140 miles in winter to 250 miles in summer, during undisturbed days.

2. F_2 layer height variability is greatest in summer; lowest in winter.

3. The night F layer heights show no regular seasonal variation; but are comparatively low, 140 to 190 miles throughout the year.

4. A fixed beam type of high-frequency antenna for daytime usage will not give maximum performance at all seasons.

5. A much larger physical structure is required at night to produce the low angle radiation needed at low operating frequencies.

6. No serious differences in minimum virtual height of the layers at oblique incidence, as compared to vertical incidence is indicated. The possible height reduction at oblique incidence appears to be offset by increased penetration accompanying the higher frequencies which oblique incidences provides.

STABILIZED MAGNETRON FOR BEACON SERVICE*†

Part I

DEVELOPMENT OF UNSTABILIZED TUBE

By

J. S. DONAL, JR.,‡ C. L. CUCCIA,‡ AND B. B. BROWN#

Summary—The frequency of a magnetron varies rather widely with temperature, current, and load impedance. This paper describes one of the first successful attempts to reduce this frequency variation by means of a method of stabilization. Part I treats particularly the mechanical and electrical design of the unstabilized tube.

The mechanical design of the tube is unconventional in that all of the parts are supported on a header to which the envelope is welded. The necessary inserts in the magnetic circuit are at cathode potential, serving both as cathode supports and as improved cathode end-shields. The tube is designed for a pulsed input power of 2500 watts. The unstabilized peak power output is approximately 1 kilowatt at an anode potential of 2500 volts. The developmental cavity stabilizer served to demonstrate the principles of stabilization and influenced the design of the tube. For production purposes, the early stabilizer was superseded by a design differing in mechanical details.

INTRODUCTION

THE pulsed magnetron described in this paper was required for use in a portable beacon system. The tube is of unusual design and represents the first magnetron to be stabilized against frequency changes by being coupled to an external resonant cavity. The frequency-stability requirements of the beacon application, together with the design of the combination of the production tube and stabilizer, with the results obtained, are described in Part II. Part I describes the electrical design of a developmental tube which has permitted rapid changes in performance requirements, and results in a high-efficiency tube, capable of about 1 kilowatt output at 2500 volts, and having

characteristics suitable for stabilization. The mechanical design described constitutes a radical departure from previous practice.

MECHANICAL DESIGN OF THE UNSTABILIZED TUBE

The tube was the first magnetron designed which used header construction. In Figure 1, it will be seen that all parts comprising the anode, resonant cavities, cathode structure and internal magnetic circuit are rigidly connected mechanically but are mounted on a comparatively flexible header. The leads, the load line, and the exhaust tubulation pass through this header. The tube may thus be completed, adjusted, and inspected immediately before the addition of the envelope.
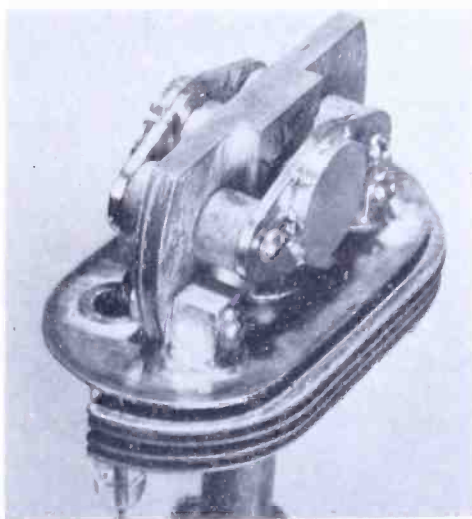
Fig. 1—An earlier pulsed magnetron for 5 kilowatts output from which basic design of the new tube was adapted.

Furthermore, rebuilding, which is frequently necessary with any developmental tube, involves merely removal of the envelope, replacement of necessary parts, and envelope replacement.

In choosing the contour of the header and the shape of the envelope it was desired to keep the dimension in the direction of the magnetic field small, yet to extend the other dimension parallel to the header to allow room for a rigid mechanical structure and for changes or additions should they prove necessary. The envelope of familiar shape shown in Figure 2 had been used earlier in a receiving tube; it is ideally suited to the requirements of the magnetron. Made originally of nonmagnetic stainless steel and later of Monel metal, it is atomic-hydrogen welded to the header.

The anode and the twelve resonant cavities are contained in an anode block of the form shown in Figures 1 and 3. This block is

bolted to posts extending through the header. Early anode blocks were formed of thin disks accurately stamped to include slot-like resonant cavities, a process developed in 1941 by P. T. Smith and L. P. Garner. Later, copper vanes were soldered into vestigial slots in disks (Figure 1) to form cavities bounded by vanes and, in the final tube, the vanes and strapping rings are supported in jigs and soldered into the central hole of the anode block to form the assembly of Figures 3 and 5.

It was necessary to support the cathode rigidly and to provide a high-permeability path through a portion of the interior of the tube in order to reduce the weight of the permanent magnet to be used external to the tube. These requirements are met by the steel buttons
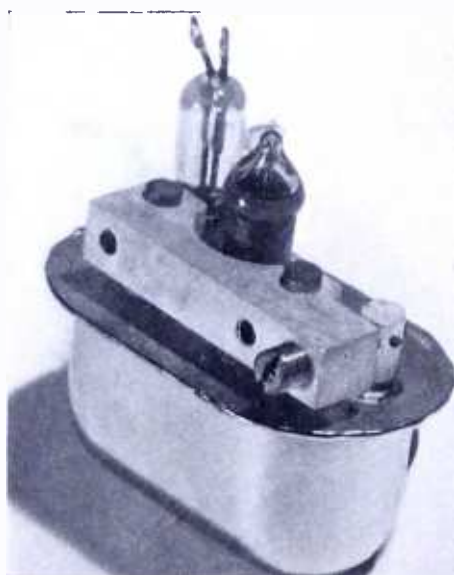
Fig. 2—Developmental tube showing the coaxial load-line seal. (This glass cup is designed to be introduced into the wave guide to which the cavity stabilizer is attached. A differential screw controls the movement of a rod which extends through the flexible header and actuates the tuning mechanism.)

shown mounted in non-magnetic brackets and bolted through ceramic insulators to the anode block. The cathode is welded to the edges of a clearance hole extending through one of the buttons (Figure 4) and projects into the anode space. The length of the cathode in contact with the button could be varied from tube to tube in order to vary the thermal path and strike the proper compromise between heater power and dissipation of heat arising from back-bombardment. The steel buttons reduce the total air gap in the magnetic circuit within the tube to 0.350 inch; the external magnetic field is thus reduced to about 37 per cent of the field within the anode space. In addition to affording
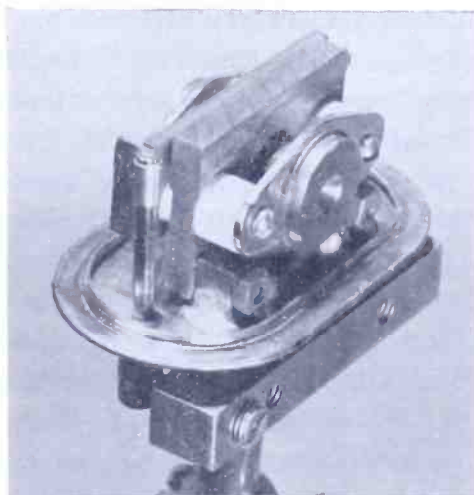
Fig. 3—Developmental tube showing the anode-block containing the twelve resonant cavities. (This block is bolted to posts extending through the header. The cylindrical steel inserts serve to reduce the weight of the external magnet and support the cathode.)

a cathode support the buttons improve upon the conventional cathode end-shields, due to their large area facing the resonant cavities, with the result that the efficiency of the tube is maintained at unusually low currents.[1] This observation has recently been confirmed by R. L.
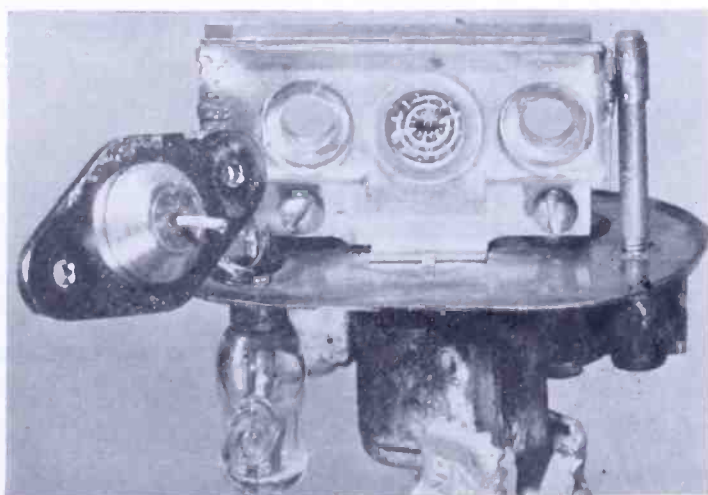
Fig. 4—Tube showing cathode, damaged in disassembling the particular tube shown, projecting through a hole in the steel insert. (The tuning plate, which varies the inductance of the resonant cavity system, is hinged at one end to the anode block.)

---

[1] The mechanical design so far described was later adopted for a 4000-megacycle continuous wave tube (G. R. Kilgore, C. Shulman, and J. Kurshan, "A Frequency-Modulated Magnetron for Super-High Frequencies", a paper presented at the I.R.E. 1947 National Convention in New York, N. Y. on March 4, 1947), and for a 10,000-megacycle continuous-wave magnetron developed by J. M. Stinchfield and J. Kurshan, of RCA Laboratories Division.

Jepsen† of the Radiation Laboratory at Columbia University.

The central conductor of the load line forms the coupling loop by being extended into a resonant cavity and attached to a vane. The outer end of the coaxial load line, designed in coöperation with H. R. Hegbar‡, is unique in that when the anode assembly is attached to the header the central conductor of the load line is accurately positioned in a glass cup (Figure 2) and does not extend through the glass; this simplifies the tube construction. The output of the tube is fed into a wave guide by inserting the glass-enclosed antenna through a hole in the broad face of the guide and providing appropriate matching adjustments.

The mechanical design of the final tube, required for beacon service, is tunable over a range of about 3 per cent in order that the frequency
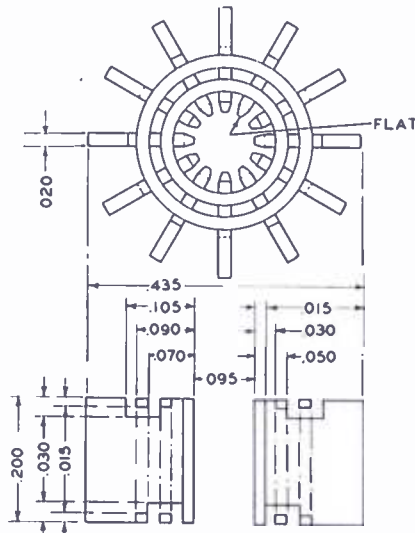
Fig. 5—The resonant cavity system with the twelve copper vanes. (Alternate vanes are connected together at one end by the inner strapping ring and at the other end by the outer ring. The vanes are tapered to make their width facing the cathode approximately equal to the gaps between the vanes. Dimensions are in inches.)

may be adjusted to 9310 megacycles before attachment of the stabilizer. After a cold-resonance investigation of various methods of tuning, advantage was taken of the flexibility of the header in the following manner. A plate is hinged to one end of the anode block as shown in Figure 4. In addition to clearance holes through which the ceramic insulators pass, a central hole in the plate is surrounded by an embossing which covers the outer portions of the resonant cavities. The free

end of the tuning plate is attached to a post extending through the header. The outer end of this post is moved by a differential screw so that, with the flexible header as a fulcrum, the tuning plate is caused to approach or to recede from the ends of the resonant cavities, varying their inductance. The tuning is reliable and reproducable, with a scarcely detectable change in power output throughout the range.

The rigidity of the mechanical design described above was confirmed by non-operating shake tests, in successive mutually perpendicular directions, at an acceleration ten times that of gravity, without mechanical failure; such shake tests at accelerations three times that of gravity, with the tube oscillating, resulted in no perceptible deterioration of the radio-frequency spectrum.

Electrical Design of the Unstabilized Tube

Development commenced with a previously-designed tube capable of a peak power output of 5 kilowatts at high efficiency, with an anode potential of 5 kilovolts. (It is of interest to note that this same basic tube was later scaled to yield a 1-kilowatt, continuous-wave magnetron,[2] in addition to the tube described in this paper.)

The final design requirements were for a tube for an ultra-portable beacon with frequency variations substantially decreased under those normally resulting from changes in temperature, current and load impedance inherent in all unstabilized magnetrons. The tube was to be tunable, and the peak power output was to be 300 watts, after frequency stabilization, with a duty cycle of 0.3 per cent.

The electrical design of the new tube was obtained by scaling the 5-kilowatt tube to the lower anode voltage and power levels. The scaling was accomplished by employing relations based upon the principle of similitude, developed by S. T. Martin.† The tube was scaled from a current and voltage at the low end of the operating range of the 5-kilowatt tube, so that the new tube proved adequate when the power requirements were increased later over original specifications. Several tubes were built in each of three different anode lengths, 0.110, 0.140, and 0.200 inches. The last length (Figure 5) was chosen to insure that power requirements could be met.

The rated current and voltage of the tube was finally set at one ampere at 2500 volts to ensure sufficient output after attachment of

---

[2] J. S. Donal, Jr., R. R. Bush, C. L. Cuccia, and H. R. Hegbar, "A 1-Kilowatt Frequency-Modulated Magnetron for 900 Megacycles", a paper presented at the I.R.E. 1947 National Convention in New York, N. Y. on March 4, 1947.

† Formerly with the Tube Department, RCA Victor Division, Harrison, N. J.
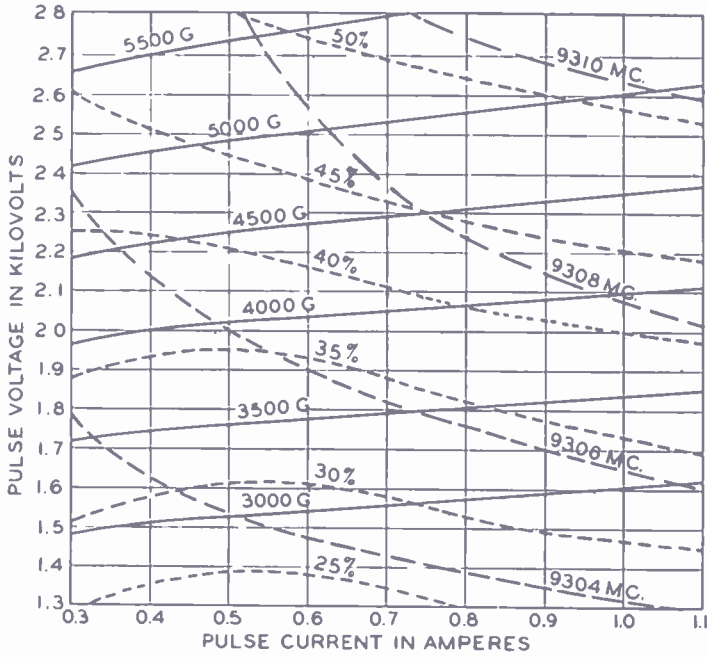
Fig. 6—Chart depicting typical variations of efficiency and frequency with pulse voltage, pulse current and magnetic field. (The magnetic fields shown by the slanting solid lines are those within the interaction space; the necessary external fields are reduced substantially by the steel inserts within the tube. These data were taken with a matched load, a pulse length of about 0.5 microsecond and a pulse repetition rate of 6000 per second.)
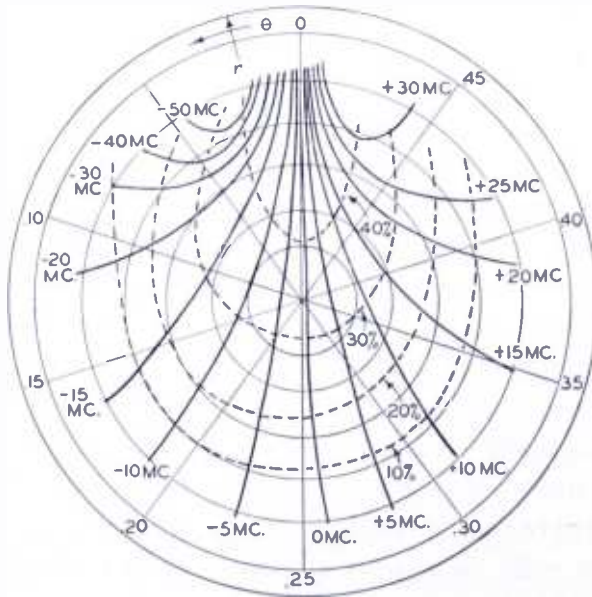
Fig. 7—"Rieke" diagram showing typical variations of frequency and efficiency, plotted on a coördinate system indicating changes of load impedance presented to the tube. (The "r"-coördinate indicates voltage standing-wave ratio while the "θ"-coördinate indicates variations of phase throughout 180 degrees. These data were taken with a pulse current of 0.5 ampere and a pulse voltage of approximately 1.8 kilovolts.)

the stabilizer. Figure 6 shows a performance chart typical of the results obtained. In the average tube the efficiency is 45 to 50 per cent at the 2500-volt level. The "pushing," or change in frequency with anode current, varies rather widely from tube to tube; the value of one megacycle for a change in current of 0.2 ampere in the un-stabilized tube, shown in Figure 6, is typical. Figure 7 is a representative "Rieke" diagram, showing the change in frequency and efficiency with variations in loading. Although these data were taken at a voltage and current lower than those at which the tubes were finally rated, there is no substantial change, other than an increase in efficiency, at the higher voltage. It will be seen that the "pulling," or frequency variation for a change in phase of 180 degrees at a 1.5 voltage standing-wave ratio, is about 20 megacycles in Figure 7.

As a result of operation at high input currents and voltages a new phenomenon was encountered with many of the tubes. As the current was increased by raising the voltage with the magnetic field constant, an abrupt frequency change of about 1 megacycle occurred, almost invariably associated with an increase in efficiency of a few per cent. A typical discontinuity extended across the performance chart, with about the shape and position of the frequency contour marked 9306 on Figure 6, and was quite reproducible in any one tube. These discontinuities were termed "space-charge modes" from their possible association with space-charge discontinuities, although efforts to eliminate them by changes in the size or shape of the cathode were unavailing. The operating range of 2500 volts and 1 ampere is relatively free from such moding, which usually occurs at lower currents and voltages. In the production tube, the moding was encountered for a time in the 2500-volt range, but later receded toward the lower voltages and currents at which it had been previously encountered. It is thought that this may have been due to an improvement in the shapes of the current and voltage pulses applied to the tube.

DEVELOPMENTAL STABILIZER

An early stabilizer development of L. E. Norton, demonstrated that the frequency could be controlled by an external stabilizing cavity to almost any degree desired, dependent upon the decrease in output power associated with the use of the device. The success of the device arose from the unique method of coupling the external high-Q cavity to the magnetron.[3] The basic theory, developed at an early date, is

---

[3] L. E. Norton, "Frequency Stabilization of Oscillators by a Method Particularly Adapted to the Higher Frequencies and Magnetron Sources", Report on Frequency Stabilization Portion of Contract OEMsr-684 with the Office of Scientific Research and Development, May 1, 1944.

substantially the same as that presented in Part II for the final stabilizer. Many developmental stabilizers were built to provide joint tests of the performance of the tube and stabilizer in combination. The results afforded criteria for changes in the design of the tubes; for example, an increase in the coupling between the load line and the resonant cavity system made the tubes capable of better stabilization by either the developmental or final production stabilizer.

The early stabilizer, shown in Figure 8, was constructed of Invar tubing in order to minimize the effects of ambient temperature. Necessary adjusting screws and a coupling to the tube were provided, and the stabilizer was designed to be pressurized. A stabilizer of different mechanical design, similar in electrical design and performance to this early stabilizer but using several parts already in production for wave meters, appeared adaptable to early production and was, therefore, substituted. The developmental stabilizer was available sufficiently
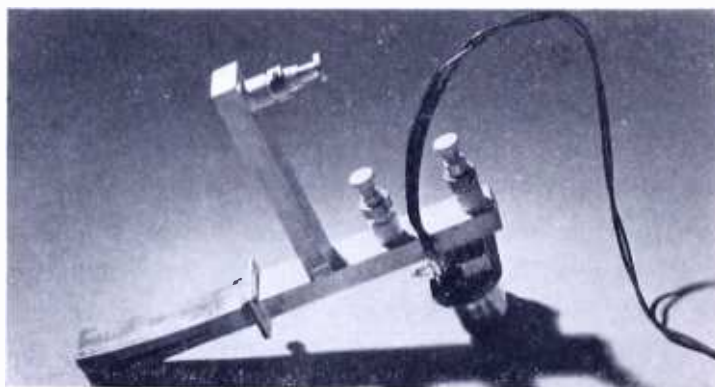
Fig. 8—The developmental stabilizer, consisting of a rectangular cavity coupled to the wave guide extending from the tube to the load termination. (In the example shown, the load was a horn matching the guide to space. The stabilizing network was constructed of Invar steel, silver plated to reduce the losses. The adjusting screws varied the degree of frequency stabilization obtained.)

early, however, to insure that the tube could be successfully stabilized upon completion of its development.

CONCLUSIONS

The pulsed, 9300-megacycle magnetron is capable in the unstabilized form of as much as 1 kilowatt peak output at 2500 volts, with a duty cycle of 0.3 per cent. The tube is tunable over a range of 3 per cent by a simple and reliable method taking advantage of the flexibility of the header.

This tube was scaled from a 5-kilowatt pulsed magnetron developed earlier. The scaling was carried out in a manner which permitted the

input to be increased later by a factor of five, without mechanical change, as the requirements placed upon the tube were altered in the course of the development.

The early developmental stabilizer, which was later modified to form the production design, not only established the principles of the method of stabilization, but ensured that the tube had such characteristics as to be usable with such a device.

The final combination of the tube and stabilizer described in Part II of this paper represents one of the first successful efforts to correct the most obvious defect, frequency instability, in a type of tube outstanding in its characteristics as regards power and efficiency.

Part II

ENGINEERING OF TUBE AND STABILIZER

By

C. P. Vogel‡ and W. J. Dodds#

Summary—*To satisfy the frequency stability requirements of a beacon system, a 9310-megacycle magnetron was fitted with a frequency stabilization device that reduced the inherent frequency changes of a magnetron by a factor of approximately 10. The device included a tunable resonant cavity for the storage of additional electromagnetic energy, and a method of coupling the cavity to the tube.*

The cavity is made of Invar steel to reduce the changes of dimension of the cavity with temperature. It is furthermore temperature-compensated by use of a higher-expansion steel for the spindle which supports the cavity tuning plunger. The tube frequency is adjusted within the specified tuning range by changing the cavity frequency. This is done by means of a tuning mechanism comprising a movable plunger actuated by rotation of an accurately ground nut which rotates in an accurately ground bearing where it is held in place by spring loading.

The cavity and stabilizer system provides for hermetic sealing so that the system may be filled with dry nitrogen at atmospheric pressure. The wave-guide system which forms the circuit that couples the tube and stabilizer to the load contains adjustable screw tuners to permit compensating for the variations of internal impedance from tube to tube and to compensate for differences in line length due to the location of the tube in the system. Stabilization procedure consists of the proper adjustment of these screw tuners.

A basic, simplified mathematical theory of stabilization is contained in the Appendix.

‡ Tube Department, RCA Victor Division, Lancaster, Pa.

Formerly with the Tube Department, RCA Victor Division, Lancaster, Pa. Now with the Research Department, RCA Laboratories Division, Princeton, N. J.

INTRODUCTION

THIS paper describes a method for stabilizing the frequency of a magnetron oscillator sufficiently to make the tube suitable for use in the transmitter of a beacon system. In a magnetron there are three major causes for frequency variation. (1) The frequency variation *with temperature* is a function of the temperature coefficient of linear expansion of the material comprising the resonant cavities. In the case of the copper-cavity tube operating at 10,000 megacycles the expected frequency decrease for a rise in the temperature of the anode assembly would be approximately 0.17 megacycles per degree Centigrade. (2) The frequency change with *anode current,* usually termed "pushing", varies greatly with the type of magnetron, but an increase in frequency of one part in one hundred thousand might reasonably be expected for a one-per cent change in anode current. (3) The frequency variation caused by changes in the *load impedance* must be considered, since in most applications it is impractical to maintain a voltage standing-wave ratio much below 1.5 in the line to the antenna. Furthermore, the phase, or position of the voltage minimum, may vary through 180 degrees due to changes in temperature (of the wave-guide output system) or in the pattern of the energy reflected to the antenna. The greatest change in frequency occurring when the position of the voltage minimum of a voltage standing-wave ratio of 1.5 is shifted through all possible phases is commonly called "pulling". This frequency change is a function of the tightness of coupling between the resonant cavities of a magnetron and the load. It may be expected to vary from 0.2 to 0.4 per cent of the tube frequency, or from 20 to 40 megacycles for a 10,000-megacycle tube.

In a beacon system it is obviously necessary to reduce these frequency variations to insure that the transmitter is operating at all times within the frequency bandwidth of the receivers. The problem, therefore, resolved itself into building a transmitter that could be tuned to a definite frequency and be stabilized to the extent that under all conditions encountered in the field, its frequency would remain within the 2.5-megacycle bandwidth of the receivers.

The proposals considered to accomplish this were:

1. Monitor the system and automatically retune the magnetron to maintain constant frequency. (This was awkward and was abandoned in favor of the second proposal.)

2. Build a tunable, stabilized magnetron that would be completely stabilized and adjusted by the manufacturer and that could be placed into any reasonably well-matched system to give the necessary per-

formance with no further adjustments except to tune to the frequency desired. This proposal was adopted when L. E. Norton demonstrated a stabilizing system comprising a resonant cavity that could be coupled to a magnetron and which would automatically control the magnetron frequency. The decision to incorporate the stabilizer as part of the tube instead of as part of the system plumbing was made because the equipment required to make the necessary circuit adjustments to obtain stabilization was not generally available in the field.

The completed unit known as type 2J41 was made up of two parts, the magnetron tube and the stabilizing network, hereinafter referred to as the stabilizer.
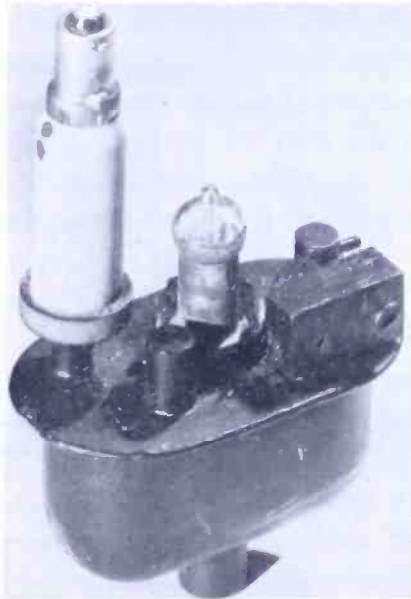
Fig. 1—The magnetron ready for attachment to the stabilizer.

THE STABILIZED TUBE

The Tube

The basic design of the magnetron tube, described in Part I, was modified to permit the use of techniques that were more suitable for production. One modification was the substitution of Monel metal for the stainless steel header and envelope used in the developmental models. Monel was chosen because of its superior brazing qualities, its non-magnetic property, its strength and its suitability as a vacuum envelope.

Another modification was in the fabrication of the anode block as described in Part I and shown therein in Figures 3 and 4. The cathode stem was modified so that it could be made on a conventional stem

machine. For protection, it is covered by a ceramic insulator and has its leads brought out to a miniature bayonet base. Figure 1 shows the completed production model of the tube ready for attachment to the stabilizer.

The Stabilizer

The stabilizer and magnetron are shown in Figure 2. The assembly includes the stabilizing cavity, a wave-guide system connecting the tube and the cavity to the output, a tuning mechanism, the permanent magnet to provide a constant magnetic field for the tube and a mounting panel.

According to the theory developed in the Appendix of this paper, the stabilizer must be a device capable of storing additional energy
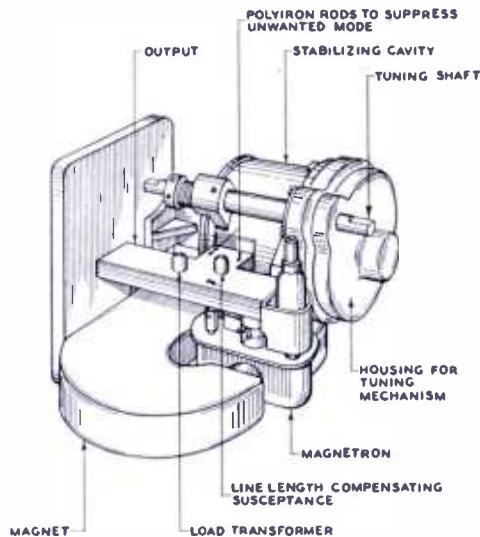
Fig. 2—Magnetron and stabilizer assembly.

at the resonant frequency; it must be mechanically rugged so th..t changes in frequency due to motion of the stabilizer parts do not occur; its changes of dimensions with temperature must be held to a low value; it must be capable of being filled with a dry inert gas; it must be tunable; and it must withstand vibration, handling and shocks.

Although the wave-guide system is capable of storing some additional energy, the major portion of the additional energy is stored in the specially built resonant stabilizer cavity. Dimensional stability of the cavity is obtained by using a rugged mechanical design and by constructing it from Invar steel, which is a nickel steel with a low thermal-expansion coefficient in the temperature range required. The cavity walls and ends are approximately ¼ inch thick and the parts are assembled with dowel pins for locating, machine screws for fastening

and soft solder to produce the final hermetic seal. The inner surfaces of the cavity are silver-plated and polished to reduce the losses caused by circulating currents.

The cavity controls the frequency of the tube to such an extent that actual tuning of the tube (over a limited range) may be accomplished by changing the frequency of the cavity alone. The cavity, consequently, is fitted with a piston type of tuning control which permits the effective size of the cavity and, therefore, its frequency to be adjusted. The plunger is supported on a non-rotating spindle on which a micrometer thread has been cut. The spindle is moved axially by rotation of a nut which supports the spindle. This nut has a ground surface and fits into a ground bearing where it is kept seated by spring loading. A flexible metal diaphragm is soldered between the spindle and the outer cavity wall to provide a pressure seal for the moving spindle. A separate tuning shaft drives the tuning mechanism through a gear train. The tuning range of the tube (± 10 megacycles) is covered in seven turns of the tuning shaft. A simple stop mechanism limits the turning of the shaft to this amount to prevent tuning the tube too far from its frequency and to prevent injury to the flexible diaphragm sealing the tuning mechanism.

The cavity is made to give a better degree of temperature stabilization than that obtainable from Invar alone by using stainless steel for the spindle that carries the cavity tuning plunger. The higher expansion of the spindle is in a direction to compensate for the changes in dimension of the Invar cavity. This feature reduces the change in frequency caused by changes in temperature from a maximum of 8 megacycles to a maximum of 3 megacycles in the temperature range specified in Table 1.

The tunable cavity is coupled to a section of ½ x 1 inch wave guide through an iris in the wall of the cavity. The wave-guide section couples the tube, the cavity and the load. An adjustable screw inserted into the wave guide is used as a compensating susceptance (Figure 2) to permit adjustment for differences in the internal admittances of individual magnetrons. A similar screw is used as a variable load coupling transformer to permit adjustment of the coupling between the tube and the load. The output end of the wave-guide section contains an iris type glass window which provides a pressure seal for the wave-guide output.

Since an unwanted mode can exist in the wave guide, pieces of polyiron have been utilized as a "lossy" material, located to damp out the unwanted mode but not to affect the desired mode. The locations of these parts are shown in Figure 2.

To prevent "breathing" of the cavity with the consequent entrapment of moisture causing a change in frequency, the stabilizer and the wave-guide assemblies are arranged for hermetic sealing after all circuit adjustments have been made. If water vapor were sealed into the cavity it would cause an additional increase of frequency with temperature. To remove the water vapor, the cavity is evacuated and baked in a manner similar to that used for vacuum tubes. It is then flushed and finally filled with dry nitrogen (dew point below -35

Table 1 — Performance of the 2J41

Anode Voltage	2400-2600 volts
Anode Current	1 ampere, peak
	3 milliamperes, average
Duty Cycle	0.3 per cent
Pulse Length	0.5 microsecond
Pulse Repetition Frequency	6000 pulses per second
Unstabilized "pulling"	20-30 megacycles
Stabilized "pulling"	1.5 megacycles, maximum
Unstabilized "pushing"	1-2 megacycles
Stabilized "pushing"	0.1 megacycle for 0.8 to 1.2 amperes
Unstabilized power output	870 watts, peak
	2.7 watts, average
Stabilized power output	500 watts, peak
	1.5 watts, average
Stabilization against temperature changes (1)	3.0 megacycles, -50 to $+85$ degrees Centigrade tube temperature
Center Frequency	9310 megacycles
Stabilized Tuning Range	± 10 megacycles
Total Weight: Tube, Stabilizer and Magnet	7 pounds, 5 ounces
Internal Magnetic Field (2)	4800 Gausses
External Magnetic Field (2)	2100 Gausses

(1) Difference between maximum and minimum frequency in temperature range shown.
(2) Provided by integral "packaged" magnet.

degrees Centigrade) and sealed with approximately atmospheric pressure of dry nitrogen inside. This operation was found to be very necessary for obtaining good temperature stabilization.

Stabilization is achieved during manufacture by the following procedure. The magnetron, Figure 1, free of the stabilizer is tuned to 9310 megacycles in a matched line and its tuning mechanism is sealed with solder. Using the stabilizer tuning mechanism, the stabilizer cavity is adjusted to 9310 megacycles. The magnetron is soldered to

the stabilizer and the permanent magnet attached. The assembly is then operated on a test bench, the line-length adjusting screw adjusted for maximum power output, and the load transformer adjusted for the desired pulling figure. The adjusting screws are sealed with solder and the characteristics of the tube re-checked. After these operations the assembly is baked, evacuated, filled with dry nitrogen as described, sealed, cleaned, painted and given its final test.

PERFORMANCE

The performance requirements of the stabilized tube were changed as tests on equipments progressed. Before stabilizer models were available, it had been hoped to be able to stabilize the tubes to within 1.0 megacycle against all variations. This requirement was found to
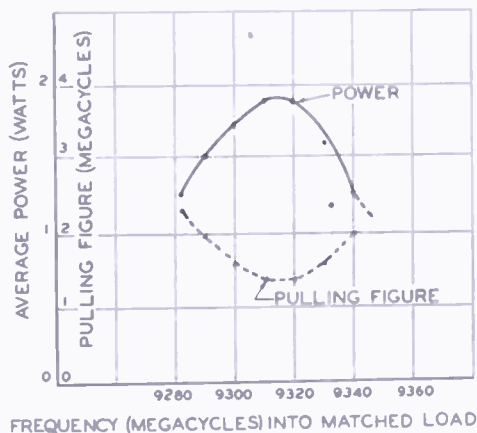
Fig. 3—Variation of average power and pulling figure with frequency.

be impractical principally because the tighter stabilization caused too great a reduction of the power output. The final specifications were established as a good compromise between the requirements of the equipment designers and the achievements of the tube manufacturer.

The performance data of the 2J41 have been condensed in Table 1. The tube must operate at a peak value of one ampere within the voltage range specified. The "pulling" is in the usual terms of frequency change in megacycles for a 1.5 voltage standing-wave ratio as previously defined and the output power is measured in a 52-ohm load matched to the wave guide at the output flange. The frequency change with variation in temperature is for the whole assembly in equilibrium with surroundings at the tube temperatures specified.

The tuning range of 10 megacycles is obtained by adjusting a single control on the stabilizer. As the tube is tuned, the power output and "pulling" vary with frequency as shown in Figure 3. The tube must

be within specifications (Table 1) at any point in the tuning range. Outside the tuning range, the power and pulling continue to change slowly in the directions indicated in Figure 3, until finally a breakout point or frequency discontinuity is reached.

CONCLUSIONS

A method of stabilizing the frequency of a magnetron was developed and shown to be practical when applied to production quantities of tubes. The frequency was stabilized to reduce the effects of changes in load impedance, temperature, tube current and changes in humidity. The tube is suitable for applications within its range of frequency stability and power.

APPENDIX

*Theory of Stabilization**

A magnetron has a certain inherent frequency stability because it incorporates in its construction a resonant circuit which stores electrical energy at its resonant frequency. The degree to which a system tends to operate near this frequency is a function of energy storage in the resonant circuit. Improvement in frequency stability can be expected by adding to the system a device for storing additional energy at the desired frequency. For the frequency under consideration, this device would take the form of a resonant cavity coupled in some way to the electromagnetic circuit of the magnetron.

For the purposes of discussion, the stabilization factor is defined as

$$\text{Stabilization factor } (S) = \frac{\text{Total energy stored in the system}}{\text{Energy stored in the unaltered magnetron}} \qquad (1)$$

E. A. Guillemin[1] derives an equation which shows that frequency changes due to varying operating conditions may be reduced by this stabilization factor, provided that the frequency of the energy-storage device stays constant. If B_{11} is the driving point susceptance of a dissipative network, E_1 is the voltage, T_{AV} is the average energy stored

---

* A very similar stabilization theory was also developed by M. A. Herlin and F. F. Rieke (consultants on this project), both members of the staff of the Radiation Laboratory, Massachusetts Institute of Technology, Cambridge, Mass.

[1] E. A. Guillemin, COMMUNICATION NETWORKS, Vol. II (p. 229), John Wiley and Sons, New York, N. Y., 1935. (Adapted by permission.)

in the magnetic field, V_{AV} is the average energy stored in the electric field and $\omega = 2\pi f$, Guillemin shows that

$$\frac{dB_{11}}{d\omega} = \left(\frac{2}{E_1}\right)^2 (T_{AV} + V_{AV}) \tag{2}$$

where B is defined as the imaginary part of the admittance. Equation (2) shows that B_{11} will change with changes in ω, and that it changes more rapidly with increased energy storage.

For any generalized, dissipative two-terminal network, the admittance over a small frequency interval near resonance in terms of an equivalent parallel resonant circuit consisting of a single lumped conductance, lumped inductance and lumped capacitance is

$$Y = G + j\omega c + \frac{1}{j\omega L} = G + j \sqrt{\frac{C}{L}} \left(\frac{\omega}{\omega_o} - \frac{\omega_o}{\omega}\right) \tag{3}$$

$$= G + j \sqrt{\frac{C}{L}} \left(\frac{\lambda_o}{\lambda} - \frac{\lambda}{\lambda_o}\right) \tag{4}$$

Simplification results from the use of the approximation

$$\left(\frac{\lambda_o}{\lambda} - \frac{\lambda}{\lambda_o}\right) = \frac{(\lambda_o - \lambda)(\lambda + \lambda_o)}{\lambda\lambda_o} \cong -2\,\delta \tag{5}$$

where

$$\delta = \frac{\lambda - \lambda_o}{\lambda_o} = \frac{\omega_o - \omega}{\omega} \tag{6}$$

then

$$Y = G - j \sqrt{\frac{C}{L}} (2\delta) \tag{7}$$

The expression for the admittance of the unaltered magnetron becomes

$$Y_t = G_t - j \sqrt{\frac{C_t}{L_t}} (2\delta\,t) \tag{8}$$

For the equivalent cavity, which is the actual physical stabilizing cavity plus the connecting lines by which it is coupled to the magnetron, the

corresponding expression becomes

$$Y_c = G_c - j \sqrt{\frac{C_c}{L_c}} \, 2\delta_c \qquad (9)$$

Let $\delta = \delta_t = \delta_c$ since tube and equivalent cavity operate at the same frequency. Then, for the tube and the equivalent cavity in parallel as shown in Figure 4.
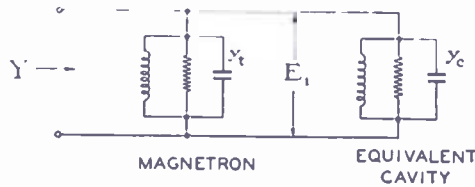
Fig. 4—Schematic of tube and stabilizer.

$$Y_t + Y_c = G_t + G_c - j \left(\sqrt{\frac{C_t}{L_t}} + \sqrt{\frac{C_c}{L_c}} \right) 2\delta \qquad (10)$$

The total stored energy from (2) is

$$T_{AV} + V_{AV} = \left(\frac{E_1}{2} \right)^2 \frac{dB}{d\omega} \qquad (11)$$

$$B = - \left(\sqrt{\frac{C_t}{L_t}} + \sqrt{\frac{C_c}{L_c}} \right) \frac{\omega_0 - \omega}{\omega} \qquad (12)$$

Then
$$\frac{dB}{d\omega} = \frac{\omega_0}{\omega^2} \left(\sqrt{\frac{C_t}{L_t}} + \sqrt{\frac{C_c}{L_c}} \right) \qquad (13)$$

When (13) is substituted in (11), the total energy stored in the magnetron and equivalent cavity circuits is

$$T_{AV} + V_{AV} = \frac{E_1^2}{4} \left(\sqrt{\frac{C_t}{L_t}} + \sqrt{\frac{C_c}{L_c}} \right) \frac{\omega_0}{\omega^2} \qquad (14)$$

The energy stored in the unaltered magnetron is

$$T'_{AV} + V'_{AV} = \frac{E_1^2}{4} \left(\sqrt{\frac{C_t}{L_t}} \right) \frac{\omega_0}{\omega^2} \qquad (15)$$

$$S = \frac{\text{Total energy stored in system}}{\text{Energy stored in the unaltered magnetron}}$$

$$S = \frac{T_{AV} + V_{AV}}{T'_{AV} + V'_{AV}} = \frac{\sqrt{\dfrac{C_t}{L_t}} + \sqrt{\dfrac{C_c}{L_c}}}{\sqrt{\dfrac{C_t}{L_t}}} \tag{16}$$

$$S = 1 + \sqrt{\frac{C_c L_t}{L_c C_t}} \tag{17}$$

This result is derived on the basis of unchanged E, when the equivalent cavity is added to the magnetron.

The quantities C_t and L_t are associated with the tube and should be considered as fixed, whereas C_c and L_c are quantities related to the equivalent cavity and by design may be given a wide latitude of values. The equivalent cavity was defined as the physical cavity plus connecting lines. It follows that for a constant quantity of stored energy in the equivalent cavity the ratio of stored energies of the physical cavity and lines may also be selected by design.

The stabilization factor obtainable with a network consisting of appropriate connecting lines and a physical cavity with a fixed value of Q has been shown[2] to have the same value as the stabilization factor obtainable with a simple physical cavity of higher Q connected to the magnetron in simple, parallel fashion.

---

[2] See Part I, Reference 3.

* * * *

ACKNOWLEDGMENTS

others contributed to the tube and stabilizer development; members of the group under V. K. Zworykin and P. T. Smith, working on a tube having similar radio-frequency characteristics, contributed many helpful suggestions to this project; P. J. Herbst coordinated the tube work with the equipment development. At RCA Victor Division, Lancaster, Pa., P. H. Morganson, J. R. Trocki, R. B. Vandegrift, L. P. Garner, D. J. Myers, Miss D. Neal, and others aided in engineering the tube and stabilizer and putting it into production. Acknowledgment is due for the constant encouragement and help of B. J. Thompson, L. P. Smith, I. Wolff, D. Ulrey and E. E. Spitzer. At the Maguire Industries Company plant at Greenwich, Connecticut, H. Langstroth and L. Beebe contributed to the design and production of the stabilizer.

CRITERIA FOR DIVERSITY RECEIVER DESIGN[*]

By

WALTER LYONS

Engineering Department, RCA Communications, Inc.,
New York, N. Y.

Summary—This article presents design criteria, especially those where differences between usual single receiver and diversity receiver design exist. Discussion is limited to those criteria concerning diversity receivers incorporating diode switching of the common diode load variety.

ALTHOUGH diversity reception has been in commercial use for nearly two decades, it is still not generally recognized that the design of a diversity receiver is materially different from that of a single receiver. Reference is made here to the literature[1,2,3] and various instruction books for diversity communication receivers for a discussion of the general aspects of diversity reception.

Except for the reception of frequency-shift signals, diode switching of the common diode load type of diversity connection is commercially used. The reception of frequency-shift signals requires the use of triggered switching diversity because multipath effects are greater due to the employment of mark and space signals. The requirement is that one and only one signal contribute to the output load at any given time with the ability for very rapid switching when an interchange occurs.

DIODE SWITCHING

A very important feature in the sound design of diversity receivers, particularly those for telephone and on-off telegraph reception, is the use of diode switching for automatically switching out all receivers of the group except the one which is temporarily receiving the highest signal voltage, and, ordinarily, the best signal-to-noise ratio. Diode switching is effected by terminating the diode outputs of the two or

---

[*] Decimal Classification: R361.107.

[1] H. H. Beverage and H. O. Peterson, "Diversity Receiving System of RCA Communications, Inc., for Radiotelegraphy," *Proc. I.R.E.*, April, 1931.

[2] H. O. Peterson, H. H. Beverage and J. B. Moore, "Diversity Telephone Receiving System of RCA Communications, Inc.," *Proc. I.R.E.*, April, 1931.

[3] J. B. Moore, "Recent Developments in Diversity Receiving Equipment," *RCA REVIEW*, Vol. II, No. 1, pp. 94-116, July, 1937.

more receivers of the group on a common load resistor. With such a common termination, the rectified voltage furnished by the receiver temporarily receiving the strongest signal operates as a counter bias on the diodes of the other receivers allowing them to contribute little or none of the rectified current flowing through the common load resistor.

For maximum effectiveness of diode switching, it is necessary that the voltage regulation of the individual diode circuits be kept low so that, as each is relieved of the load by counter bias action, its output voltage will not rise greatly and unduly resist relief of the load. To this end resistance of the interconnections between the low potential sides of the several intermediate-frequency transformers and their common interconnection should be as low as possible and intermediate-frequency transformer circuit design considerations should be applied as indicated below.

Sensitivity and Gain

In order that automatic receiver switching be complete when receivers are connected in diversity by interconnecting their several diode output terminals to a common diode load, it is necessary first that the diode voltage be large enough to overcome the contact potential presented by the signal rectifier. A practical value for the diode voltage is 5 volts minimum, obtained from a 0.5 microvolt signal. The conclusion, therefore, is that the total voltage gain from antenna to diode load be at least ten million times.

Automatic Gain Control

Since that instrument receiving the strongest signal from its particular antenna develops the highest automatic-gain-control (AGC) potential, interconnection of the AGC circuits will accelerate switching action by reducing the gain of the other receivers in diversity. Diversity receivers require the highest degree of flat AGC characteristic in order to have little change in signal weight when receiving on-off keyed signals due to fades not fully compensated for by the switching action. The same reasoning applies for the reception of telephone signals where commercial requirements are far more severe than those for ordinary home entertainment. Voltage delay on the AGC action should be employed for two reasons—in order that the AGC should be substantially flat (at least 120 decibels change in input for 10 decibels change in diode voltage), and in order to obtain high level detection to fulfill the requirements mentioned under Sensitivity above. The

delay voltage should be that value which is above the rectified noise level appearing across the diode load plus the value of the rectified signal voltage obtained from the lowest usable signal level so that the normal signal-to-noise ratio appearing at the input terminals of the receiver is not decreased as it is presented across the diode load resistor. Thus, if reference is made to the foregoing, it is evident that the delay voltage in no case should be below 5 volts.

Gain Control

The gain control should not alter the differential gain characteristic for any setting of the control, in order that each receiver may have identical opportunity to switch reception. This type control is best obtained by controlling the gain of the intermediate-frequency amplifier in such manner as not to alter the slope of the AGC characteristic. A gain control is necessary for receivers in diversity connection in order that the gain from antenna to diode of each receiver in diversity can be made equal. This control should have a range on the order of not less than 100, nor more than 1,000 times, in order to accommodate production variations in receiver gain in addition to variations in antenna sensitivity.

AGC Time Constants

Since the reception of CW code signals represents a great part of the service for diversity receivers, it is advisable to include variable automatic-gain-control (AGC) time constants. Three time constants are usually deemed advisable although two are used in most cases. If three time constants are to be incorporated, they should have values of approximately one second, 1/10 of a second, and 1/100 of a second. If two time constants are used, it is preferable that they be approximately one second and 1/20 of a second. A fast time constant is required when recording signals which have a fast fading characteristic causing drop-outs. The slow time constant is desirable when noise occuring between code pulses is encountered.

Frequency Stability

Frequency stability of the local oscillator is highly important in diversity reception since a shift in frequency in any one of the receivers tends to remove it from diversity action and cause phase distortion. In order to reduce these faults, it is not only necessary to have extremely high frequency stability, but it is also desirable in most cases

to utilize one heterodyne oscillator for all the receivers. In some multiple receiver installations, however, it may be desirable to utilize separate heterodyne oscillators for each receiver in order to obtain greater flexibility in the use of the equipment.

BFO MONITORING

In order to monitor receivers in diversity, it is important that no extraneous voltages be introduced into the diode load circuit which will impair the diversity action of the several receivers. Reference is made in particular to the common practice of injecting beat-frequency-oscillator (BFO) potentials into the intermediate-frequency amplifier as this increases the potential of the diode out of proportion to the received signal and therefore causes that particular receiver to control switching without regard to the strength of the signal. Since diversity receivers must be tuned to exact frequency as nearly as possible and resonance maintained throughout operation, the requirement is that beat frequency injection be divorced from the main intermediate-frequency amplifier. This may be accomplished by the use of a separate intermediate-frequency amplifier, BFO detector and audio amplifier operated from coupling circuits in the individual intermediate-frequency amplifiers connected in diversity.

FINAL INTERMEDIATE-FREQUENCY TRANSFORMER DESIGN

In order to obtain fast diode switching action, it is desirable to design the last intermediate-frequency transformer so that its output voltage does not increase substantially when its diode is inoperative. When no signal is received, the final transformer is unloaded and conversely is loaded by half its diode load resistance when its diode is operating. It is, therefore, desirable to use the highest value diode load resistor consistent with the remainder of the design and the audio fidelity desired. Furthermore, the transformer secondary may be shunted so that the removal of the diode load does not cause the diode output voltage to rise objectionably and counter the action. Adjusting the coupling between the primary and secondary of the transformer so that optimum coupling is obtained when the diode is operating tends to prevent an objectionable rise in voltage when the diode is inoperative.

RADIATION

Installations utilizing diversity receivers usually include expensive antenna systems that, in many cases, cost considerably more than the

receiving equipment. It is, therefore, economical to operate several receivers from the same antenna. This brings up the problem of oscillator radiation and its effect on other receivers connected to the same antenna. In multiple receiver installations, unless sufficient operating care is exercised it is probable that one of the receivers may be tuned to the oscillator frequency of another receiver. This makes it necessary that the oscillator radiation be held down to a level no greater than the receiver noise. No simple method to accomplish this will be outlined herein; it is sufficient for the purpose of this paper to mention the usual precautions of filtering, shielding, and careful choice of grounds.

BALANCED INPUT

In order to reduce local noise interference effects, it is desirable to utilize balanced antenna input. The ratio between the voltage on the first grid of the receiver, due to the antenna voltage across the transmission line, to the voltage on the grid, due to potentials between the transmission line and ground, should be greater than 40 decibels. This latter figure is commonly referred to as the antenna input balance ratio. Neglecting balanced input may result in local noise interference causing a particular antenna and the receiver connected to it to control the diode switching, resulting in the loss of signal and the substitution of noise.

CONCLUSION

In summation, diversity design criteria may be tabulated as shown below:

   (1) Voltage gain antenna to diode load 10 million times.
   (2) Automatic gain control effect not more than 10 decibels change of output from 120 decibels change of radio-frequency input voltage above 0.5 microvolt.
   (3) Manual gain control on intermediate-frequency amplifier of 100 to 1,000 times.
   (4) Automatic-gain-control time constant, one second and 1/20 second.
   (5) Frequency stability better than 30 parts per million per degree centigrade. (Stability in presence of all other variations should be on the same order.)
   (6) Separate beat-frequency-oscillator monitoring channel.
   (7) Final intermediate-frequency transformer designed for low voltage regulation.
   (8) Oscillator radiation less than 0.5 microvolts.
   (9) Input balance 40 decibels or better.

ACKNOWLEDGMENTS

RCA TECHNICAL PAPERS†

First Quarter, 1947

Any requests for copies of papers listed herein should be addressed to the publication to which credited.

"A Coaxial-Line Diode Noise Source for U-H-F", H. Johnson, *RCA REVIEW* (March) 1947

"A De Luxe Film Recording Machine", M. E. Collins, *Jour. Soc. Mot. Pic. Eng.* (February) 1947

"Antennas for FM and Television", M. Kaufman, *Radio Maintenance* (March and April) 1947

"Automatic Frequency-Phase Control in TV Receivers", A. Wright, *Tele-Tech* (February) 1947

"Carbide Structures in Carburized Thoriated-Tungsten Filaments", C. W. Horsting, *Jour. Appl. Phys.* (January)....... 1947

"Civil Service Electrical Engineering", D. F. Shapiro, Pamphlet, Board of Transportation, New York, N. Y. (March)........ 1947

"Convex Wood Splays for Broadcast and Motion Picture Studios", M. Rettinger, *Jour. Acous. Soc. Amer.*, (March).... 1947

"Design of Recording Studios for Speech and Music", G. M. Nixon, and J. Volkmann, *Tele-Tech* (February).......... 1947

"Determination of Current and Dissipation Values for High-Vacuum Rectifier Tubes", A. P. Kauzmann, *RCA REVIEW* (March) 1947

"Excess Noise in Cavity Magnetrons", R. L. Sproull, *Jour. Appl. Phys.* (March) 1947

"Explanation of the Ratio Detector as an Aid in FM Servicing", J. A. Cornell, *RCA Rad. Serv. News* (March-April) 1947

"Film Projectors for Television", R. V. Little, Jr., *Jour. Soc. Mot. Pic. Eng.* (February) 1947

"Headphone Measurements and Their Interpretation" D. W. Martin and L. J. Anderson, *Jour. Acous. Soc. Amer.* (January) 1947

"High Frequency Gluing—Fact and Fantasy", E. S. Winlund, *Wood Products Magazine* (March and April) 1947

"Input Circuit Noise Calculations for F-M and Television Receivers", W. J. Stolze, *Communications* (February)........ 1947

"International Plan for Air Navigation", D. H. Pain, *Electronics* (February) 1947

"Magnetic Recording", H. E. Roys, *Inter. Project.*, (January). 1947

---

† Report all corrections or additions to RCA REVIEW, Radio Corporation of America, RCA Laboratories Division, Princeton, N. J.

"Magnetic Throat Microphones of High Sensitivity" D. W. Martin, *Jour. Acous. Soc. Amer.*, (January)............. 1947

"Mechano-Electronic Transducers", H. F. Olson, *Jour. Acous. Soc. Amer.*, (March) 1947

"Military Television", George M. K. Baker, TELEVISION, Volume IV (January) 1947

"Model 1947 Theatre Voice Doctor Has Modern Instruments", F. W. Wentker, *Box Office Magazine* (Modern Theatre Section) (February 1) 1947

"Multi-Channel Radiotelephone for Inland Waterways" G. G. Bradley, *Tele-Tech* (January) 1947

"Multivibrators", T. Gootée, *Radio News* (February and March) 1947

"Power Measurements of Class B Audio Amplifier Tubes", D. P. Heacock, *RCA REVIEW* (March) 1947

"Radio's Contribution to International Understanding", David Sarnoff, Editorial, *Proc. I.R.E.* (February) 1947

RCA TECHNICAL PAPERS (1919-1945)—INDEX, Volume I, RCA REVIEW, RCA Laboratories Division, Princeton, N. J. (February) 1947

RCA TECHNICAL PAPERS (1946)—INDEX, Volume II(a), RCA REVIEW, RCA Laboratories Division, Princeton, N. J. (March) 1947

"Relation of the Engineering Profession to Industry", C. B. Jolliffe, Pamphlet, RCA Department of Information, New York, N. Y. (March) 1947

"Relative Amplitude of Side Frequencies in On-Off and Frequency-Shift Telegraph Keying", G. S. Wickizer, *RCA REVIEW* (March) 1947

"Ring Oscillators for U.H.F. Transmission", T. Gootée, *Radio News* (January) 1947

"Science at New Altitudes", David Sarnoff, Pamphlet, RCA Department of Information, New York, N. Y. (February 11)... 1947

"Technical Educational Requirements of the Modern Radio Industry", P. L. Gerhart, *RCA REVIEW* (March) 1947

TELEVISION, Volume III (1938-1941), RCA REVIEW, RCA Laboratories Division, Princeton, N. J. (January).......... 1947

TELEVISION, Volume IV (1942-1946), RCA REVIEW, RCA Laboratories Division, Princeton, N. J. (January).......... 1947

"Television—A Review, 1946", E. W. Engstrom, TELEVISION, Volume IV (January) 1947

"Television Broadcasting—1946", O. B. Hanson, TELEVISION, Volume IV (January) 1947

"Television Deflection Circuits", A. W. Friend, *RCA REVIEW* (March) 1947

"Television, Films and the Human Eye", A. Rose, *Inter. Project.* (March) 1947

"Television High Voltage R-F Supplies", R. S. Mautner and O. H. Schade, *RCA REVIEW* (March) 1947

"Television Receivers", A. Wright, *RCA REVIEW* (March) ... 1947

"Television Today and Its Problems—1946", A. N. Goldsmith, TELEVISION, Volume IV (January) 1947

"Test Equipment for Theatre Servicing", E. Stanko and P. B. Smith, *Inter. Project.* (February) 1947

"Testing Audio Amplifiers with Square Waves", K. A. Simons, *RCA Rad. Serv. News* (January-February) 1947

"The Clamp Circuit—Part I", C. L. Townsend, *Broad. Eng. Jour.* (January) 1947

"The Magnetic Electron Microscope Objective: Contour Phenomena and the Attainment of High Resolving Power", J. Hillier and E. G. Ramberg, *Jour. Appl. Phys.* (January) ... 1947

"The Maximum Efficiency of Reflex-Klystron Oscillators", E. G. Linder and R. L. Sproull, *Proc. I.R.E.* (March) 1947

"The Outlook for Television—1941", A. F. Van Dyck, TELEVISION, Volume III (January) 1947

"The Pocket Ear", J. L. Hathaway and W. Hotine, *RCA REVIEW* (March) 1947

"The Present Status and Future Possibilities of the Electron Microscope", J. Hillier, *RCA REVIEW* (March) 1947

"The Progress of Television, 1938-1941", A. N. Goldsmith, TELEVISION, Volume III (January) 1947

"The Significance of Bikini", A. F. Van Dyck (coauthor), *Elec. Eng.* (January) 1947

"The Theory and Design of Speech Clipping Circuits", M. H. Dean, *Tele-Tech* (May) 1947

THEORY AND APPLICATION OF RADIO - FREQUENCY HEATING, G. H. Brown, C. N. Hoyler and R. A. Bierwirth, D. Van Nostrand Company, Inc., New York, N. Y. (March) . 1947

"Transmission Lines and Antennas for F.M. and Television", M. Kaufman, *Radio Maintenance* (March and April) 1947

"24-Frame/p.s. Projection vs. 30-Frame Video Rate", RCA Laboratories Division, Princeton, N. J., *Inter. Project.* (April) ... 1947

NOTE—Omissions or errors in these listings will be corrected in the yearly index.

AUTHORS

JACK AVINS received the A.B. degree in Physics from Columbia University in 1932. From 1931 to 1934 he was an assistant in the Physics Department at Columbia. From 1935 to 1938 he was employed by John F. Rider, Publisher, Inc. and from 1939 to 1941 by Service Instruments, Inc., where he designed radio test equipment. In August 1941 he reported for active duty in the Signal Corps and during 1942 and 1943 he served as senior American radar instructor at the Military College of Science in England. In 1944 he became Chief of the Radar Division, Signal Corps Publications Agency, Fort Monmouth. In January 1946, he joined the Industry Service Laboratory, RCA Laboratories Division, New York, N. Y., where he has been engaged in receiver design. Mr. Avins is a Member of Phi Beta Kappa and an Associate Member of the Institute of Radio Engineers.

BARREMORE B. BROWN received the B.E. degree in Chemical Engineering in 1937 and the M.S. degree in Physics in 1939 (both from Tulane University) and in 1942, he was awarded the D.Sc. degree in Physics by M.I.T. From 1942 to 1944, he was a research engineer at RCA Laboratories Division, Princeton, N. J., working on magnetron research and development. In 1944, he was associated with the Stromberg-Carlson Company as a senior physicist, performing research on magnetrons and equipment for microwave communications. During this period he was also a Research Associate on the Staff of Cornell University. In 1946, he joined the Tube Department, RCA Victor Division, Lancaster, Pa., as supervisor of the Special Development Group, working on the design of magnetrons and microwave power tubes. Dr. Brown is a member of Tau Beta Pi, Sigma Xi, the American Physical Society, the Institute of Radio Engineers, and the American Association for the Advancement of Science.

GEORGE H. BROWN received the B.S. degree at the University of Wisconsin in 1930; the degree of M.S. in 1931; the Ph.D. degree in 1933; and his professional degree of E.E. in 1942. From 1930 until 1933 he was a Research Fellow in the electrical engineering department at the University of Wisconsin, and from 1933 to 1942 he was in the research division of the RCA Manufacturing Company at Camden, N. J. Since 1942, he has been at RCA Laboratories Division, Princeton, N. J. Dr. Brown is a Member of Sigma Xi, the American Institute of Electrical Engineers, New York Academy of Sciences, and a Fellow of the Institute of Radio Engineers.

WILLIAM BROWN was graduated from the Pratt Institute in 1936. He was associated with the Cities Service Oil Company until 1941 when he joined the Columbia Broadcasting System as a Sound Engineer. Since 1943 he has been a member of the Industry Service Laboratory, RCA Laboratories Division, Princeton, N. J. Dr. Brown is a engaged in television development and licensee consultation. Mr. Brown is a Member of the Institute of Radio Engineers.

C. Louis Cuccia received the B.S. and M.Sc. degrees in Electrical Engineering from the University of Michigan in 1941 and 1942 respectively. He was associated with the General Motors Corporation during 1941 and 1942 working on high power induction heating. In 1942, Mr. Cuccia joined the RCA Manufacturing Company and, since November, 1942, has been a research engineer with RCA Laboratories Division, Princeton, N. J. He has been engaged in research on ultra-high-frequency transmitting tubes and associated modulation problems. During 1944 and 1945, Mr. Cuccia was also a member of the ESMWT faculty of Rutgers University, where he taught evening courses in Advanced Mathematics and Electrical Engineering. Mr. Cuccia is a member of Sigma Xi and an Associate Member of the Institute of Radio Engineers.

Wellesley J. Dodds received the B.S. degree from South Dakota State College in 1939, and the M.Sc. degree in Physics from the University of Kansas, where he was the Edwin Emory Slosson Scholar in Science in 1941. In 1941 and 1942 he was engaged in graduate work in biophysics at the University of Illinois. In 1942 he joined the Power Tube Design Section of the RCA Victor Division, Lancaster, Pa. Since 1945, he has been in the Research Department of RCA Laboratories Division, Princeton, N. J., performing research on microwave amplifier tubes. Mr. Dodds is a member of Sigma Xi, Pi Nu Epsilon, Sigma Pi Sigma and a Senior Member of the Institute of Radio Engineers.

John S. Donal, Jr. received the A.B. degree from Swarthmore College in 1926 and the Ph.D. degree in physics from the University of Michigan in 1930. From 1930 to 1936, he was associated with the Johnson Foundation for Research in Medical Physics and with the department of Pharmacology of the University of Pennsylvania. In 1936, he joined the research laboratories of the RCA Manufacturing Company, Inc., and is now associated with RCA Laboratories Division, Princeton, N. J., where he is engaged in research on light valves for television reproduction and in research on microwave transmitting tubes and their modulation. Dr. Donal is a member of Sigma Xi, Sigma Tau, the American Physical Society and a Senior Member of the Institute of Radio Engineers.

Simon Goldman received the B.Sc. degree in electrical engineering from Pratt Institute in 1940. After graduation he was employed by the U. S. Government as an assistant electrical engineer. Later, he entered the field of ionospheric research in the Department of Terrestrial Magnetism, Carnegie Institute of Washington, D. C., first in Washington and then in Iceland and Clyde, Baffin Island, in which latter place he was Chief Physicist and Observer-in-Charge. In 1946, he joined the Radio Systems Research Laboratory of RCA Laboratories Division, New York, N. Y. Mr. Goldman is an Associate Member of the American Institute of Electrical Engineers.

NORVAL H. GREEN received the degree of B.S. in Electrical Engineering from the University of Ohio in 1930. From 1930 to 1932 he was in the Long Lines Engineering Department of the American Telephone and Telegraph Company. In 1932, he attended Ohio State University for graduate work in Communications and received his M.S. degree in 1933. He joined the RCA Radiotron Company in 1933 and was in the Standardizing Section until 1938. In 1938, he transferred to the Receiving Tube Design Group of RCA Victor Division, Harrison, N. J.; he has been supervisor of this group since 1942. Mr. Green is a Member of the Institute of Radio Engineers.

HENRY E. HALLBORG graduated from Brown University in 1907 with a degree of B.Sc. in electrical engineering. After graduation, he joined the General Electric Company, first as a student engineer and then in the Testing Department. Following this, he was associated with the following organizations: 1909-1912, National Electric Signaling Company; 1912-1915, Marconi Wireless Telegraph Company of America; 1915-1923, U.S. Navy Department as an expert on radio aids; and 1923-1925, consulting engineer, C. Brandes Company. In 1925, he joined the Radio Corporation of America, and until 1932 worked on short-wave transmitter development. Since 1932, he has been performing research on terrestrial magnetism and ionosphere and space circuit analysis, first with RCA Communications, Inc., and since 1942, with the Radio Systems Research Laboratory of RCA Laboratories Division, New York, N. Y. Mr. Hallborg is President of the Brown Engineering Association and a Fellow of the Institute of Radio Engineers.

J. LEWIS HATHAWAY received his B.S. degree in Electrical Engineering from the University of Colorado in 1929. In the same year, he joined the National Broadcasting Company where, as a member of the Development Group, he has since been engaged in all fields of the Company's engineering activities. While on a leave of absence 1941 to 1944, he served as a Special Research Associate at Harvard University performing underwater sound development work. Mr. Hathaway was appointed a Staff Engineer of the National Broadcasting Company in 1945.

HARLEY IAMS graduated from Stanford University in 1927, with the B.A. degree in mechanical engineering. From 1927 to 1930, he was associated with the Westinghouse Electric Company, first in their student course and then as a research engineer working on facsimile transmission and television. In 1931, he joined the research laboratories of RCA Manufacturing Company, Inc., and since 1942 has been with RCA Laboratories Division, Princeton, N. J., developing television, infrared, centimeter-wave and radar tubes and apparatus. Mr. Iams is a member of Sigma Xi and Phi Beta Kappa, and a Senior Member of the Institute of Radio Engineers.

ROBERT L. JEPSEN, following his graduation with a B.S. degree in Electrical Engineering from the State College of Washington in 1944, joined the Special Development Division of the RCA Victor Division at Lancaster, Pa. He is currently employed at the Columbia Radiation Laboratory, and is studying graduate physics at Columbia University.

RALPH C. KENNEDY received the B.A. degree from San Jose State College in 1943 and the M.A. and E.E. degrees in Electrical Engineering from Stanford University in 1945 and 1946 respectively. In 1938 he became Chief Engineer at KRE. After serving as transmitter engineer at KROY and KQW, he joined the Hewlett-Packard Company as a development engineer in 1943. In 1944 he became a transmitter engineer at KPO, the National Broadcasting Company transmitting station in San Francisco, Calif. In 1946 he was transferred to the Sound Broadcasting Development Group of the National Broadcasting Company, New York, N. Y. Mr. Kennedy is a Member of the Institute of Radio Engineers.

WALTER LYONS received the B.Sc. degree in electrical engineering in 1928 from McGill University in Montreal, Canada. During 1929-1930 he attended the Columbia University Graduate School and in 1932 received the M.Sc. degree from McGill University. From 1924 to 1932, he was associated with various activities including Bell Telephone Laboratories, Inc., N. Y. Edison Co., Victor Talking Machine Co., Western Union Telegraph Co., Balkeit Radio Co., and the Hazeltine Corp. In 1932 he joined Wells-Gardner, in 1933-34 Emerson Radio and Television Corp., in 1934-1937 Hazeltine Corp., in 1937-1938 Majestic Radio and Television Corp., and in 1938 RCA Victor Division. In 1945 he became Staff Engineer of RCA International Division and in 1946 Plant Design Engineer for RCA Communications, Inc. Mr. Lyons is a Member of Sigma Xi and the Institute of Radio Engineers.

WILLIAM MILWITT received the B.S. degree in Electrical Engineering from the Newark College of Engineering in 1944. In that year he joined the Industry Service Laboratory, RCA Laboratories Division, New York, N. Y. Mr. Milwitt is a member of Tau Beta Pi and an Associate Member of the Institute of Radio Engineers.